doi : 10.17596/0002685

R/V Mirai Cruise Report

MR18-05C

Arctic Challenge for Sustainability (ArCS)

Arctic Ocean, Bering Sea and North Pacific

24 October 2018 – 7 December 2018

Japan Agency for Marine-Earth Science and Technology

(JAMSTEC)

Contents

1. Cruise Summary

1.1 Objectives

Unusual states of the Arctic regions, for example, less sea-ice extent, high temperatures in the atmosphere and ocean, much snow fall, and extreme weather events in the Arctic and beyond, has been prominent in recent years in particular during winter time. Those phenomena are scientifically important for understanding the air-ice-sea coupled physical processes and improving skills of numerical models. Skillful forecasts of weather, sea ice, and ocean are useful for ship navigation as well as activities of indigenous people. The Year of Polar Prediction (YOPP) proposed by World Meteorological Organization (WMO) Polar Prediction Project (PPP) provides a great opportunity to collaborate with observing and modeling platforms (Figure 1.1-1). This cruise contributes to the YOPP by

(1) collecting the in-situ data to understand the physical processes during early winter Arctic Ocean,

(2) evaluating and improving operational models based on the in-situ data, and

(3) monitoring the temporal and spatial variability of the basic parameters during a period of sea-ice advancing.

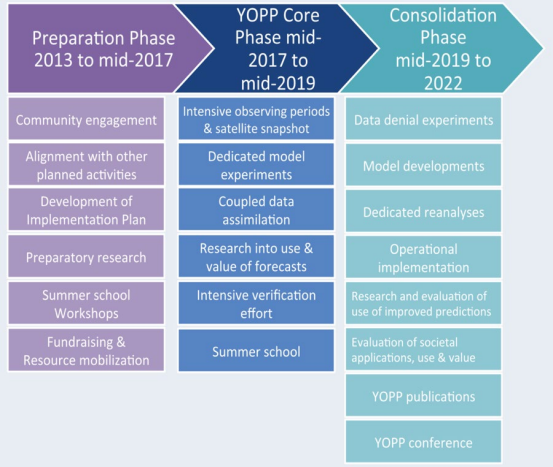

Figure 1.1-1: Three stages of the YOPP (Jung et al. 2016).

1.2 Basic information

Cruise ID:	MR18-05C
Name of vessel:	R/V Mirai
	L x B x D 118.02m x 19.0m x 13.2m
	Gross Tonnage: 8,706 tons
	Call Sign JNSR
Title of the cruise:	Arctic Challenge for Sustainability (ArCS)
Undertaking institute:	Japan Agency for Marine-Earth Science and Technology (JAMSTEC)
Chief scientist:	Jun Inoue (National Institute of Polar Research)
Cruise period:	24 October 2018 – 7 December 2018
Ports of call:	24 October 2018, Sekinehama (leave port)
	25 October 2018, Hachinohe (arrival in and leave port)
	7 December 2018, Shimizu (arrival in port)
Research area:	The North Pacific Ocean, the Bering Sea, and the Arctic Ocean

Research Map:

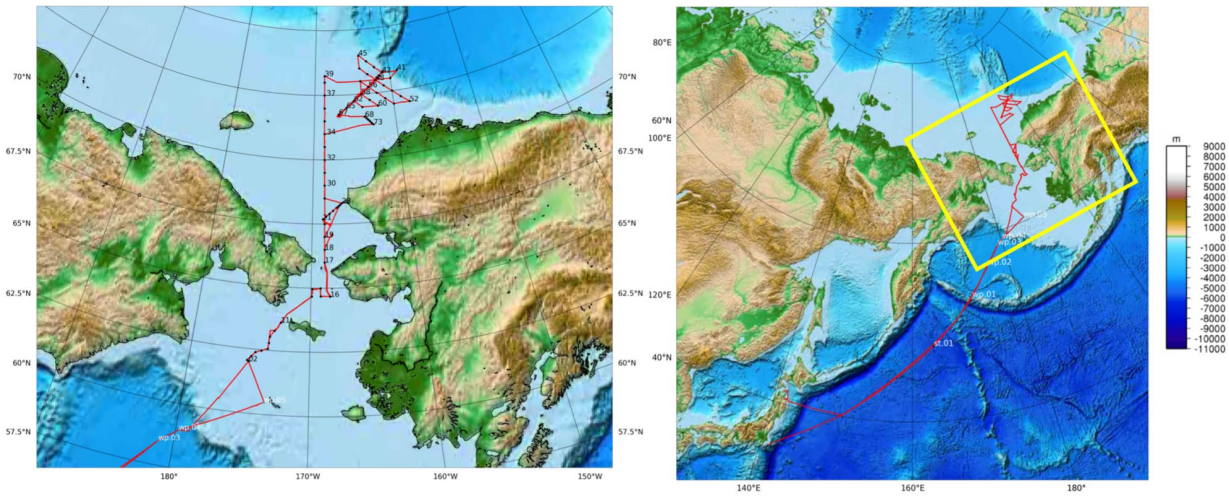

Figure 1.2-1: Cruise track and CTD stations of MR18-05C.

1.3 Atmospheric and Oceanographic Overview during the cruise

Meteorological and oceanographic observations were made in the North Pacific Ocean, the Bering Sea and the Arctic Ocean on board the R/V Mirai from 24 October 2018 to 7 December 2018 as a part of the Arctic Challenge for Sustainability (ArCS) project. Because the sea ice extent during November in the southern Chukchi Sea was low comparing with early 2000's, it is possible to enter the Arctic Ocean by RV Mirai. Based on the AMSR-2 satellite, the sea surface temperature (SST) was abnormally high (> 5℃) at the south of Bering Strait (Figure 1.3-1), suggesting that the delay of freezing in the southern Chukchi Sea was expected due to warm water inflow from the strait.

To understand the ocean structures and its temporal changes at the upstream regions of the Arctic Ocean, we made CTD sections and those revisits at the Distributed Biological Observatory (DBO 1: Sts. 2-11, DBO 2: Sts. 12-16, and Sts.21-28). The structure had been well mixed up to 40-m depth at each section on 2-5 November, and the mixed layers were well developed and cooled up to the bottom except for DBO 1 on 24-26 November. This would be caused by wind forced mixing. Shallow warm water inflow (< 30 m) in the early November as well as deep water inflow (> 40 m) with relatively low temperature in the late November would keep the heat content high in the southern Chukchi Sea.

After wave buoy deployments over the ice-free and ice-covered regions on 6 November (Sts. 40 & 41: Figure

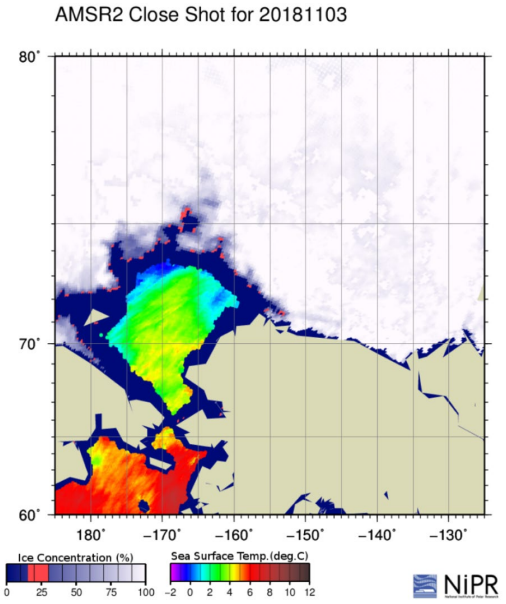

Figure 1.3-1: Ice concentration and sea surface temperature on 3rd November 2018 derived from AMSR-2 sensor.

1.3-2), we made a regional CTD survey to decide the repeat CTD section (Figure 1.3-3). Because a high SST region (> 2℃) was expected between St. 48 (73°N 162°W) and St. 67 (71.75°N 167°W) based on the medium range forecast provided by ECMWF, we set this line as a daily repeat section. This repeat section consists of a station of marginal ice zone (MIZ: Sts. 63, 64, and 66), and Sts. 42, 48, 56, 58, 62, 65, and 67. The position of the station of MIZ varied every day due to sea-ice advance/retreat. A CTD cast was made at each station, and 6-hourly radiosonde observations were conducted. There are three weather regimes (Figure 1.3-4). The first one is a moderate northerly wind condition with low air temperature (around -8℃) from pack ice area (9-13 November). Grease ice and nilas starts to form at the MIZ with small amount of snow fall on it (Figure 1.3-5 left). The second period is a strong warm south-westerly wind condition (around -4℃) (14-16 November). Sea ice was broken into brash ice by attenuated waves from open ocean (Figure 1.3-5 middle). The last period is a strong easterly and north-easterly wind condition from cold pack ice area (< -10℃) (17-21 November). Cloud streets with snow fall were observed by a ship-board Doppler radar due to the strong air mass modification. However, the sea ice was not advected neither formed at the MIZ due to relatively high SST from the freezing point.

Figure 1.3-2: A wave buoy deployment at St. 41 on 6 November 2018.

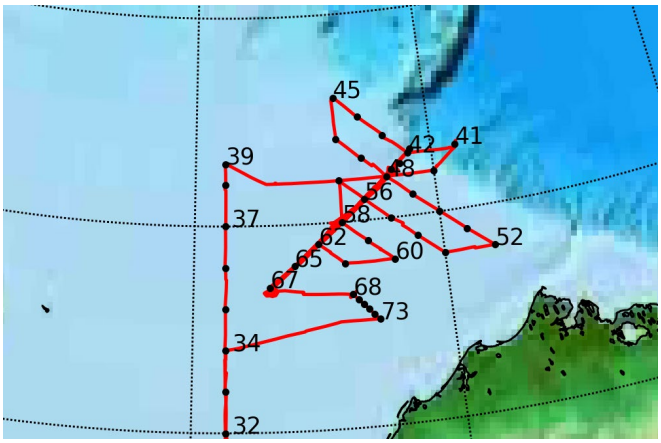

Figure 1.3-3: A map of CTD stations for a regional survey and a repeat section.

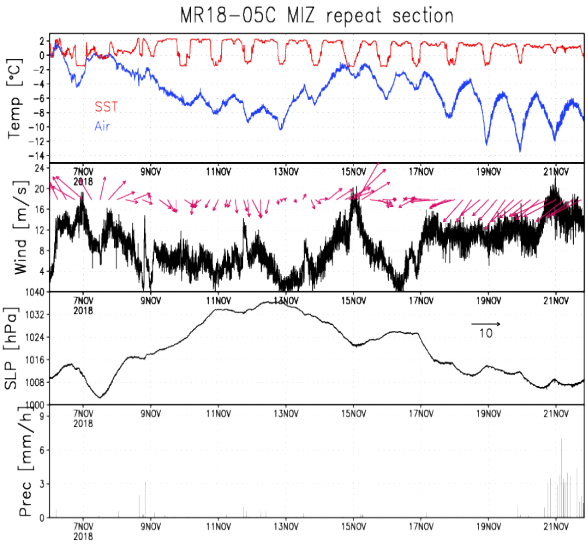

Figure 1.3-4: Time series of surface temperatures of water and air, wind speeds, sea level pressure, and precipitation rate observed by RV Mirai during the repeat section.

Figure 1.3-5: Photos taken at St. 64 on 11 November, at St.64 on 14 November, and St. 48 on 20 November.

The ocean structure at the MIZ during the repeat section was very complicated. The water masses with low temperature/salinity and high dissolved oxygen (DO) and with high temperature/salinity and low DO were periodically observed from surface to 25-m depth partly due to the several passages of eddies along the shelf slope. This periodical warm and saline water inflow into the MIZ would prevent from new ice formation. Both water masses could be identified at DBO 3 section (Sts. 21-28). The Alaskan coastal water with low temperature and high DO was found at DBO 4 (Sts. 68-73), while the Bering Sea water with high temperature and low DO was found at the repeat section (Sts. 48-67). Overall, this repeat section provides unique opportunities to understand the recent delay of freezing during early winter and to evaluate an atmosphere-ice-ocean coupled model.

To achieve this challenging cruise, precise weather and sea-ice forecasts are necessary for safe navigation and valuable observing activities. This cruise was supported by the operational forecasts provided from ECMWF and ECCC as a part of Year of Polar Prediction (YOPP). In addition to this, the Japanese National Institute of Polar Research (NIPR) has developed the Vessel Navigation Unit support System (VENUS) to receive and process the forecast data automatically on the ship. The chief scientist used the real time forecasts to manage the cruise schedule on time scales from a day to a week (Figure 1.3-6). For example, because a closing of Bering Strait by sea ice is critical for this ice-strengthen ship, several parameters (air temperature, winds, sea ice cover, etc) should be considered and compared with both weather centers to decide the final date in the Arctic Ocean. At a daily observation meeting, the captain and the

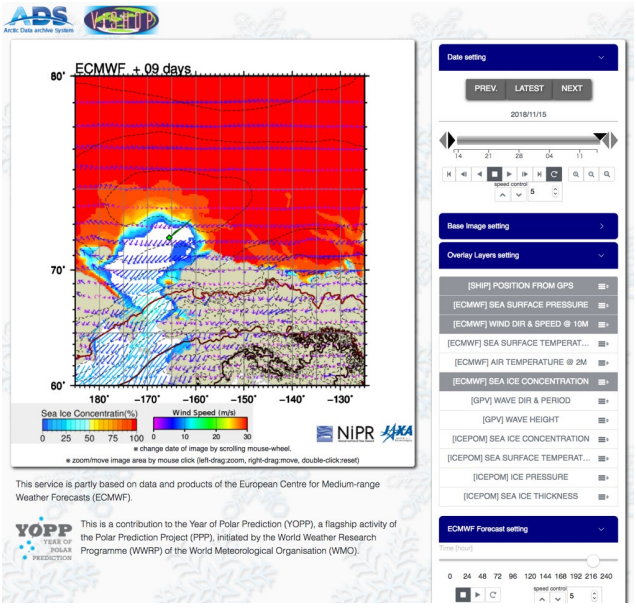

Figure 1.3-6: A screenshot of the VENUS. The forecast products by ECMWF is displayed (ice concentration, SLP, and winds).

ice-pilot learned how high-resolution multiple center forecasts are valuable for them.

1.4 List of participants

Table 1.4-1 List of participants of MR18-05C

No.	Name	Organization	Position
1	Jun Inoue	National Institute of Polar Research	Associate professor
2	Kazutoshi Sato	Kitami Institute of Technology	Project assistant professor
3	Kodai Takebe	Kitami Institute of Technology	Under graduate student
4	Akio Yamagami	University of Tsukuba	Graduate student
5	Takehiko Nose	The University of Tokyo	Project researcher
6	Shuichi Fushimi	The University of Tokyo	Graduate student
7	Fumikazu Taketani	Japan Agency for Marine-Earth Science and Technology (JAMSTEC)	Senior scientist
8	Chunmao Zhu	Japan Agency for Marine-Earth Science and Technology (JAMSTEC)	Scientist
9	Kazuho Yoshida	Nippon Marine Enterprises, Ltd.	Technical staff
10	Souichiro Sueyoshi	Nippon Marine Enterprises, Ltd.	Technical staff
11	Shinya Okumura	Nippon Marine Enterprises, Ltd.	Technical staff
12	Kenichi Katayama	Marine Works Japan Ltd.	Technical staff
13	Shungo Oshitani	Marine Works Japan Ltd.	Technical staff
14	Keisuke Takeda	Marine Works Japan Ltd.	Technical staff
15	Rio Kobayashi	Marine Works Japan Ltd.	Technical staff
16	Yasuhiro Arii	Marine Works Japan Ltd.	Technical staff
17	Keitaro Matsumoto	Marine Works Japan Ltd.	Technical staff
18	Elena Hayashi	Marine Works Japan Ltd.	Technical staff
19	Erii Irie	Marine Works Japan Ltd.	Technical staff
20	Mikio Kitada	Marine Works Japan Ltd.	Technical staff
21	David Snider	Martech Polar Consulting Ltd.	Ice Navigator

2. Meteorology

2.1 GPS Radiosonde

(1) Personnel

Jun Inoue	NIPR	- PI
Kazutoshi Sato	Kitami Institute of Technology (KIT)	
Akio Yamagami	University of Tsukuba	
Kodai Takebe	KIT	
Kazuho Yoshida	Nippon Marine Enterprises Ltd. (NME)	
Soichiro Sueyoshi	NME	
Shinya Okumura	NME	
Hattori Takehito	MIRAI Crew	

(2) Objectives

To understand the thermodynamic structure of the boundary layer, and migratory cyclones and anticyclones, a 6-hourly radiosonde observation was conducted over the Arctic Ocean from 4 November through 24 November 2018 which includes some additional radiosonde observations over the Arctic ocean. The dataset includes 12-hourly initial- and last-observations over the Bering Sea and North Pacific Ocean during 26 October to 3 November 2018 and 25 November to 3 December 2018, respectively. In addition, the GPS radiosonde was launched with the Cloud Particle Sensor (CPS) sonde in the observation at 06 UTC on 28 November 2018 (CPS exp.). Obtained data will be used mainly for studies of clouds, validation of reanalysis data as well as satellite analysis, and data assimilation.

(3) Parameters

Temperature

Humidity

Pressure

Wind speed and direction.

(4) Instruments and Methods

Radiosonde observations were carried out from 26 October to 3 December 2018, by using GPS radiosonde (RS41-SPG). We used software (MW41 Vaisala Sounding System; version 2.11), processor (SPS311), GPS antenna (GA20), UHF antenna (RB21) and balloon launcher (ASAP) made by Vaisala Oyj. Prior to launch, humidity, air temperature, and pressure sensors were calibrated by using the calibrator system (RI41 and PTB330, Vaisala). In case the relative wind to the ship is not appropriate for the launch, the handy launch was selected.

(5) Station List

Table 2.1-1 summarizes the log of upper air soundings. Almost all of data were sent to the world meteorological community by the global telecommunication system (GTS) through the Japan Meteorological Agency immediately after each observation. Raw data was recorded as binary format during ascent. ASCII data was converted from raw data.

(6) Preliminary results

Location of all radiosonde observations during the cruise is shown in Figure 2.1-1. Time-height section of observed air temperature and wind during the cruise are shown in Figure 2.1-2.

On 7-22 November, we carried out radiosonde observation on a daily repeat section. During this period, the radiosonde observation was conducted near the marginal ice zone (MIZ) at 00 UTC, and that was conducted at the furthest point from the MIZ at 18 UTC.

The former period is characterized by southerly wind near the outer rim of low pressure system over the Chukchi Sea. During middle period, GPS radiosonde observation was primarily conducted under a strong northerly wind along the outer rim of the anticyclone over the Chukchi Sea. The latter period is characterized by north-easterly wind under a strong pressure gradient between a high-pressure system over the central Arctic Ocean and a low-pressure system over the Alaska.

During MR18-05C cruise, we used 350g balloons, except for some early observations. Most of observations reached ~20 hPa levels. Although the radiosonde observation did not reach 10 hPa in the previous cruise, the observation at 06UTC on 12 November 2018 reached at 9.11 hPa in this cruise. Also, the observation at 06 UTC on 28 November 2018 (CPS exp.) was reached at 24.2 hPa. This result and Figure 2.1-2 indicate that the observation is consistent with the usual radiosonde observations.

(7) Data Archive

These data obtained in this cruise will be submitted to the Data Management Group of JAMSTEC, and will be opened to the public via “Data Research System for Whole Cruise Information in JAMSTEC (DARWIN)” in JAMSTEC web site. http://www.godac.jamstec.go.jp/darwin/e

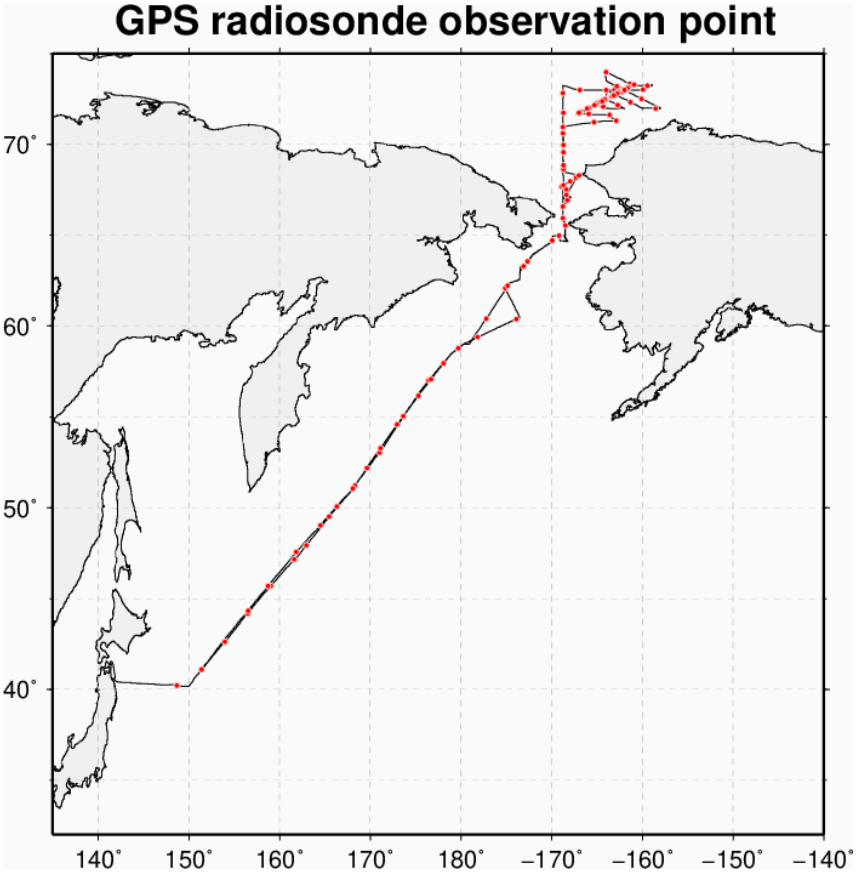

Figure 2.1-1: Sounding stations during the cruise.

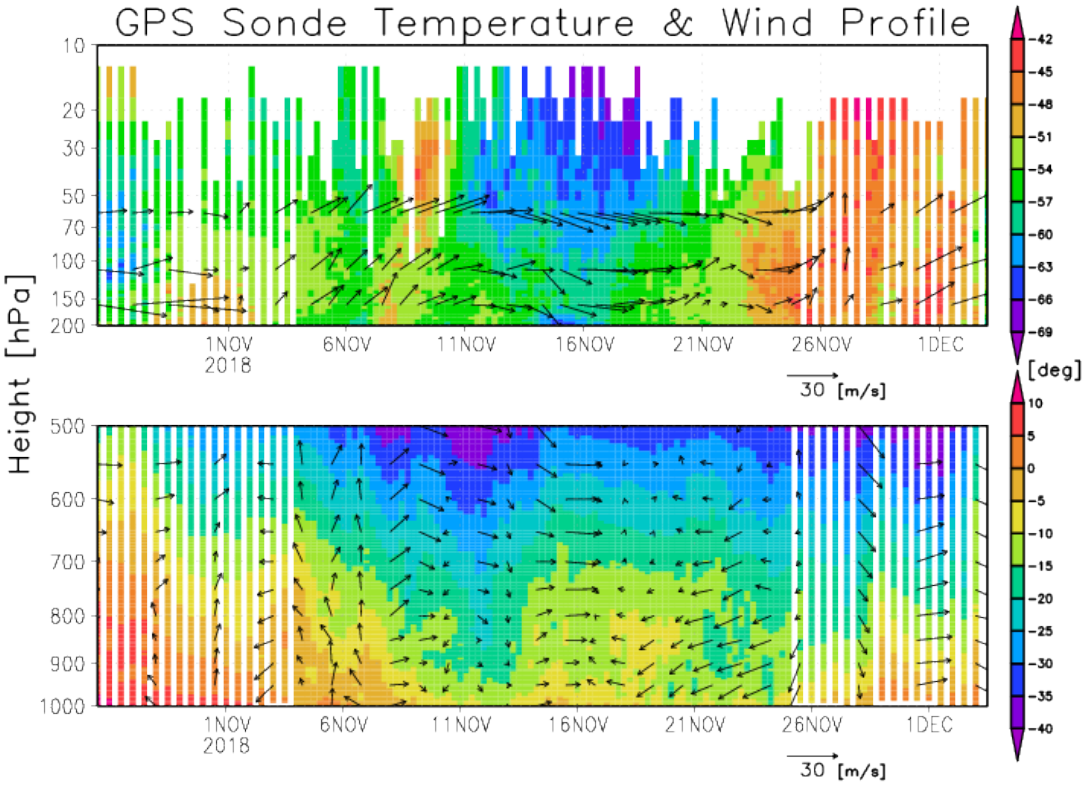

Figure 2.1-2: Time-height section of air temperature (shade) and wind (vectors).

Table 2.1-1: Launch log

ID	Date	Latitude	Longitude	Psfc	Tsfc	RHsfc	WD	Wsp	SST	Max height			Cloud	
	YYYYMM DDHH	degN	degE	hPa	degC	%	deg	m/s	degC	hPa	m	Duration	Amount	Type
RS001	2018102612	40.218	148.687	1020.5	14.3	55	93	5.1	21.20	13.2	29179	6549	1	Cu
RS002	2018102700	41.084	151.417	1020.5	13.9	59	125	6.7	18.66	13.5	29012	6738	5	Cc
RS003	2018102712	42.616	153.957	1017.3	11.2	67	142	10.4	12.70	11.4	30141	6972	8	Cs
RS004	2018102800	44.156	156.466	1014.5	11.4	70	143	12.8	12.73	13.3	29181	5897	10	St
RS005	2018102812	45.675	159.034	1012.7	9.9	77	124	10.6	10.66	23.1	25567	6495	10	St
RS006	2018102900	47.150	161.646	1011.3	8.6	89	127	8.2	9.20	25.4	24967	5852	10	St
RS007	2018102912	47.925	162.955	1009.8	7.6	96	138	6.5	8.05	22.2	25784	6110	9	As
RS008	2018103000	49.497	165.467	1008.5	7.5	90	165	5.3	8.32	16.9	27467	6039	10	St
RS009	2018103012	51.219	168.309	1003.7	7.2	91	185	10.5	8.19	124.4	14608	3491	10	St
RS010	2018103100	53.029	171.009	997.6	6.9	89	173	12.5	7.56	18.4	26825	6061	7	St
RS011	2018103112	55.030	173.657	996.6	6.8	89	163	8.2	7.10	39.1	21940	4565	10	St
RS012	2018110100	57.011	176.457	998.0	6.5	82	164	9.3	6.09	17.7	26976	6049	3	Ac,Ci
RS013	2018110112	58.787	179.711	999.6	5.7	75	102	8.3	6.88	39.2	21870	5107	10	St
RS014	2018110200	60.408	-177.231	997.7	5.7	86	80	12.1	6.28	13.7	28554	6713	10	St
RS015	2018110212	62.110	-175.099	998.1	3.1	81	76	13.3	5.38	18.3	26696	6216	10	Unknown
RS016	2018110300	63.301	-173.069	996.2	3.0	75	44	15.1	5.31	21.7	25593	6221	8	St
RS017	2018110312	64.725	-169.912	995.8	1.5	66	53	10.1	4.36	16.9	27162	6609	0	-
RS018	2018110400	65.554	-168.496	998.3	-1.5	74	70	2.8	4.51	18.0	26775	6087	3	Ci,St
RS019	2018110406	66.601	-168.749	999.9	-0.3	67	105	8.5	4.56	52.8	19939	4832	4	Unknown
RS020	2018110412	67.671	-168.918	1002.4	0.5	72	138	8.6	2.68	30.1	23493	5657	2	Sc
RS021	2018110418	68.188	-167.313	1003.8	-0.3	72	147	10.2	3.71	23.1	25162	5724	10	St
RS022	2018110500	68.646	-168.716	1003.5	1.5	83	153	12.3	3.75	39.0	21831	5830	10	St
RS023	2018110506	69.575	-168.729	1003.1	1.9	90	150	13.8	4.21	52.1	19948	6430	10	Unknown
RS024	2018110512	70.635	-168.747	1004.5	1.8	67	191	15.8	3.02	24.9	24599	6254	10	Unknown
RS025	2018110518	71.747	-168.718	1005.5	1.1	87	170	9.1	2.91	12.0	29179	6714	3	St
RS026	2018110600	72.852	-168.735	1007.0	-0.2	94	212	6.7	1.20	11.9	29167	6836	8	Sc,St
RS027	2018110606	73.000	-166.881	1009.0	1.1	95	157	10.5	2.18	10.7	29865	6903	10	Unknown
RS028	2018110612	73.000	-163.084	1011.6	-1.1	87	137	12.2	0.07	36.5	22108	4812	10	Unknown
RS029	2018110618	73.027	-159.915	1011.4	-3.0	90	112	13.1	1.11	13.5	28394	6513	9	Unknown
RS030	2018110702	73.238	-159.453	1006.9	-2.0	91	124	12.5	-1.24	104.7	15451	3551	10	St
RS031	2018110706	73.351	-161.380	1003.1	-0.7	95	153	10.5	0.43	13.4	28542	5893	7	Unknown

RS032	2018110712	73.999	-164.000	1000.3	-0.2	98	199	11.2	-0.33	15.2	27747	6718	10	St
RS033	2018110718	73.207	-162.811	1003.4	-0.3	75	231	12.6	-0.30	27.2	22747	5510	10	St
RS034	2018110800	72.532	-160.104	1008.6	-1.4	84	236	13.4	-0.06	25.6	24544	6210	10	St
RS035	2018110806	71.998	-158.531	1013.1	-2.3	67	302	7.8	0.59	26.2	24448	5151	10	Unknown
RS036	2018110812	72.343	-161.349	1014.6	-2.3	62	276	8.9	0.80	58.4	19204	4510	10	St
RS037	2018110818	72.998	-163.991	1014.2	-3.4	81	300	5.8	-0.04	99.5	15696	3885	10	St
RS038	2018110900	72.178	-162.712	1015.7	-2.8	89	227	1.7	0.51	17.8	26982	6293	9	Sc
RS039	2018110906	72.091	-164.344	1017.0	-4.3	61	321	8.5	2.02	18.9	26594	6154	6	Sc
RS040	2018110912	72.736	-162.977	1017.7	-5.2	67	324	7.2	2.29	15.8	27669	6533	0	-
RS041	2018110918	72.751	-163.021	1019.1	-5.8	66	357	5.6	2.27	16.8	27233	6167	10	Sc?
RS042	2018111000	73.297	-160.923	1020.8	-6.7	66	318	9.0	-1.45	77.2	17262	4468	10	Sc
RS043	2018111006	72.746	-162.990	1023.6	-6.6	70	33	6.9	2.22	18.0	26654	6409	10	Sc
RS044	2018111009	72.501	-163.996	1025.2	-6.1	67	21	2.3	2.14	20.4	25821	5942	10	Sc
RS045	2018111012	72.251	-164.994	1026.0	-5.4	62	56	5.8	1.93	27.4	23883	5995	10	Sc
RS046	2018111018	72.768	-162.965	1029.0	-6.7	68	38	6.4	2.22	11.5	29316	7187	10	Sc
RS047	2018111100	73.155	-161.504	1031.2	-8.3	67	25	6.7	-1.41	12.6	28642	6657	10	Sc
RS048	2018111006	72.766	-162.953	1031.4	-6.6	65	18	4.9	2.16	21.2	25345	5813	10	Sc
RS049	2018111009	72.500	-163.993	1031.1	-6.1	55	40	4.9	2.24	38.4	21667	4997	10	Sc
RS050	2018111112	72.251	-164.997	1030.7	-5.7	59	339	6.2	1.55	12.8	28554	6808	10	Sc
RS051	2018111118	72.756	-163.028	1030.3	-6.6	52	336	6.8	0.60	15.7	27177	6606	10	Sc
RS052	2018111121	73.092	-161.627	1031.0	-9.3	83	6	8.2	-1.15	12.6	28495	6804	10	Sc
RS053	2018111200	72.951	-162.199	1031.3	-8.3	61	1	5.8	-0.44	27.2	23728	5669	8	Sc
RS054	2018111206	72.298	-164.809	1033.0	-7.4	79	4	9.9	2.01	9.1	30640	7169	10	Sc
RS055	2018111212	72.251	-165.001	1033.9	-7.8	65	6	6.7	1.98	11.9	28918	6326	10	Sc
RS056	2018111218	72.753	-162.990	1033.8	-8.9	69	337	4.4	1.79	13.0	28311	6946	10	Sc
RS057	2018111221	73.071	-161.795	1034.3	-10.4	67	122	2.2	-1.20	14.1	27772	6183	6	Sc
RS058	2018111300	72.944	-162.214	1033.2	-8.8	64	343	0.8	-0.73	29.0	23359	5603	8	Sc
RS059	2018111306	72.277	-164.877	1032.3	-6.1	62	307	2.7	2.06	21.7	25216	5817	10	Sc
RS060	2018111312	72.243	-164.992	1030.7	-5.2	67	248	3.1	1.96	13.3	28201	6378	10	Sc
RS061	2018111318	72.751	-163.017	1029.6	-6.0	66	333	5.0	0.34	14.6	27582	6239	10	Sc
RS062	2018111321	73.048	-161.795	1028.9	-7.0	76	327	1.5	-1.38	20.8	25404	6082	10	Sc
RS063	2018111400	72.998	-162.003	1028.0	-5.7	72	262	5.4	-0.85	14.6	27599	6264	10	Sc
RS064	2018111406	72.330	-164.679	1026.8	-4.3	70	240	7.9	1.88	14.8	27564	6333	10	Sc
RS065	2018111412	72.248	-164.971	1024.8	-2.6	69	252	11.5	1.82	12.9	28388	6442	10	Sc
RS066	2018111418	72.744	-162.986	1021.6	-1.6	69	249	11.8	0.30	11.3	29073	7131	10	Sc
RS067	2018111421	73.056	-161.752	1020.3	-1.9	75	249	10.5	-1.55	11.3	29073	7131	10	Sc

RS068	2018111500	73.096	-161.615	1018.6	-2.7	82	236	16.9	-1.57	19.6	25683	5209	10	St
RS069	2018111503	72.898	-162.370	1018.9	-2.9	86	207	17.3	0.05	26.8	23826	5408	10	Unknown
RS070	2018111506	72.647	-163.377	1019.3	-1.6	80	229	13.5	1.41	14.3	27642	6625	10	Sc
RS071	2018111512	72.025	-165.893	1020.7	-1.8	66	279	9.8	1.44	11.8	28872	6665	10	Sc
RS072	2018111518	72.730	-163.026	1020.8	-4.3	67	317	5.9	-0.18	29.3	23247	5681	10	Sc
RS073	2018111521	73.050	-161.850	1021.6	-5.1	66	275	7.0	-1.47	22.4	24872	5879	3	Sc
RS074	2018111600	73.001	-161.992	1022.6	-6.3	78	344	4.0	-1.45	13.5	27947	6550	3	Sc,Cu
RS075	2018111606	72.384	-164.456	1023.5	-3.3	68	89	2.6	1.91	13.4	28062	6255	10	Sc
RS076	2018111612	72.253	-165.044	1023.2	-2.5	60	244	0.5	1.72	19.3	25837	6213	10	Sc
RS077	2018111618	72.753	-163.022	1022.5	-4.0	73	63	9.6	0.97	13.2	28073	6600	10	Sc
RS078	2018111621	73.001	-162.087	1023.0	-4.8	63	90	2.6	-1.55	15.2	27209	6286	10	Sc
RS079	2018111700	72.808	-162.759	1021.2	-4.0	67	89	7.2	1.11	18.3	26132	6155	10	Sc
RS080	2018111706	72.178	-165.299	1016.1	-3.2	82	106	10.6	1.43	21.9	25092	6268	10	Sc
RS081	2018111712	71.988	-166.067	1013.5	-5.1	77	88	12.5	1.30	23.3	24741	5919	10	St
RS082	2018111718	72.712	-163.171	1012.6	-8.0	88	76	8.8	0.92	18.0	26231	6029	10	Sc
RS083	2018111721	73.048	-161.845	1012.4	-8.5	87	81	12.2	-0.96	19.9	25633	6069	2	Sc
RS084	2018111800	73.054	-161.850	1011.5	-7.2	85	74	12.6	-1.37	18.6	26053	5906	2	Sc
RS085	2018111806	72.429	-164.266	1009.0	-4.7	74	54	11.8	1.76	13.3	28118	6574	3	Sc
RS086	2018111812	71.751	-167.003	1008.2	-3.6	75	48	11.5	1.41	37.8	21875	4891	6	St
RS087	2018111818	72.454	-164.205	1009.2	-6.2	76	70	13.3	1.74	19.4	25919	6165	2	St
RS088	2018111900	73.099	-161.646	1011.1	-11.7	92	56	12.6	-1.35	31.4	22970	5661	4	Sc
RS089	2018111906	72.479	-164.067	1010.3	-6.4	81	59	11.4	1.62	34.4	22450	5210	6	Sc
RS090	2018111912	71.771	-166.917	1009.3	-5.4	80	41	14.6	1.19	26.1	24194	5688	6	St
RS091	2018111918	72.416	-164.385	1008.6	-8.9	87	69	12.5	1.60	18.6	26227	5943	10	Sc
RS092	2018112000	73.019	-162.003	1008.8	-12.4	88	49	15.0	-1.05	18.1	26394	6192	10	Sc
RS093	2018112006	72.350	-164.603	1005.5	-7.1	81	73	12.1	1.36	39.9	21541	5272	10	Sc
RS094	2018112012	71.793	-166.861	1004.1	-5.7	86	59	13.6	1.21	28.4	23710	5418	10	Sc
RS095	2018112018	72.488	-164.143	1004.4	-8.6	87	73	16.1	1.49	22.4	25129	5595	10	Sc
RS096	2018112100	73.004	-161.986	1006.2	-11.3	86	57	17.9	0.29	59.8	18949	3404	10	Sc
RS097	2018112106	72.391	-164.426	1004.8	-8.6	85	58	15.1	1.18	36.2	22172	5192	10	Sc
RS098	2018112112	71.749	-167.000	1004.9	-6.8	75	65	14.9	1.09	16.0	27312	6217	10	Sc
RS099	2018112118	71.690	-165.943	1005.6	-8.1	87	71	14.3	0.99	50.8	20044	4642	10	Sc
RS100	2018112200	71.648	-163.655	1008.1	-8.9	82	76	14.7	-0.86	34.0	22623	5383	10	Sc
RS101	2018112206	71.322	-162.898	1009.6	-9.8	77	68	14.2	-0.76	41.1	21410	4388	10	Sc
RS102	2018112212	71.233	-165.346	1013.1	-8.9	85	70	16.0	0.94	41.5	21403	4919	10	Sc
RS103	2018112218	70.984	-168.748	1015.1	-6.9	79	76	16.7	1.01	33.6	22789	5237	10	Sc

RS104	2018112300	69.994	-168.725	1014.6	-5.3	63	72	15.1	1.88	26.7	24302	4957	10	Sc
RS105	2018112306	68.852	-168.721	1013.1	-6.9	80	67	17.8	1.73	26.1	24524	5939	10	Sc
RS106	2018112312	67.760	-168.712	1010.4	-7.3	75	57	15.5	2.05	21.0	25930	6085	6	Sc
RS107	2018112318	67.522	-168.402	1009.9	-7.9	73	39	17.8	2.20	31.7	23323	5379	7	Sc
RS108	2018112400	67.980	-167.964	1011.1	-10.3	70	38	20.3	1.85	22.8	25392	5606	3	Sc
RS109	2018112406	68.290	-166.996	1009.7	-12.8	70	62	17.4	1.08	17.9	26922	6217	1	Sc
RS110	2018112412	67.240	-168.405	1005.2	-7.8	72	44	12.9	1.82	47.7	20666	5189	8	Sc
RS111	2018112418	66.923	-168.279	1001.8	-6.7	78	50	12.2	2.43	47.2	20713	5422	10	Sc
RS112	2018112500	65.946	-168.735	997.4	-6.8	80	59	14.9	2.73	39.9	21835	5140	5	Sc
RS113	2018112512	64.988	-169.180	992.5	-5.9	77	28	13.8	2.76	21.3	25901	6496	4	Sc
RS114	2018112600	63.566	-172.645	993.0	-5.2	78	10	18.8	2.54	23.3	25370	6366	10	Sc
RS115	2018112612	62.218	-174.874	993.2	-3.8	56	14	7.8	2.98	18.3	27014	6094	10	Unknown
RS116	2018112700	60.391	-173.907	991.8	-2.5	63	326	15.9	4.02	18.0	27157	6111	9	Sc
RS117	2018112712	59.385	-178.151	1000.8	-3.1	68	352	11.1	4.52	18.3	27063	6640	4	Cu
RS118	2018112800	57.952	178.078	1002.3	-2.4	50	0	9.2	4.29	14.5	28672	6786	6	Sc,Cu
CPS exp. *1	2018112806	57.060	176.693	1006.6	-2.0	52	317	6.8	4.01	24.2	25229	6321	4	Sc
RS119	2018112812	56.170	175.311	1008.8	-0.8	49	185	3.8	4.73	14.0	28941	6819	2	Cu
RS120	2018112900	54.586	172.981	987.1	4.6	67	262	12.0	5.77	14.0	28905	6651	3	Ac,Sc,Cu
RS121	2018112912	53.264	171.118	986.8	4.0	71	238	11.5	5.75	18.6	26927	5541	6	Unknown
RS122	2018113000	52.183	169.623	986.3	2.9	58	240	16.7	5.67	20.1	26345	6280	4	Sc,Cu
RS123	2018113012	51.045	168.077	986.7	0.2	82	245	10.2	5.83	20.2	26343	6019	0	-
RS124	2018120100	50.075	166.328	990.8	2.3	60	263	9.7	5.81	19.5	26527	6048	4	Sc,Cu
RS125	2018120112	49.039	164.530	1004.6	1.1	64	270	11.5	4.84	48.2	20554	4540	5	Unknown
RS126	2018120200	47.551	161.856	1004.5	3.0	53	178	3.8	7.01	17.2	27346	6348	9	As,Sc,Cu
RS127	2018120212	45.693	158.7	1012.8	0.0	70	313	13.2	6.7	13.88	28723	6540	7	Unknown
RS128	2018120300	44.334	156.6	1017.4	5.1	82	290	12.4	7.0	14.39	28513	6404	8	Cu

*1 GPS radiosonde launched with the CPS sonde

2.2 CPS sonde

(1) Personnel

Jun Inoue	NIPR	- PI
Kazutoshi Sato	KIT	
Akio Yamagami	University of Tsukuba	
Kodai Takebe	KIT	
Kazuho Yoshida	NME	
Soichiro Sueyoshi	NME	
Shinya Okumura	NME	
Hattori Takehito	MIRAI Crew	

(2) Objectives

To understand the vertical profiles of Arctic clouds, we conducted Cloud Particle Sensor (CPS) sonde observations over the Arctic Ocean and Bering Sea. The CPS sonde, which is developed by Japanese Meisei Electric Co., Ltd. (Meisei), measures vertical distributions of cloud particles (number of density, size and the phase (water cloud or ice cloud)) in addition to the meteorological elements (Temperature, Relative Humidity, Height, Wind direction and Wind speed). This is a first trial of cloud particles observation over the Arctic Ocean on R/V Mirai.

(3) Parameters

Cloud particles (number of density, Particle size and Output signal voltage)
Wind speed and direction
Pressure
Temperature
Relative Humidity

(4) Instruments and methods

Twelve (12) CPSs were launched during 01 and 28 November 2018 only when we identified cloud covered by the satellite cloud images or radar echo by the C-band Weather Radar. The CPS sonde consists of CPS sonde and GPS radiosonde transmitter (RS-11G, Meisei). The CPS sonde was connected with 350g balloon (Totex TA-350) and parachute. We used MEISEI standard GPS sonde ground system (RD-08AC), software (MGPS-R) and 400MHz antenna.

(5) Station list or Observation log

See Table 2.2-1 “CPS sonde launch log with surface observation and maximum sounding height”.

(6) Preliminary results

Figure 2.2-1 shows Mirai tracks during MR18-05C and CPS sonde points over the Arctic Ocean. Figures 2.2-2 to 2.2-25 show NOAA Ch.4 and radar reflectivity (ZH) images at the time close to CPS observations (No.01-12), vertical profiles of temperature and relative humidity obtained by RS-11G GPS radiosonde, and number of particle, degree of polarization and P output obtained by CPS sonde. We successfully observed 22 clouds including low, middle and high clouds.

(7) Data archive

These data obtained in this cruise will be submitted to the Data Management Group of JAMSTEC, and will be opened to the public via "Data Research System for Whole Cruise Information in JAMSTEC (DARWIN)" in JAMSTEC web site. <http://www.godac.jamstec.go.jp/darwin/e>

(8) Remarks

To confirm a difference between Meisei GPS radiosonde and Vaisala GPS radiosonde, we launched Meisei RS-11G GPS radiosonde and CPS sonde with Vaisala GPS radiosonde (RS41-SPG) at 06UTC 28 November ("CPS exp." in table 2.1-1).

Table 2.2-1: CPS sonde launch log with surface observation and maximum sounding height.

No.	Date (YYYY/MMDD)	Lat (degN) Lon	Psfc (hPa)	Tsfc (℃)	RHsfc (%)	WDsfc (deg)	Max Alt (m)
01	2018/1101 14:00	59.00614 179.32788	998.4	5.1	84	94 9.4	1282
02	2018/1105 00:29	68.80009 168.72383	1003.1	1.5	82	153 12.1	23701
03	2018/1107 05:59	73.46884 161.93007	1002.9	-0.4	92	154 10.7	21893
04	2018/1112 11:59	72.24722 164.98750	1033.9	-8.7	58	27 5.3	25861
05	2018/1113 12:04	72.25264 164.98283	1031.2	-5.1	75	259 5.0	15866
06	2018/1114 14:19	72.49088 164.41503	1023.5	-2.0	69	224 11.6	15822
07	20181116 12:00	72.25213 165.00309	1023.1	-2.5	59	200 3.5	16116
08	20181119 02:40	72.75639 163.00433	1011	-8.2	84	59 12.0	22961
09	20181120 01:36	72.75522 163.00178	1007	-10.1	85	70 11.2	22102
10	20181120 06:09	72.25287 165.04153	1005.3	-7.2	80	41 13.7	18972
11	20181120 10:30	71.75251 167.00821	1003.8	-5.2	79	54 12.0	22138
12	20181128 05:30	56.9867 -176.60233	1006.6	-2.0	52	317 6.8	25250

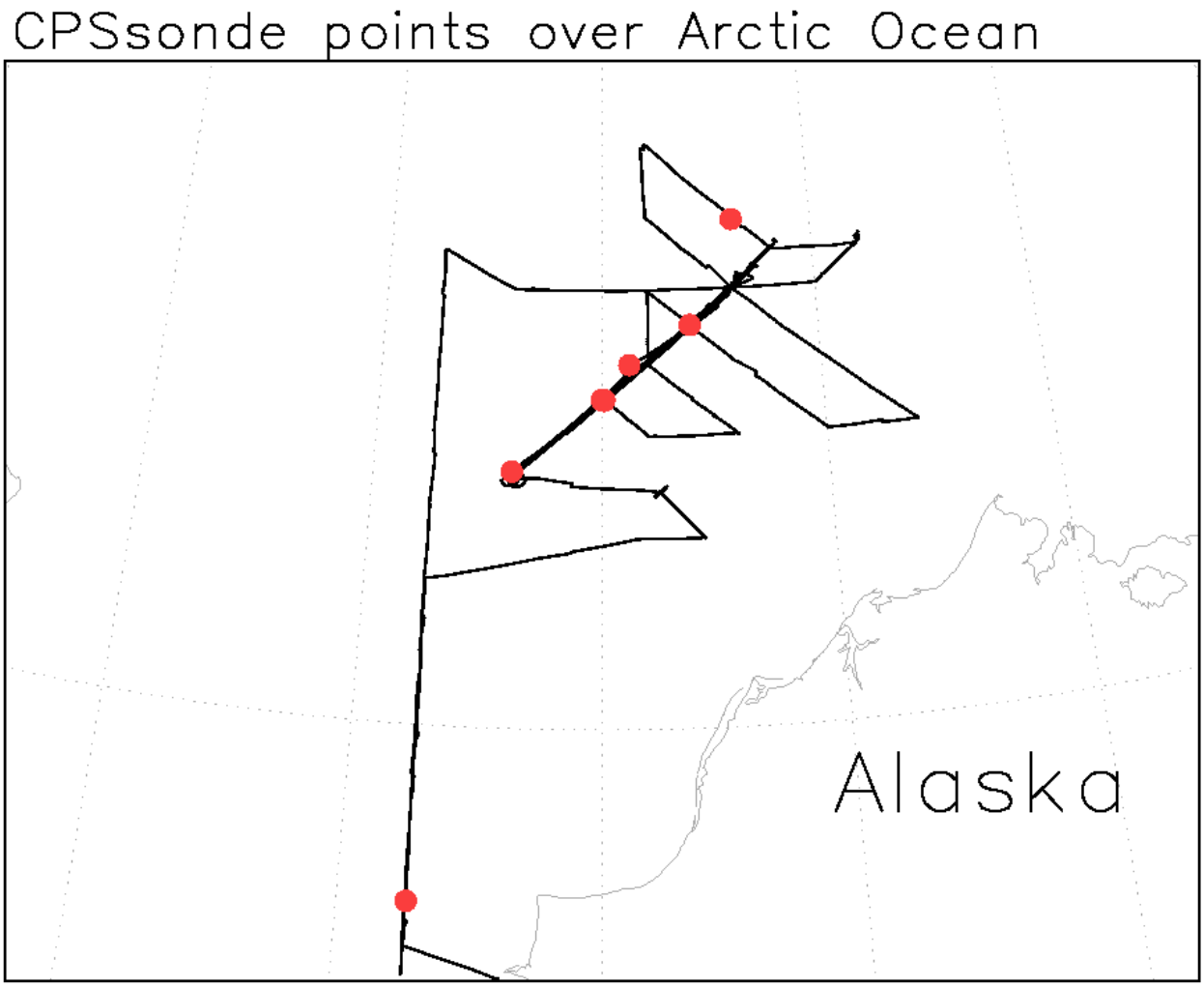

Figure 2.2-1: Mirai track (black line) and CPS sonde points (red dots) over the Arctic Ocean during No.2 and No.11.

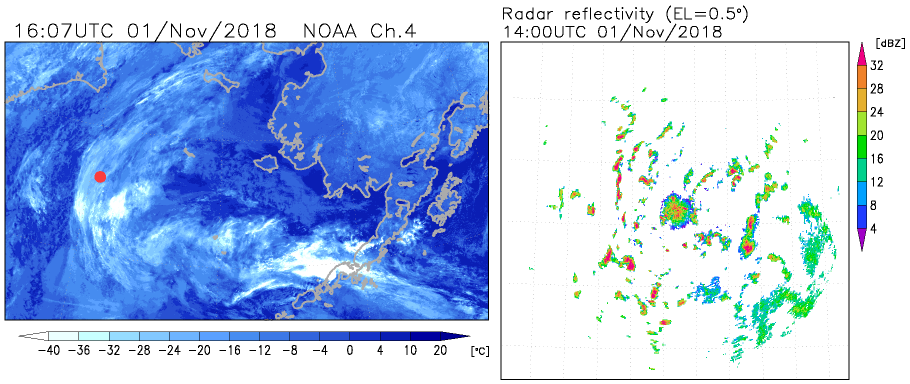

Figure 2.2-2: (a) NOAA satellite image with Mirai position, (b) PPI image obtained by the first volume scan at elevation angle of 0.5 degree for No.1 launch (01 November).

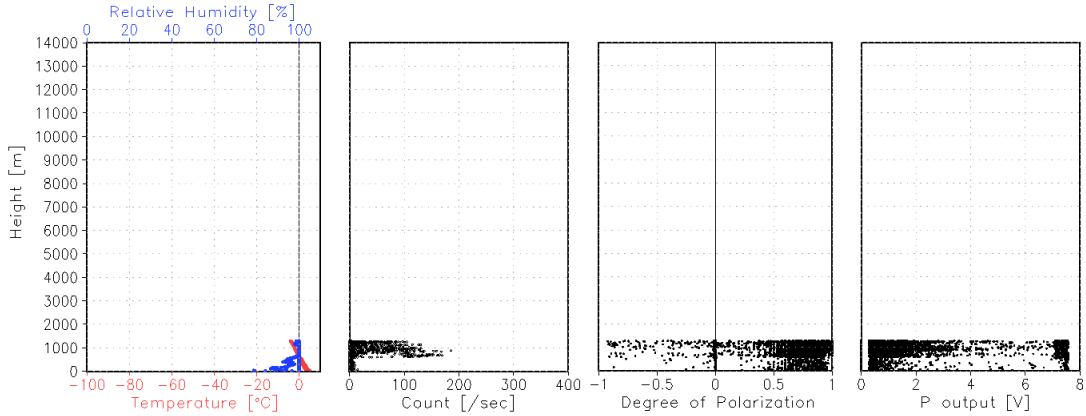

Figure 2.2-3: Vertical profiles of Temperature (red) and Humidity (blue) obtained by RS-11G radiosonde, and number of particle, degree of polarization and P output obtained by CPS sonde for No.1 launch (01 November).

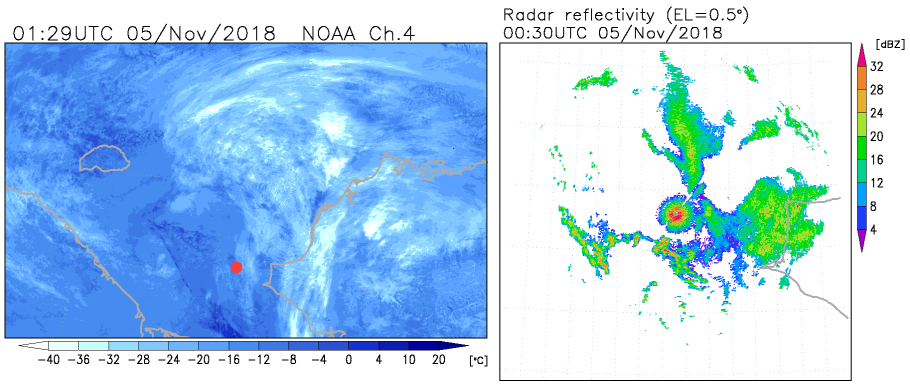

Figure 2.2-4: Same as in Figure 2.2-2, but for No.2 launch (05 November).

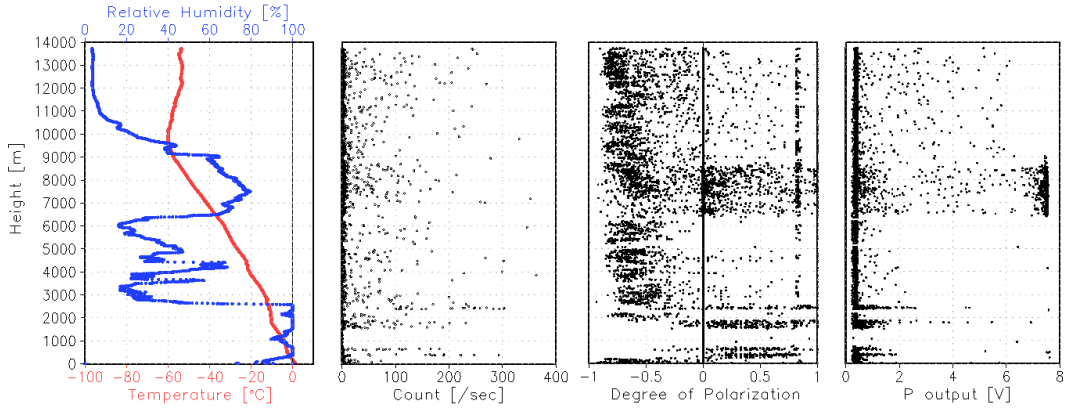

Figure 2.2-5: Same as in Figure 2.2-3, but for No.2 launch (05 November).

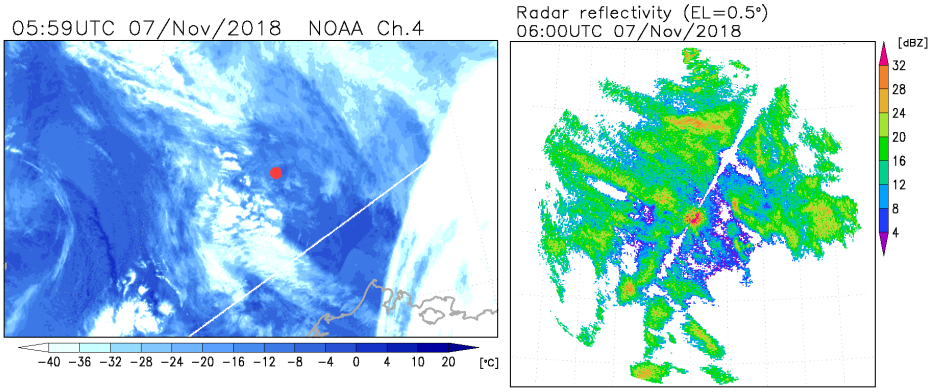

Figure 2.2-6: Same as in Figure 2.2-2, but for No.3 launch (07 November).

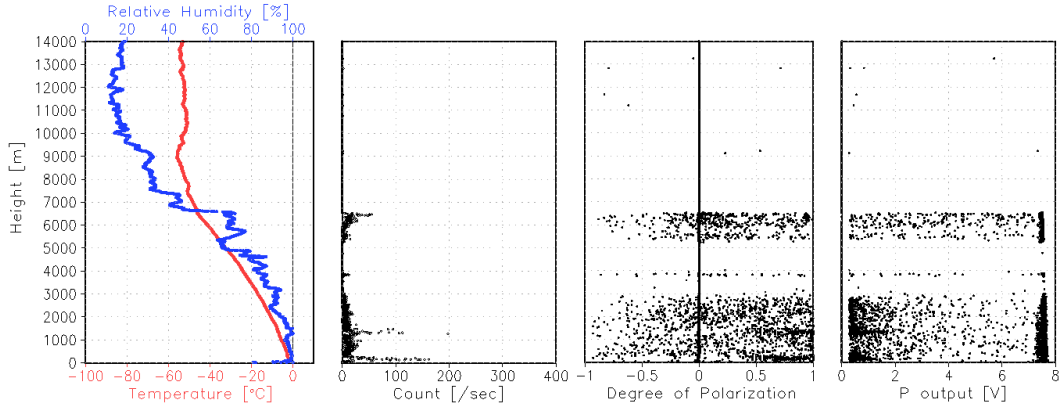

Figure 2.2-7: Same as in Figure 2.2-3, but for No.3 launch (07 November).

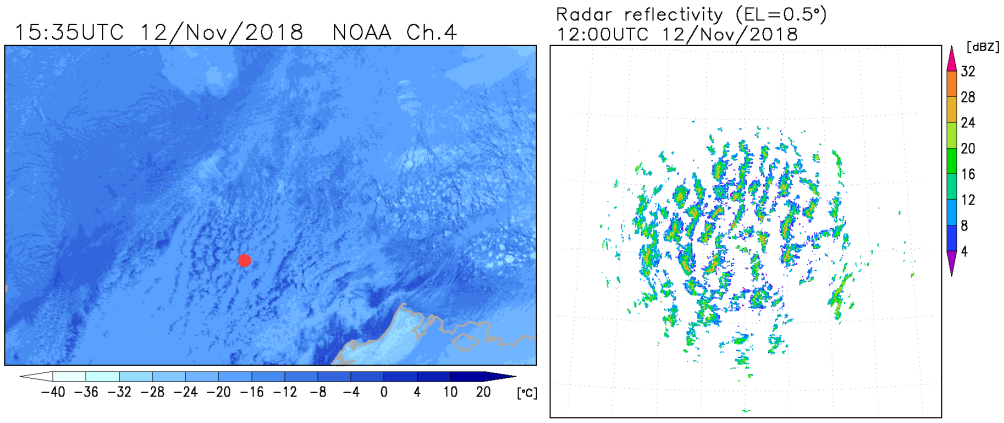

Figure 2.2-8: Same as in Figure 2.2-2, but for No.4 launch (12 November).

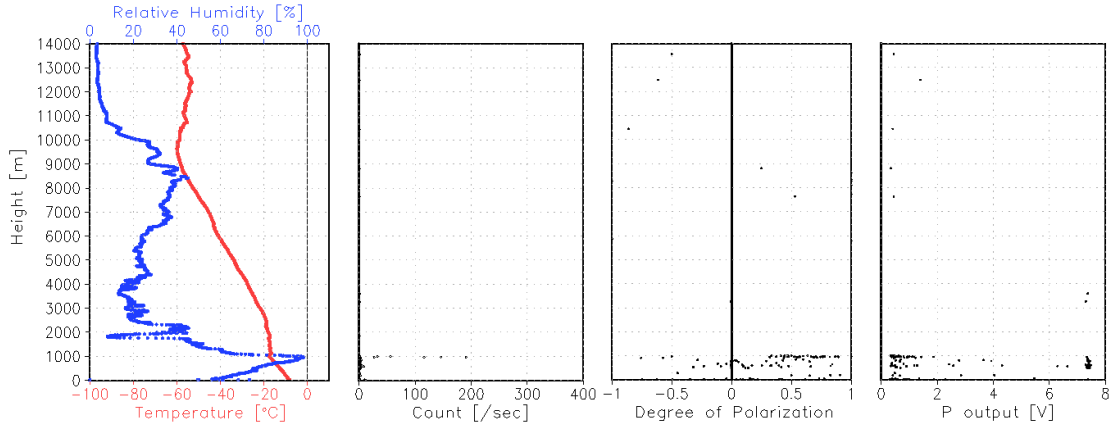

Figure 2.2-9: Same as in Figure 2.2-3, but for No.4 launch (12 November).

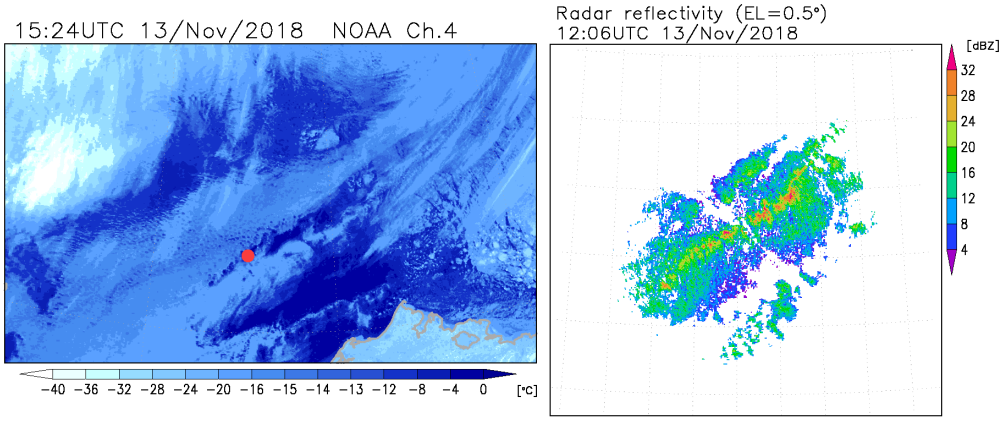

Figure 2.2-10: Same as in Figure 2.2-2, but for No.5 launch (13 November).

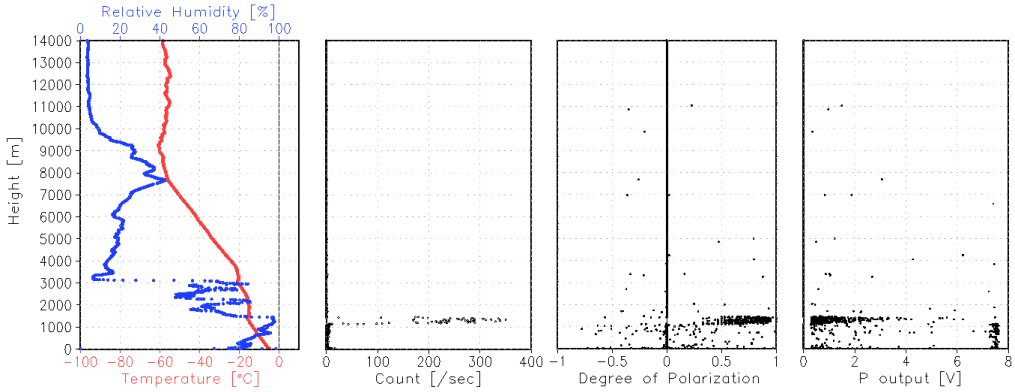

Figure 2.2-11: Same as in Figure 2.2-3, but for No.5 launch (13 November).

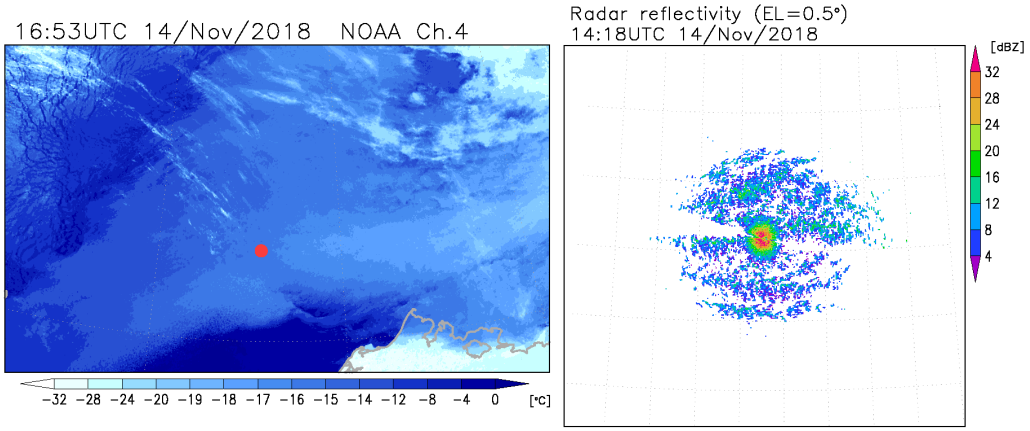

Figure 2.2-12: Same as in Figure 2.2-2, but for No.6 launch (14 November).

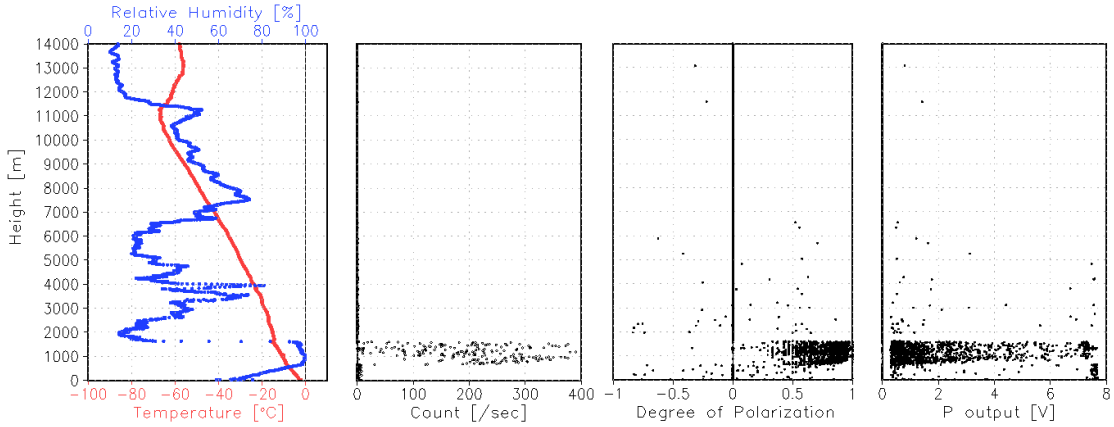

Figure 2.2-13: Same as in Figure 2.2-3, but for No.6 launch (14 November).

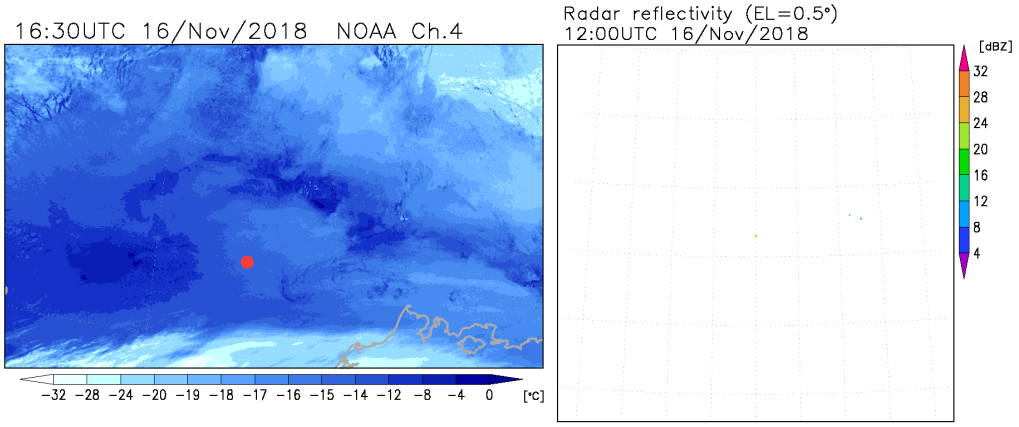

Figure 2.2-14: Same as in Figure 2.2-2, but for No.7 launch (16 November).

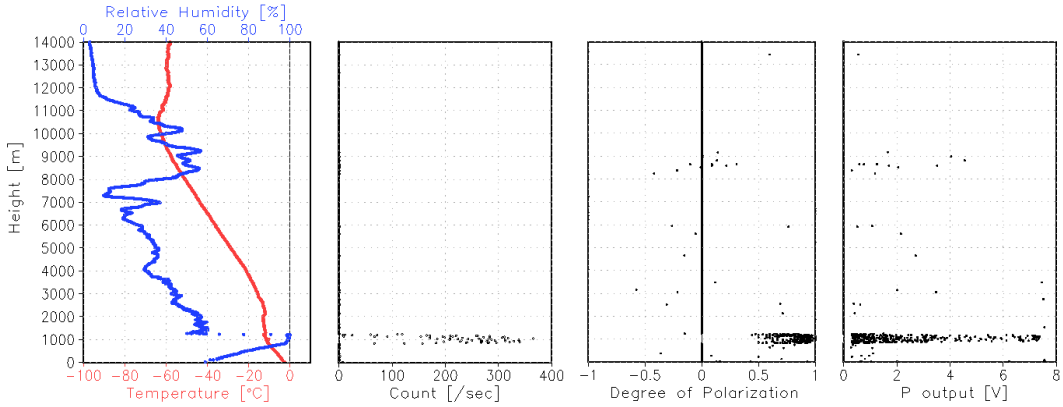

Figure 2.2-15: Same as in Figure 2.2-3, but for No.7 launch (16 November).

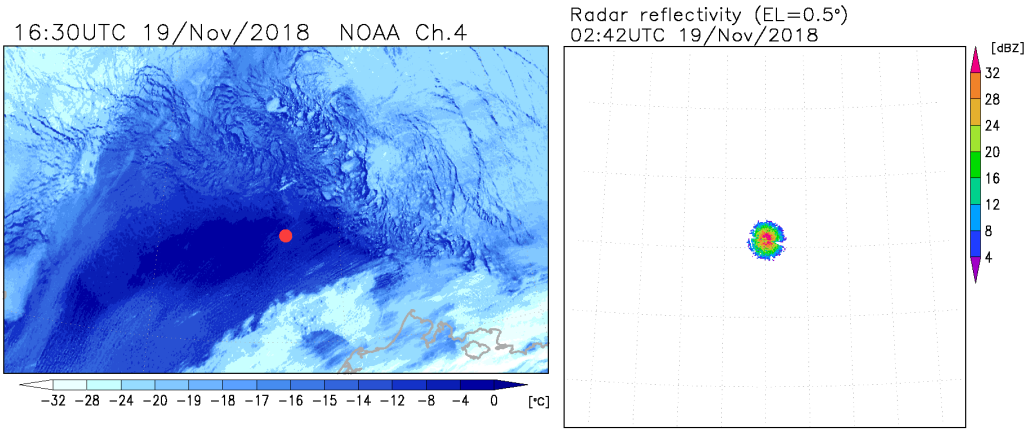

Figure 2.2-16: Same as in Figure 2.2-2, but for No.8 launch (19 November).

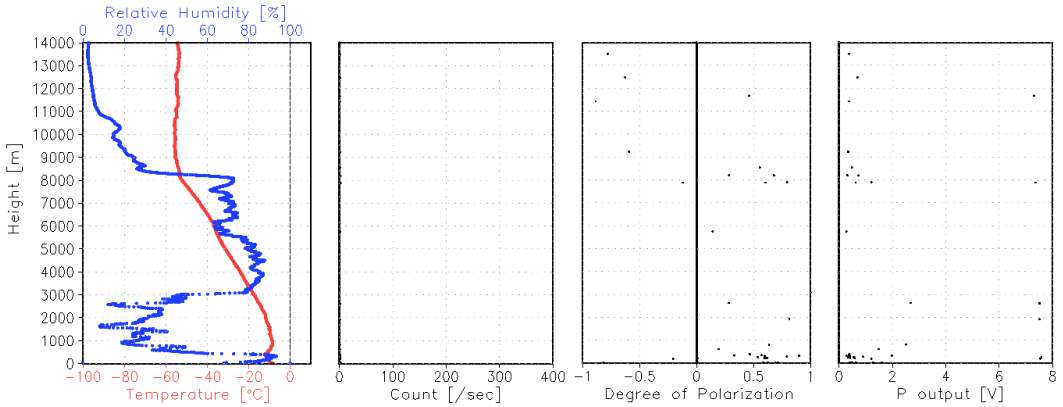

Figure 2.2-17: Same as in Figure 2.2-3, but for No.8 launch (19 November).

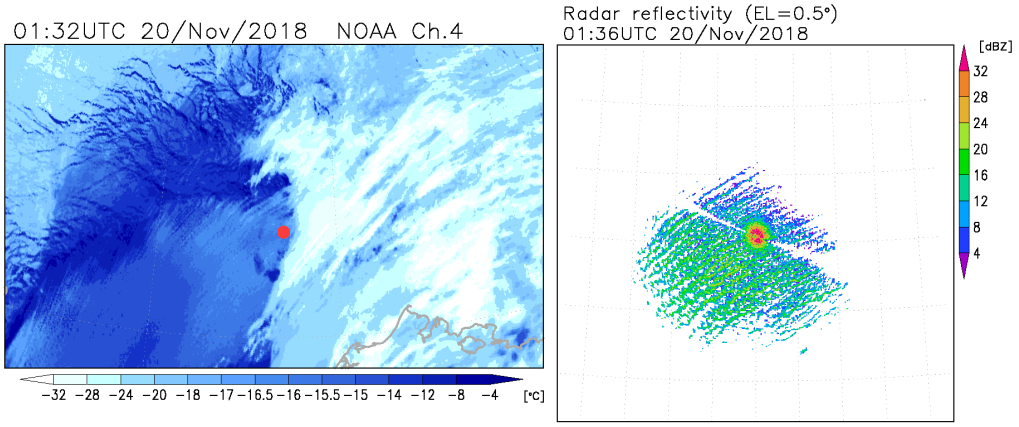

Figure 2.2-18: Same as in Figure 2.2-2, but for No.9 launch (20 November).

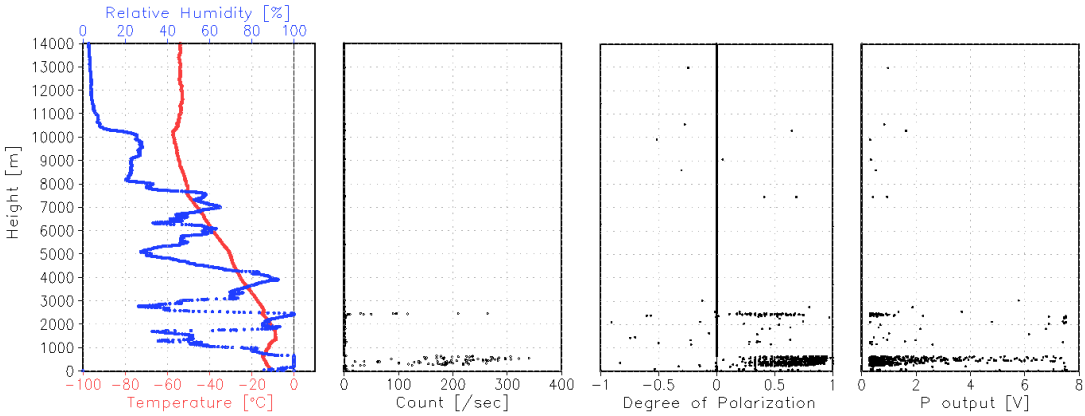

Figure 2.2-19: Same as in Figure 2.2-3, but for No.9 launch (20 November).

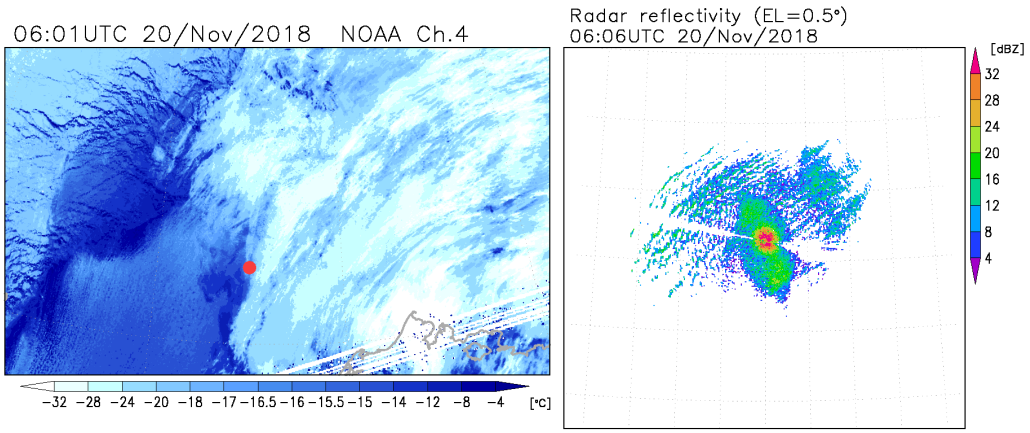

Figure 2.2-20: Same as in Figure 2.2-2, but for No.10 launch (20 November).

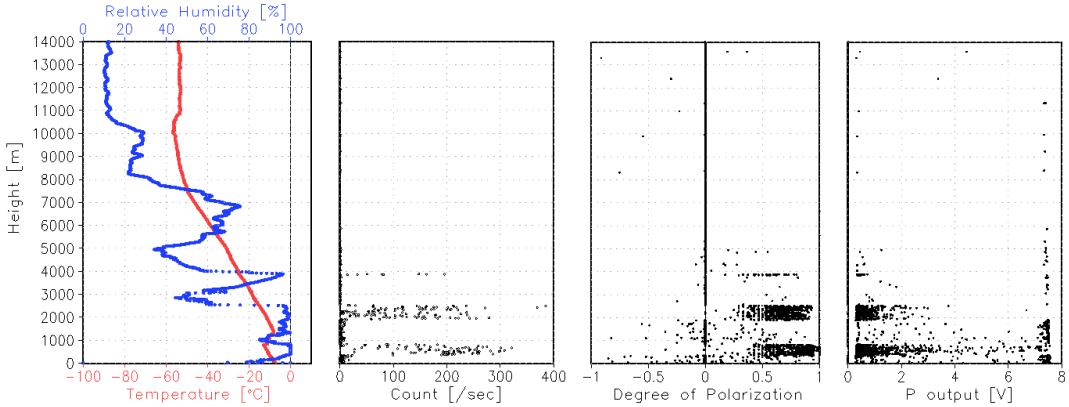

Figure 2.2-21: Same as in Figure 2.2-3, but for No.10 launch (20 November).

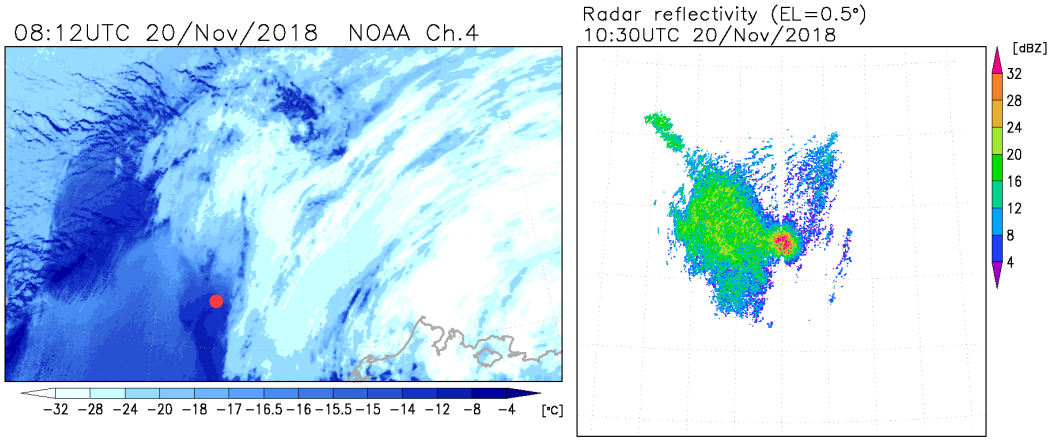

Figure 2.2-22: Same as in Figure 2.2-2, but for No.11 launch (20 November).

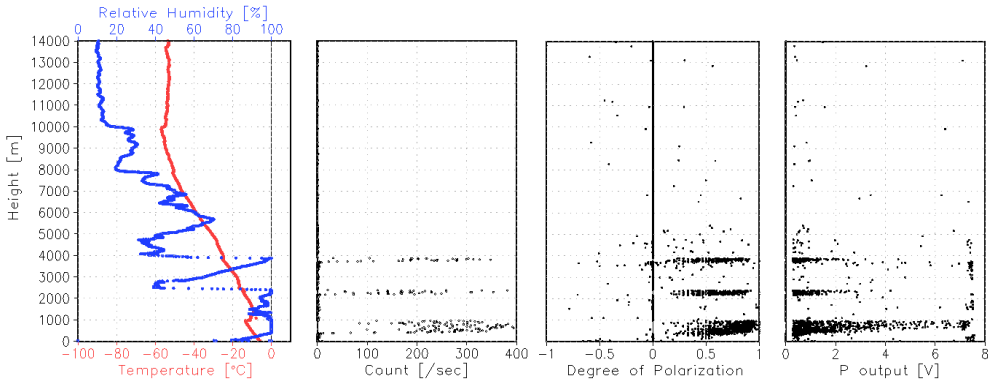

Figure 2.2-23: Same as in Figure 2.2-3, but for No.11 launch (20 November).

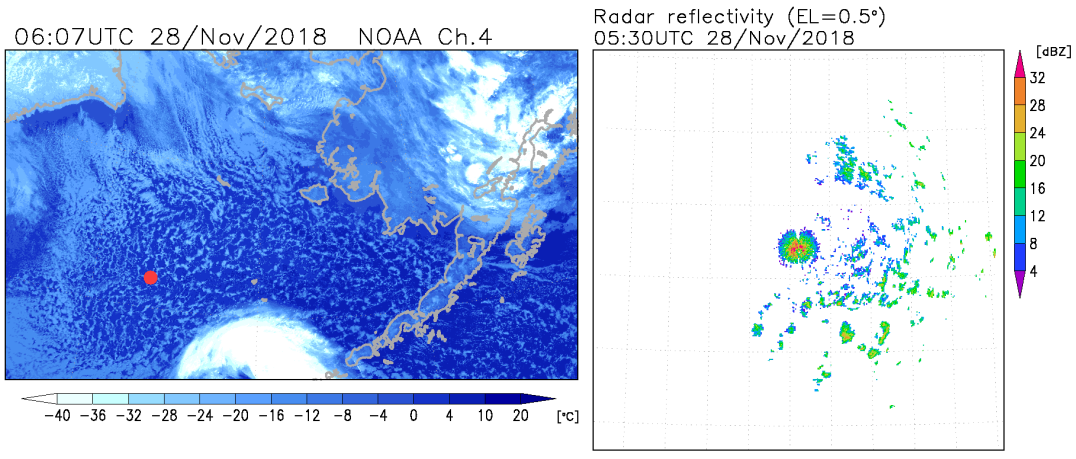

Figure 2.2-24: Same as in Figure 2.2-2, but for No.12 launch (28 November).

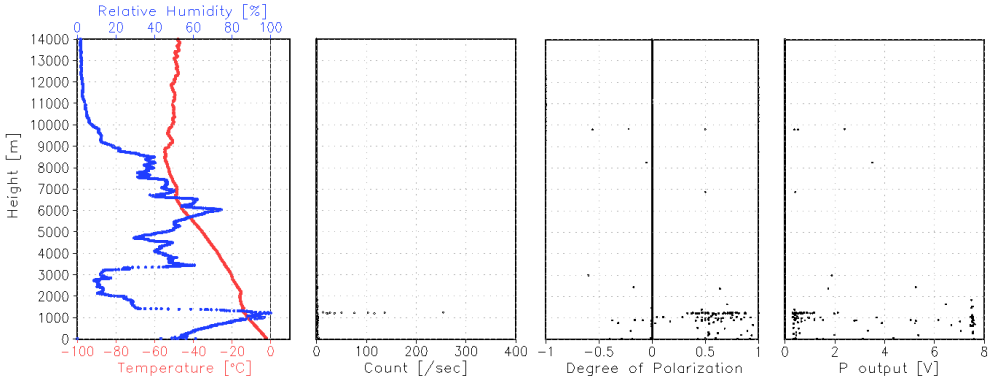

Figure 2.2-25: Same as in Figure 2.2-3, but for No.12 launch (28 November).

2.3. C-band Weather Radar

(1) Personnel

Jun Inoue	NIPR	- PI
Kazutoshi Sato	KIT	
Akio Yamagami	University of Tsukuba	
Kodai Takebe	KIT	
Kazuho Yoshida	NME	
Souichiro Sueyoshi	NME	
Shinya Okumura	NME	
Takehito Hattori	MIRAI Crew	

(2) Objectives

Low level clouds over the Arctic Ocean which usually dominate during early winter have a key role for sea/ice surface heat budget. To capture the broad cloud-precipitation systems and their temporal and spatial evolution over the Arctic Ocean, three-dimensional radar echo structure and wind fields of rain/snow clouds were obtained by C-band Doppler radar observation.

(3) Parameters

The C-band Weather radar observed three-dimensional radar echo structure and wind fields of rain/snow cloud.

Radar variables, which are converted from the power and phase of the backscattered signal at vertically-and horizontally-polarized channels, are as follows:

Radar reflectivity:	Z
Doppler velocity:	Vr
Spectrum width of Doppler velocity:	SW
Differential reflectivity:	ZDR
Differential propagation phase:	ΦDP
Specific differential phase:	KDP
Co-polar correlation coefficients:	ρHV

(4) Instruments and methods

The C-band Weather radar on board R/V Mirai is used. The basic specification of the radar is as follows:

Frequency:	5370 MHz (C-band)
Polarimetry:	Horizontal and vertical (simultaneously transmitted and received)
Transmitter:	Solid-state transmitter
Pulse Configuration:	Using pulse-compression
Output Power:	6 kW (H) + 6 kW (V)
Antenna Diameter:	4 meter
Beam Width:	1.0 degrees
INU (Inertial Navigation Unit):	PHINS (IXBLUE S.A.S.)

The antenna is controlled to point the commanded ground-relative direction, by controlling the azimuth and elevation to cancel the ship attitude (roll, pitch and yaw) detected by the INU. The Doppler velocity is also corrected by subtracting the ship motion in beam direction.

As the maintenance, internal parameters of the radar are checked and calibrated at the beginning and the end of the cruise. Meanwhile, the following parameters are checked daily; (1) frequency, (2) peak output power and (3) pulse width.

During the cruise, the radar was operated typically by repeating a volume scan with 17 PPIs (Plan Position Indicators) every 6-minute. A dual PRF mode with the maximum range of typically 100 km is used for the volume scan. A surveillance PPI scan is performed every 30 minutes in a single PRF mode with the maximum range of 300 km. RHI (Range Height Indicator) scans are operated whenever detailed vertical structures are necessary in certain azimuth directions. During this cruise, the scan strategy is kept same, as in Table 2.3-1, to provide the same data quality to highlight the temporal variation of the precipitating systems.

(5) Station list or Observation log

The radar was operated continuously from 05:06UTC Oct. 23 to 00:00UTC Dec. 05.

(6) Preliminary results

The radar was operated continuously from Oct. 23 to Dec. 05 during the cruise. During the cruise, several precipitation systems passed near the R/V Mirai. The C-band weather radar captured strong precipitation systems during MR18-05C. Figure 2.3-1 shows the temporal variation of the areal coverage of the radar echo within 100-km range on the PPI for precipitating events (Top in figure 2.3-1). The event was captured on November 7 when the low pressure system approached R/V Mirai. The strong echo associated with convergence was observed near coast of Barrow where wind sheer was found on November 11 and 12. Snowfall accompanied with the northeast wind was observed near ice edge and coast of Alaska during

November 20-24.

(7) Data archive

These data obtained in this cruise will be submitted to the Data Management Group of JAMSTEC, and will be opened to the public via "Data Research System for Whole Cruise Information in JAMSTEC (DARWIN)" in JAMSTEC web site. <http://www.godac.jamstec.go.jp/darwin/e>

(8) Remarks

1. The following period, data acquisition was suspended due to the work station error.

06:12UTC 29 Oct. 2018 - 07:12UTC 29 Oct. 2018

2. After around 19 Nov., transmit power of horizontal polarization has been depressed due to performance decline in one of the power amplifiers.

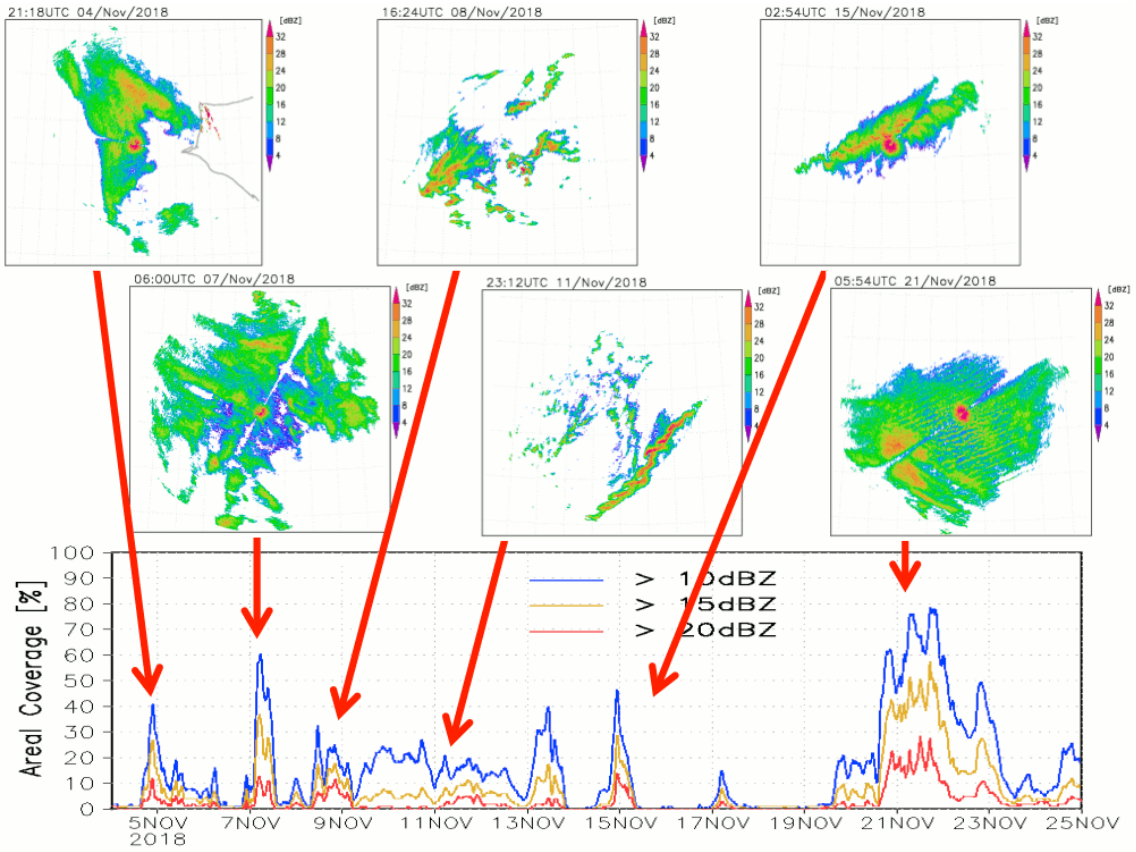

Figure 2.3-1: (Bottom) The temporal variations of the areal coverage of the echo exceeding threshold as 10 dBZ (blue), 15 dBZ (yellow) and 20 dBZ (red), within 100-km range distance on the PPI scans. (top) the six representing PPI images for characteristic precipitating event, obtained by the first PPI in the volume scan (at elevation angle of 0.5 degrees).

Table 2.3-1: Parameters for scan strategy in the Arctic Ocean.

	Surveillance PPI Scan	Volume Scan						RHI Scan
Repeated Cycle (min.)	30	6						6
Times in One Cycle	1	1						3
Pulse Width (long / short, in microsec)	200 / 2	64 / 1		32 / 1		32 / 1		32 / 1
Scan Speed (deg/sec)	18	18		24		36		9 (in el.)
PRF(s) (Hz)	400	dual PRF (ray alternative)						1250
		667	833	938	1250	1333	2000	
Pulses / Ray	16	26	33	27	34	37	55	32
Ray Spacing (deg.)	0.7	0.7		0.7		1.0		0.23
Azimuth	Full Circle							Optional
Bin Spacing (m)	150							
Max. Range (km)	300	150		100		60		100
Elevation Angle(s) (deg.)	0.5	0.5		1.0, 1.8, 2.6, 3.4, 4.2, 5.1, 6.2, 7.6, 9.7, 12.2 15.2		18.7, 23.0, 27.9, 33.5, 40.0		-0.2 to 70.0

2.4. Surface Meteorological Observations

(1) Personnel

Jun Inoue	NIPR	-PI
Kazuho Yoshida	NME	
Souichiro Sueyoshi	NME	
Shinya Okumura	NME	
Takehito Hattori	MIRAI Crew	

(2) Objectives

Surface meteorological parameters are observed as a basic dataset of the meteorology. These parameters provide the temporal variation of the meteorological condition surrounding the ship.

(3) Instruments and methods

Surface meteorological parameters were observed during this cruise. In this cruise, we used two systems for the observation.

i. MIRAI Surface Meteorological observation (SMet) system

Instruments of SMet system are listed in Table 2.4-1 and measured parameters are listed in Table 2.4-2. Data were collected and processed by KOAC-7800 weather data processor made by Koshin-Denki, Japan. The data set consists of 6-second averaged data.

ii. Shipboard Oceanographic and Atmospheric Radiation (SOAR) measurement system

SOAR system designed by BNL (Brookhaven National Laboratory, USA) consists of major five parts.

a) Portable Radiation Package (PRP) designed by BNL – short and long wave downward radiation.
b) Analog meteorological data sampling with CR1000 logger manufactured by Campbell Scientific Inc. Canada – wind pressure, and rainfall (by a capacitive rain gauge) measurement.
c) Digital meteorological data sampling from individual sensors - air temperature, relative humidity and rainfall (by optical rain gauge (ORG)) measurement.
d) Photosynthetically Available Radiation (PAR) sensor manufactured by Biospherical Instruments Inc. (USA) - PAR measurement.
e) Scientific Computer System (SCS) developed by NOAA (National Oceanic and Atmospheric Administration, USA) – centralized data acquisition and logging of all data sets.

SCS recorded PRP, air temperature, relative humidity, CR1000 and ORG data. SCS composed Event

data (JamMet) from these data and ship's navigation data every 6 seconds. Instruments and their locations are listed in Table 2.4-3 and measured parameters are listed in Table 2.4-4.

For the quality control as post processing, we checked the following sensors, before and after the cruise.

i. Young Rain gauge (SMet and SOAR)

Inspect of the linearity of output value from the rain gauge sensor to change Input value by adding fixed quantity of test water.

ii. Barometer (SMet and SOAR)

Comparison with the portable barometer value, PTB220, VAISALA

iii. Thermometer (air temperature and relative humidity) (SMet and SOAR)

Comparison with the portable thermometer value, HM70, VAISALA

(4) Observation log

24 Oct. 2018 to 07 Dec. 2018

(5) Preliminary results

Figure 2.4-1 shows the time series of the following parameters;

Wind (SMet)
Air temperature (SMet)
Relative humidity (SMet)
Precipitation (SMet, ORG)
Short/long wave radiation (SOAR)
Pressure (SMet)
Sea surface temperature (SMet)
Significant wave height (SMet)

(6) Data archives

These data obtained in this cruise will be submitted to the Data Management Group of JAMSTEC, and will be opened to the public via "Data Research System for Whole Cruise Information in JAMSTEC (DARWIN)" in JAMSTEC web site. <http://www.godac.jamstec.go.jp/darwin/e>

(7) Remarks (Times in UTC)

i) The following periods, Sea surface temperature of SMet data was available.
09:00, 25 Oct. 2018- 05:35, 05 Dec. 2018

ii) The following time, increasing of SMet capacitive rain gauge data were invalid due to test transmitting for MF/HF radio.
23:41 27 Nov. 2018
23:49 27 Nov. 2018

iii) The following periods, PRP data acquisition was suspended due to maintenance.
01:11 28 Oct. 2018 - 01:21 28 Oct. 2018
01:21 31 Oct. 2018 - 01:23 31 Oct. 2018
23:42 28 Nov. 2018 - 00:02 29 Nov. 2018
09:35 29 Nov. 2018 - 09:37 29 Nov. 2018

iv) The following period, FRSR data acquisition was suspended.
01:23 31 Oct. 2018 - 00:00 07 Dec. 2018

v) The following periods, SMet wind data were invalid due to some trouble in anemometer.
23:38 23 Nov. 2018 - 23:39 23 Nov. 2018
04:28 29 Nov. 2018 - 04:30 29 Nov. 2018
09:21 29 Nov. 2018
13:06 29 Nov. 2018 - 13:08 29 Nov. 2018
17:55 29 Nov. 2018 - 17:56 29 Nov. 2018

vi) The following period, PAR data acquisition was suspended due to software freeze.
07:00 24 Oct. 2018 - 09:44 24 Oct. 2018

vii) After 07:27 22 Nov. 2018, PAR data acquisition was stopped due to sensor power supply failure.

viii) The following period, Navigation data (position, speed and course) were not updated due to the server error.
04:37:00 24 Oct. 2018 - 04:37:18 24 Oct. 2018

ix) The amount of SMet long wave radiation data contains bias (about -50 W/m2) throughout the cruise.

x) The amount of PRP long wave radiation (PIR) contains bias in a temperature environment under about -5.5 degC, because output of PIR case and dome thermistor for radiation correction fell below the measurement range.

Table 2.4-1: Instruments and installation locations of SMet system

Sensors	Type	Manufacturer	Location(altitude from surface)
Anemometer	KS-5900	Koshin Denki, Japan	foremast (25 m)
Tair/RH	HMP155	Vaisala, Finland	
with 43408 Gill aspirated radiation shield		R.M. Young, USA	compass deck (21 m) starboard and port side
Thermometer: SST	RFN2-0	Koshin Denki, Japan	4th deck (-1m, inlet -5m)
Barometer	Model-370	Setra System, USA	captain deck (13 m) weather observation room
Rain gauge	50202	R. M. Young, USA	compass deck (19 m)
Optical rain gauge	ORG-815DR	Osi, USA	compass deck (19 m)
Radiometer (short wave)	MS-802	Eko Seiki, Japan	radar mast (28 m)
Radiometer (long wave)	MS-202	Eko Seiki, Japan	radar mast (28 m)
Wave height meter	WM-2	Tsurumi-seiki, Japan	bow (10 m)

Table 2.4-2: Parameters of MIRAI Surface Meteorological observation system

Parameter	Units	Remarks
1 Latitude	degree	
2 Longitude	degree	
3 Ship's speed	knot	Mirai log, DS-30 Furuno
4 Ship's heading	degree	Mirai Gyro, TOKYO-KEIKI, TG-8000
5 Relative wind speed	m/s	6sec./10min. averaged
6 Relative wind direction	degree	6sec./10min. averaged
7 True wind speed	m/s	6sec./10min. averaged
8 True wind direction	degree	6sec./10min. averaged
9 Barometric pressure	hPa	adjusted to sea surface level 6sec. averaged
10 Air temperature (starboard)	degC	6sec. averaged
11 Air temperature (port side)	degC	6sec. averaged
12 Dewpoint temperature (starboard)	degC	6sec. averaged
13 Dewpoint temperature (port side)	degC	6sec. averaged
14 Relative humidity (starboard)	%	6sec. averaged
15 Relative humidity (port side)	%	6sec. averaged
16 Sea surface temperature	degC	6sec. averaged
17 Rain rate (optical rain gauge)	mm/hr	hourly accumulation
18 Rain rate (capacitive rain gauge)	mm/hr	hourly accumulation
19 Down welling shortwave radiation	W/m^2	6sec. averaged
20 Down welling infra-red radiation	W/m^2	6sec. averaged
21 Significant wave height (bow)	m	hourly
22 Significant wave height (aft)	m	hourly
23 Significant wave period (bow)	second	hourly
24 Significant wave period (aft)	second	hourly

Table 2.4-3: Instruments and installation locations of SOAR system

Sensors (Meteorological)	Type	Manufacturer	Location (altitude from surface)
Anemometer	05106	R.M. Young, USA	foremast (25 m)
Barometer	PTB210	Vaisala, Finland	foremast (23 m)
with 61002 Gill pressure port,		R.M. Young, USA	
Rain gauge	50202	R.M. Young, USA	foremast (24 m)
Tair/RH	HMP155	Vaisala, Finland	foremast (23 m)
with 43408 Gill aspirated radiation shield		R.M. Young, USA	foremast (23 m)
Optical rain gauge	ORG-815DR	Osi, USA	foremast (24 m)

Sensors (PRP)	Type	Manufacturer	Location (altitude from surface)
Radiometer (short wave)	PSP	Epply Labs, USA	foremast (25 m)
Radiometer (long wave)	PIR	Epply Labs, USA	foremast (25 m)
Fast rotating shadowband radiometer		Yankee, USA	foremast (25 m)

Sensors (PAR)	Type	Manufacturer	Location (altitude from surface)
PAR sensor	PUV-510	Biospherical Instruments Inc., USA	Navigation deck (18m)

Table 2.4-4: Parameters of SOAR system (JamMet)

Parameter	Units	Remarks
1 Latitude	degree	
2 Longitude	degree	
3 SOG	knot	
4 COG	degree	
5 Relative wind speed	m/s	
6 Relative wind direction	degree	
7 Barometric pressure	hPa	
8 Air temperature	degC	
9 Relative humidity	%	
10 Rain rate (optical rain gauge)	mm/hr	
11 Precipitation (capacitive rain gauge)	mm	reset at 50 mm
12 Down welling shortwave radiation	W/m^2	
13 Down welling infra-red radiation	W/m^2	
14 Defuse irradiance	W/m^2	
15 PAR	microE/cm2/sec	

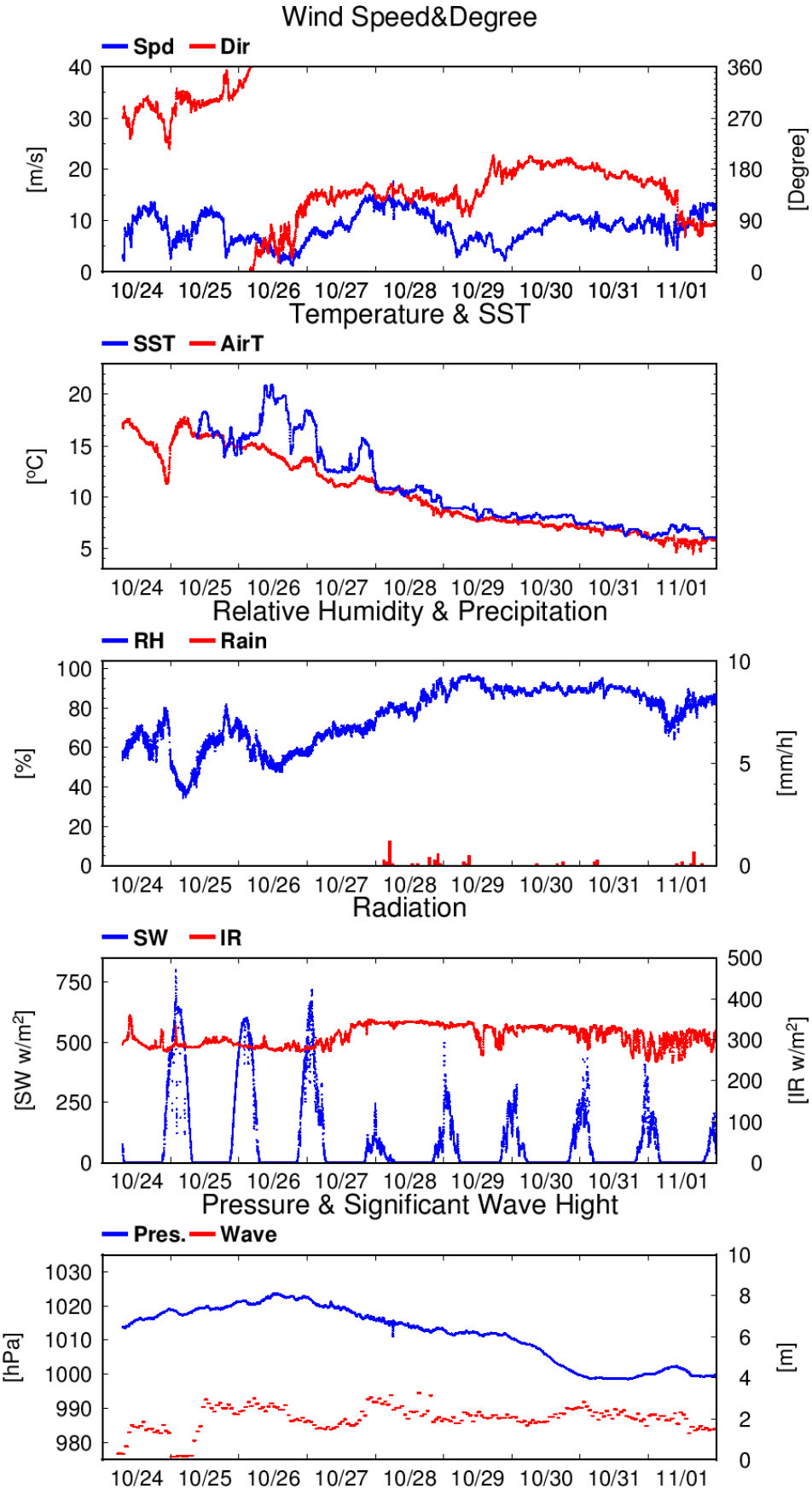

Figure 2.4-1: Time series of surface meteorological parameters during this cruise

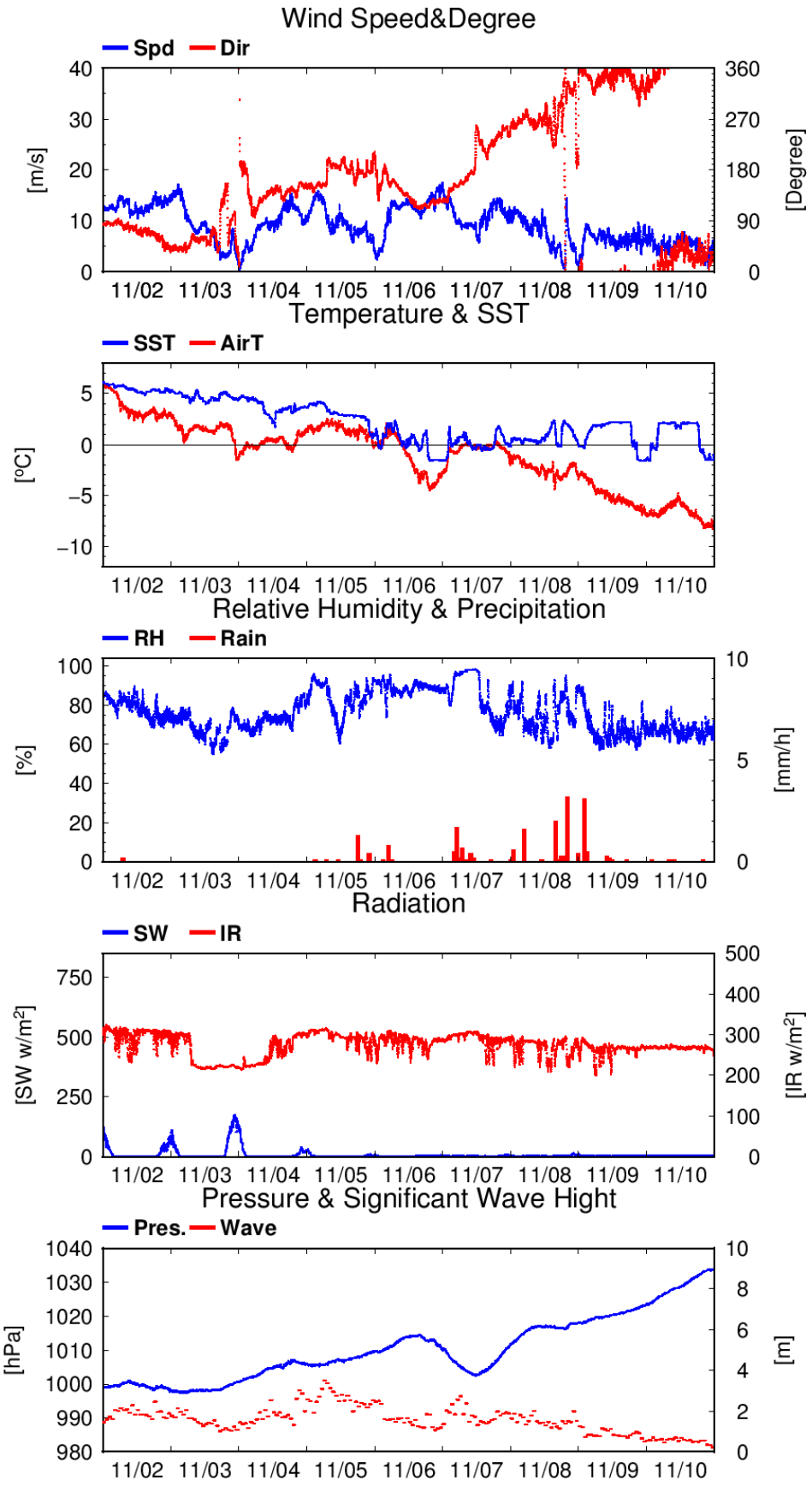

Figure 2.4-1: (Continued)

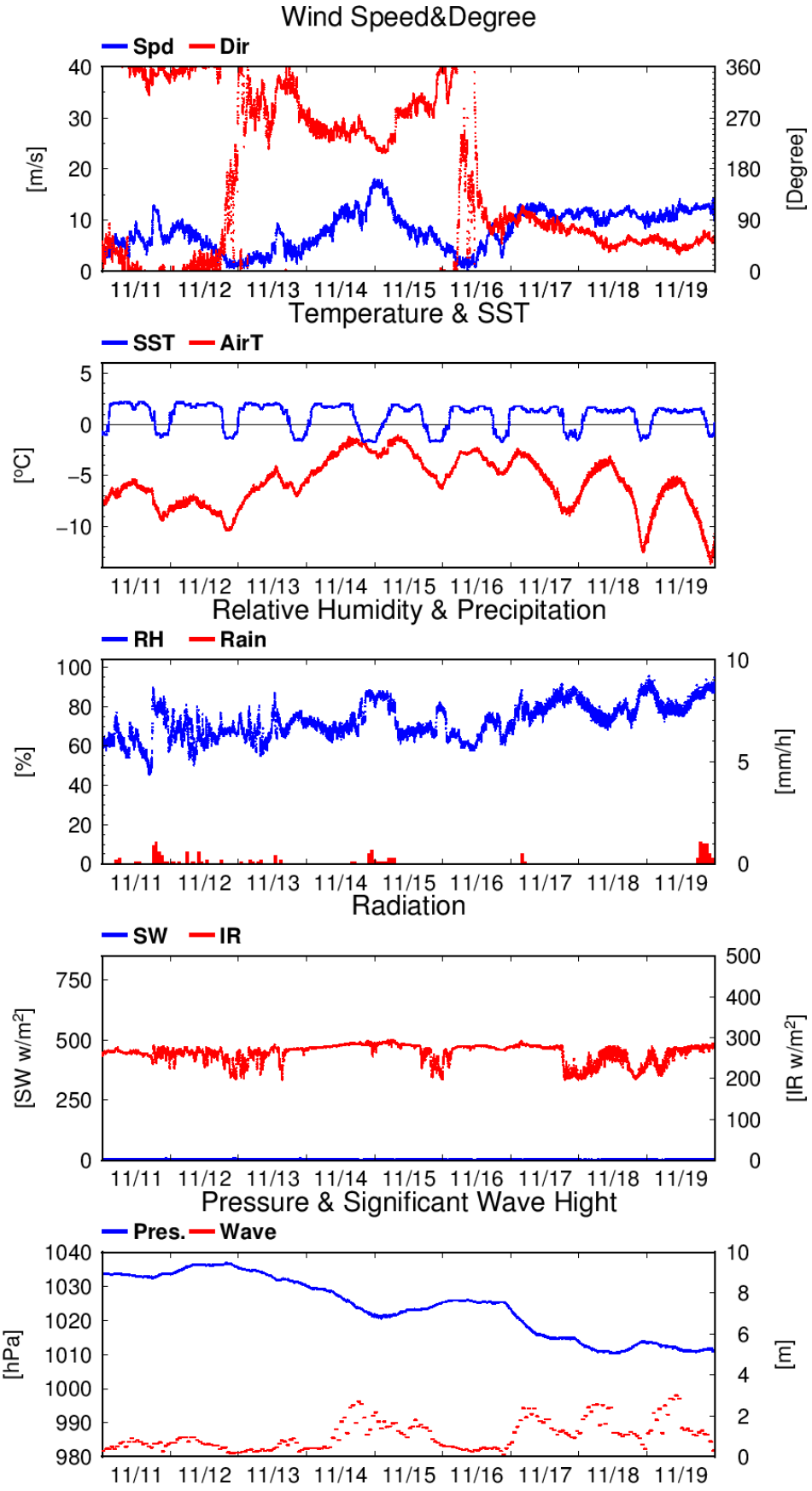

Figure 2.4-1: (Continued)

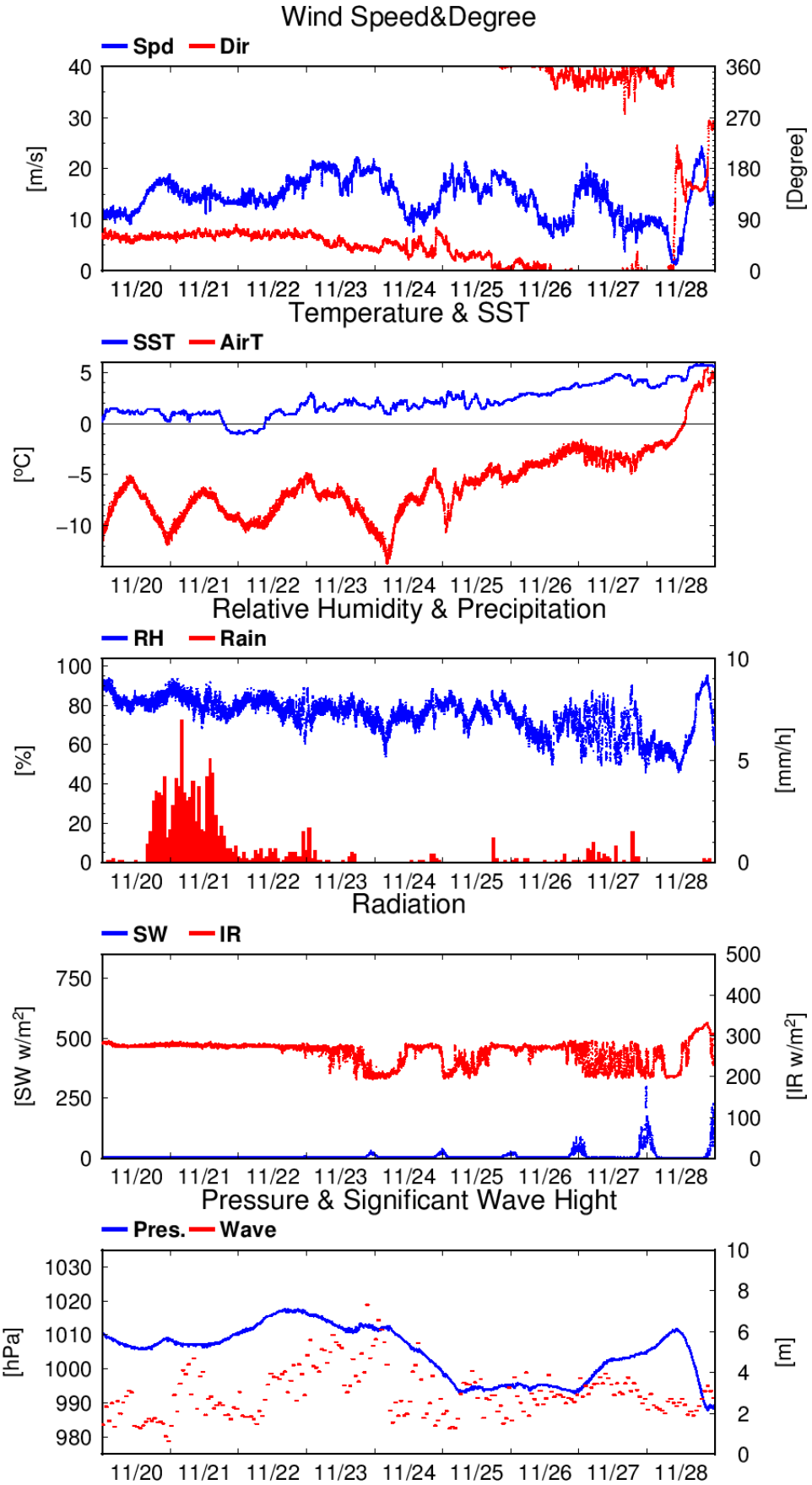

Figure 2.4-1: (Continued)

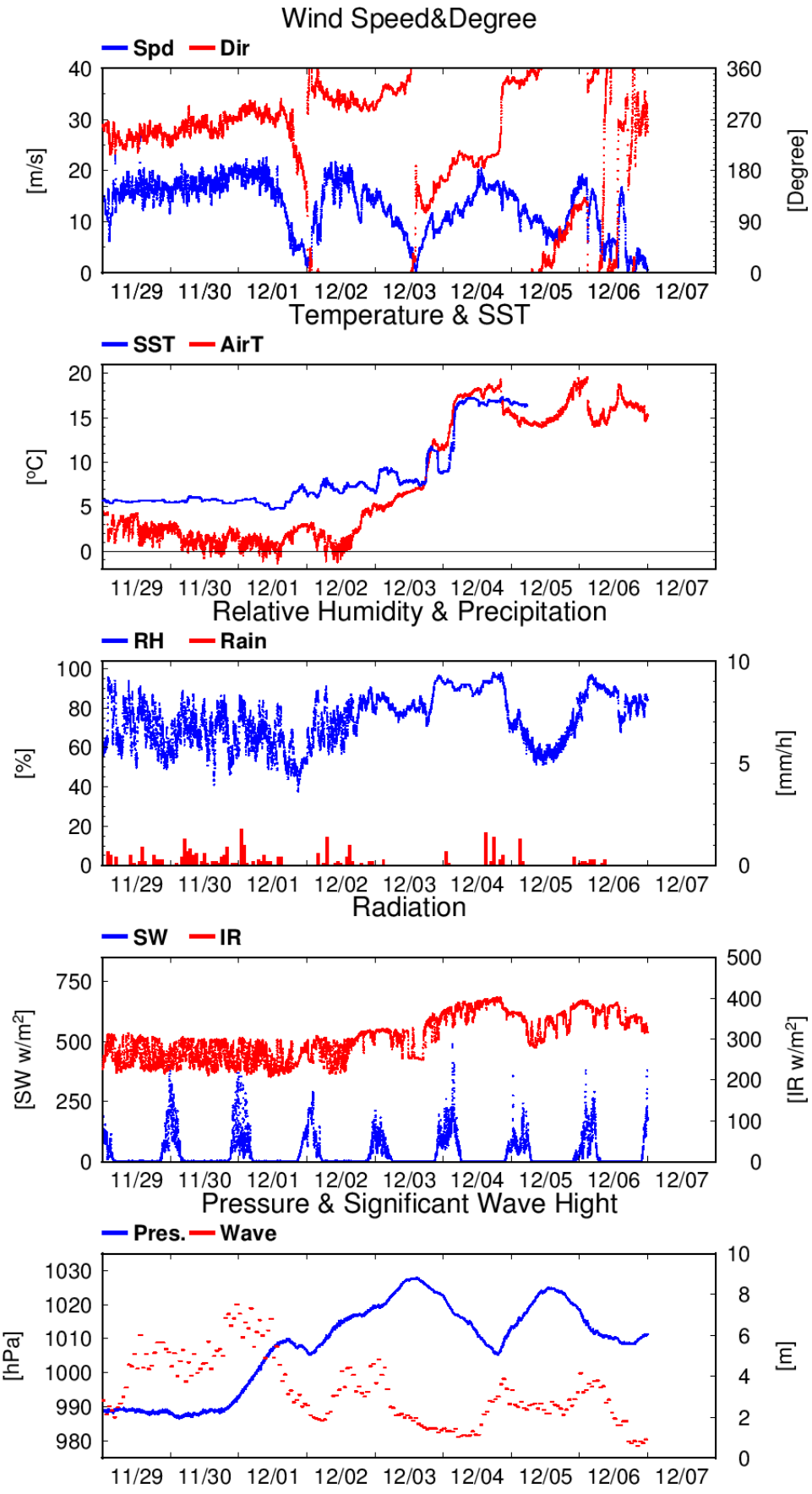

Figure 2.4-1: (Continued)

2.5. Ceilometer

(1) Personnel

Jun Inoue	NIPR	- PI
Kazuho Yoshida	NME	
Souichiro Sueyoshi	NME	
Shinya Okumura	NME	
Takehito Hattori	MIRAI Crew	

(2) Objectives

The information of cloud base height and the liquid water amount around cloud base is important to understand the process on formation of the cloud. As one of the methods to measure them, the ceilometer observation was carried out.

(3) Parameters

Cloud base height [m].

Backscatter profile, sensitivity and range normalized at 10 m resolution.

Estimated cloud amount [oktas] and height [m]; Sky Condition Algorithm.

(4) Instruments and methods

We measured cloud base height and backscatter profile using ceilometer (CL51, VAISALA, Finland) throughout this cruise.

Major parameters for the measurement configuration are as follows;

Laser source:	Indium Gallium Arsenide (InGaAs) Diode Laser
Transmitting center wavelength:	910±10 nm at 25 degC
Transmitting average power:	19.5 mW
Repetition rate:	6.5 kHz
Detector:	Silicon avalanche photodiode (APD)
Measurement range:	0 ~ 15 km
	0 ~ 13 km (Cloud detection)
Resolution:	10 meter in full range
Sampling rate:	36 sec
Sky Condition	0, 1, 3, 5, 7, 8 oktas (9: Vertical Visibility)
	(0: Sky Clear, 1: Few, 3: Scattered, 5-7: Broken, 8: Overcast)

On the archive dataset, cloud base height and backscatter profile are recorded with the resolution of 10 m.

(5) Observation log

24 Oct. 2018 - 07 Dec. 2018

(6) Preliminary results

Figure 2.5-1 shows the time series of cloud-base heights derived from the ceilometer during this cruise.

(7) Data archives

These data obtained in this cruise will be submitted to the Data Management Group of JAMSTEC, and will be opened to the public via “Data Research System for Whole Cruise Information in JAMSTEC (DARWIN)” in JAMSTEC web site.
<http://www.godac.jamstec.go.jp/darwin/e>

(8) Remarks (Times in UTC)

Window cleaning

23:42 25 Oct. 2018
23:39 01 Nov. 2018
21:25 08 Nov. 2018
20:00 17 Nov. 2018
22:34 24 Nov. 2018
23:27 28 Nov. 2018
22:58 01 Dec. 2018

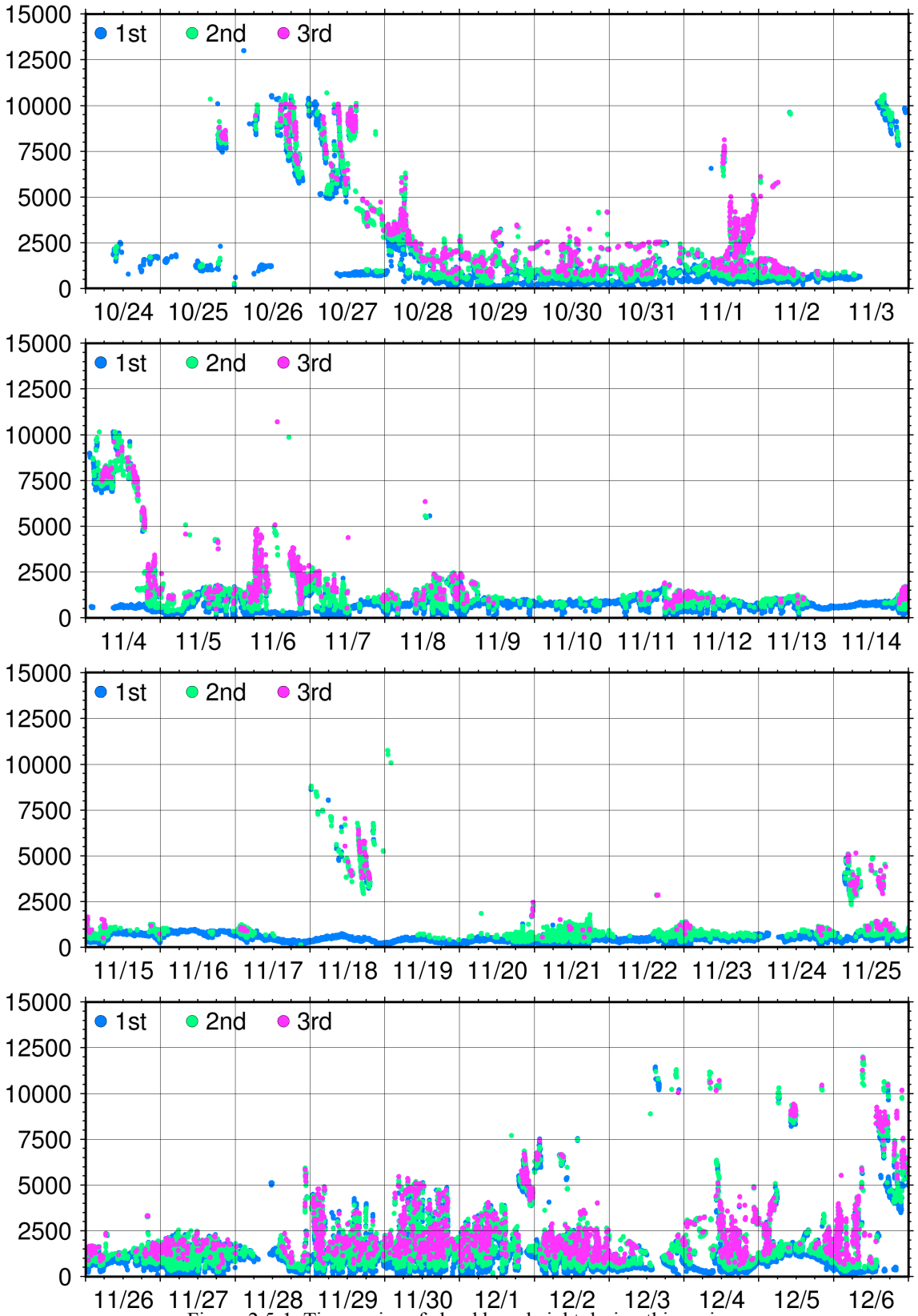

Figure 2.5-1: Time series of cloud base height during this cruise

2.6 Sea spray

(1) Personal

Jun Inoue	NIPR	- PI
Toshihiro Ozeki	Hokkaido Univ. of Education	- not on board
Hajime Yamaguchi	University of Tokyo	- not on board
Shuichi Fushimi	University of Tokyo	

(2) Objectives

Marine disasters caused by ship icing occur frequently in cold regions. The typical growth mechanism of sea spray icing is as follows. First, sea spray is generated from the bow of the ship. Next, the spray drifts and impinges upon the superstructure, after which there is a wet growth of ice from the brine water flow. To address icing on the ship, we focus on the impinging seawater spray. We investigated the drop size of seawater spray on R/V Mirai.

(3) Parameters

Number of sea spray particles

Spray particle size distribution

Liquid water contents

The amount of spray impinging on ships

(4) Instruments and methods

The amount of seawater spray and the size distribution of seawater particles were measured by a spray particle counter (SPC) and a marine rain gauge type spray gauge (MRS).

(4-1) Spray particle counter (SPC)

The SPC, which was originally developed for the measurement of drifting snow, was improved to be a seawater spray particle counter. The flux distribution and the transport rate can be calculated as a function of particle size. The SPC (SPC-S7; Niigata Denki) consists of a sensor, data processor, and personal computer, and the measuring range is set from 100 to 1,000 μm in diameter. The sensing area is 25 mm wide, 3 mm high, and 0.5 mm deep, and SLD light is used as a parallel ray. The sensor measures light attenuation caused by particles that pass through the sensing area. The processor divides the particles into 32 classes depending on their diameters. The particles in each class are counted every second. The volume flux of the spray was calculated by $(4\pi r_c^3/3)$ where r_c is class value of particle radius. The unit of the volume flux is millimeters [mm] per unit time, which is also the unit of precipitation.

(4-2) Marine rain gauge type spray gauge (MRS)

The marine rain gauge type spray gauge (MRS) consists of a marine rain gauge (CYG-50202, R M Young) and a cylindrical spray trap. The marine rain gauge was developed to measure rainfall on ships. It collects seawater spray or precipitation in a catchment funnel which has a cross sectional area of 100 cm^2. The inside diameter of the funnel is 112 mm. The cylindrical spray trap is attached above the marine rain gauge to capture the seawater spray from the horizontal direction instead of precipitation. The impinging spray particle is drained into the catchment funnel. The spray trap has a diameter of 76.3 mm, a height of 120 mm, and the projected area is 92 cm^2. The amount of seawater spray is measured every minute. The smallest measurable unit is 0.1 mm.

To reveal the positional relationship of the amount of seawater spray, observations were conducted from three different points on the deck. SPC were installed on center of the compass deck. The two MRSs were installed one on the port side and one on the starboard side of the bridge deck. They were set on the bulwark behind 42 m from the bow.

(5) Station list or Observation log

The data of SPCs, MRS were obtained continuously through the cruise from Oct. 25 to Dec. 5. Experimental cruise for generating sea spray is given at Nov. 21 11:35, Nov. 23 13:45, Nov. 24 13:55 UTC.

(6) Preliminary results

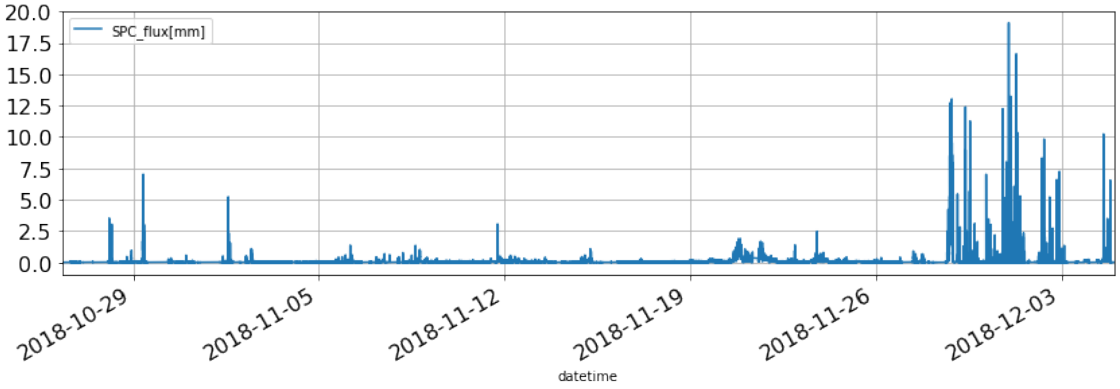

Figure2.6-1: Spray and rainfall flux observed by SPC

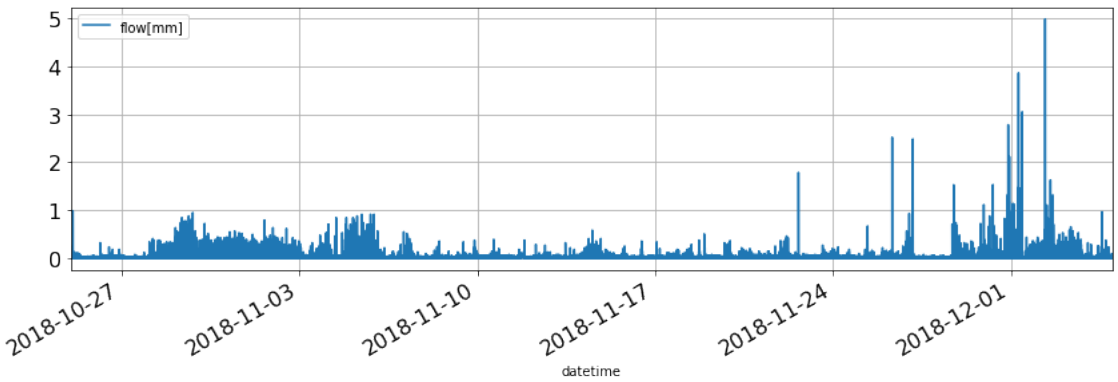

Figure 2.6-2: Spray and rainfall flux observed by the starboard side MRS

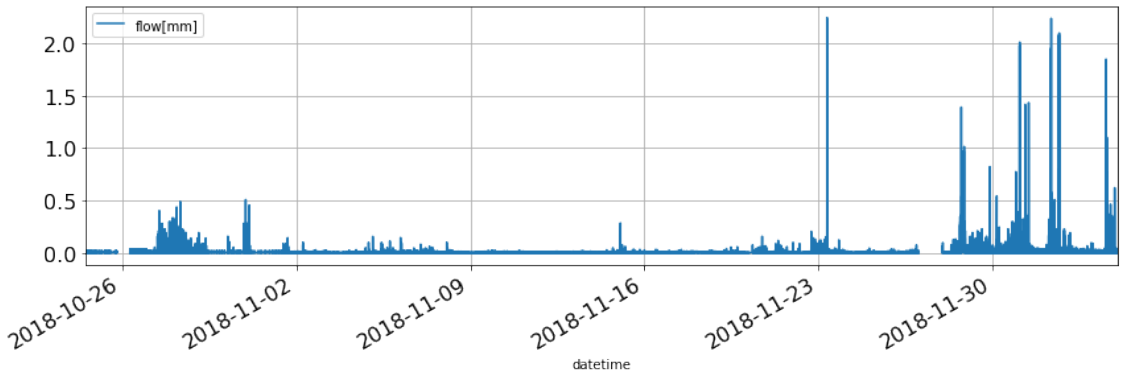

Figure 2.6-3: Spray and rainfall flux observed by the port side MRS

(6) Data archives

These data obtained in this cruise will be submitted to the Data Management Group of JAMSTEC, and will be opened to the public via “Data Research System for Whole Cruise Information in JAMSTEC (DARWIN)” in JAMSTEC web site.

2.7 Vessel icing

(1) Personal

Jun Inoue	NIPR	- PI
Toshihiro Ozeki	Hokkaido Univ. of Education	- not on board
Hajime Yamaguchi	University of Tokyo	- not on board
Shuichi Fushimi	University of Tokyo	

(2) Objectives

Marine disasters caused by vessel icing occur frequently in cold regions. Freezing spray is the main cause of vessel icing; however, spray ice accretion often occurs during intense snowfall. Additionally, brine pockets trapped in spray ice during ice growth are structural features of sea spray icing. We made sampling of superstructure ice accretion on R/V Mirai.

(3) Parameters

Samples of sea spray ice (incl. snow and sea surface water samples)

Thickness

Structure

Salinity

δ18O value of the ice.

(4) Instruments and methods

The structural characteristics of the sea spray ice are analyzed using conventional thin-section and NMR imaging. The salinity of the melted sample is analyzed using a refractometer and an electric conductivity. The oxygen isotopic composition of the melted samples is analyzed using a standard mass spectrometer. These samples are going to be analyzed in laboratory.

(5) Station list or observation log

Table. 2.7-1 List of sampling locations of the sea spray ice, snow and sea surface water. Severe vessel icing event happened on Nov. 23.

Table. 2.7-1: List of sampling locations

No.	On board ID	Sample Category	YYYY	MM	DD	time(UTC)
1	MR1805C_spray_20181108_1	snow	2018	11	08	0:00
2	MR1805C_spray_20181108_2	snow	2018	11	08	0:00
3	MR1805C_spray_20181108_3	snow	2018	11	08	0:00
4	MR1805C_spray_20181109_1	snow	2018	11	09	0:00
5	MR1805C_spray_20181115_1	snow	2018	11	15	0:00
6	MR1805C_spray_20181116_1	icing	2018	11	16	0:00
7	MR1805C_spray_20181116_2	snow	2018	11	16	0:00
8	MR1805C_spray_20181117_1	icing	2018	11	17	0:00
9	MR1805C_spray_20181117_2	icing	2018	11	19	0:00
10	MR1805C_spray_20181117_3	snow	2018	11	19	0:00
11	MR1805C_spray_20181118_1	icing	2018	11	19	0:00
12	MR1805C_spray_20181119_1	icing	2018	11	19	0:00
13	MR1805C_spray_20181119_2	snow	2018	11	19	0:00
14	MR1805C_spray_20181120_1	icing	2018	11	20	0:00
15	MR1805C_spray_20181120_2	icing	2018	11	20	0:00
16	MR1805C_spray_20181121_1	icing	2018	11	21	0:00
17	MR1805C_spray_20181121_2	icing	2018	11	21	0:00
18	MR1805C_spray_20181121_3	icing	2018	11	21	0:00
19	MR1805C_spray_20181121_4	icing	2018	11	21	0:00
20	MR1805C_spray_20181121_5	snow	2018	11	21	0:00
21	MR1805C_spray_20181121_6	snow	2018	11	21	9:00
22	MR1805C_spray_20181123_1	snow	2018	11	23	5:30
23	MR1805C_spray_20181124_1	icing	2018	11	24	5:00
24	MR1805C_spray_20181124_2	icing	2018	11	24	5:00
25	MR1805C_spray_20181124_3	icing	2018	11	24	5:00
26	MR1805C_spray_20181124_4	icing	2018	11	24	5:00
27	MR1805C_spray_20181124_5	icing	2018	11	24	5:00

28	MR1805C_spray_20181125_1	icing	2018	11	25	0:00
29	MR1805C_spray_20181125_2	icing	2018	11	25	0:00
30	MR1805C_spray_20181125_3	icing	2018	11	25	0:00
31	MR1805C_spray_20181125_4	icing	2018	11	25	0:00
32	MR1805C_spray_20181125_5	icing	2018	11	25	0:00
33	MR1805C_spray_20181126_1	icing	2018	11	26	2:30
34	MR1805C_spray_20181126_2	icing	2018	11	26	2:30
35	MR1805C_spray_20181126_3	icing	2018	11	26	2:30
36	MR1805C_O18_040_1_0	Seawater	2018	11	06	16:09
37	MR1805C_O18_041_1_0	Seawater	2018	11	06	21:08
38	MR1805C_O18_057_1_0	Seawater	2018	11	08	17:12
39	MR1805C_O18_063_1_0	Seawater	2018	11	09	22:54
40	MR1805C_O18_064_1_0	Seawater	2018	11	10	22:10
41	MR1805C_O18_064_2_0	Seawater	2018	11	11	20:51
42	MR1805C_O18_066_1_0	Seawater	2018	11	12	20:54
43	MR1805C_O18_066_2_0	Seawater	2018	11	13	21:17
44	MR1805C_O18_064_3_0	Seawater	2018	11	14	21:52
45	MR1805C_O18_066_3_0	Seawater	2018	11	15	21:18
46	MR1805C_O18_048_9_0	Seawater	2018	11	16	20:49
47	MR1805C_O18_064_4_0	Seawater	2018	11	17	21:59
48	MR1805C_O18_064_5_0	Seawater	2018	11	18	22:49
49	MR1805C_O18_048_12_0	Seawater	2018	11	19	22:41
50	MR1805C_O18_056_13_0	Seawater	2018	11	21	1:56
51	MR1805C_O18_067_5_0	Seawater	2018	11	21	11:06
52	MR1805C_O18_068_1_0	Seawater	2018	11	22	0:53
53	MR1805C_O18_020_2_0	Seawater	2018	11	23	12:36
54	MR1805C_O18_019_2_0	Seawater	2018	11	24	12:40
55	MR1805C_O18_007_2_0	Seawater	2018	11	26	6:33

(6) Data archives

These data obtained in this cruise will be submitted to the Data Management Group of JAMSTEC, and will be opened to the public via “Data Research System for Whole Cruise Information in JAMSTEC (DARWIN)” in JAMSTEC web site.

2.8 Tropospheric gas and particles observation in the Arctic Marine Atmosphere

(1) Personnel

Fumikazu Taketani	JAMSTEC	- PI
Zhu Chunmao	JAMSTEC	
Yugo Kanaya	JAMSTEC	- not on board
Takuma Miyakawa	JAMSTEC	- not on board
Yutaka Tobo	NIPR	- not on board
Masayuki Takigawa	JAMSTEC	- not on board
Kazuyuki Miyazaki	JAMSTEC	- not on board
Kazuyo Yamaji	JAMSTEC/Kobe Univ.	- not on board

(2) Objectives

To investigate roles of aerosols in the marine atmosphere in relation to climate change

To investigate processes of biogeochemical cycles between the atmosphere and the ocean.

To investigate contribution of suspended particles to the rain, and snow

(3) Parameters

Black carbon(BC) and fluorescent particles

Particle size distribution

Particle number concentration

Composition of ambient particles

Composition of snow and rain

Surface ozone(O_3), and carbon monoxide(CO) mixing ratios

(4) Instruments and methods

(4-1) Online aerosol observations:

(4-1-1) Particle umber concentration and size distribution

The number concentration of particles was measured by handheld optical particle counter (OPC, KR-12A, Rion).

(4-1-2) Black carbon (BC)

Number and mass BC concentration were measured by an instrument based on laser-induced incandescence, single particle soot photometer (SP2) (model D, Droplet Measurement Technologies). The laser-induced incandescence technique based on intracavity Nd:YVO4 laser operating at 1064 nm were used for detection of single particles of BC.

(4-1-3) Fluorescent property

Fluorescent properties of aerosol particles were measured by a single particle fluorescence sensor, Waveband Integrated bioaerosol sensor (WIBS4) (WIBS-4A, Droplet Measurement Technologies). Two pulsed xenon lamps emitting UV light (280 nm and 370 nm) were used for excitation. Fluorescence emitted from a single particle within 310–400 nm and 420–650 nm wavelength windows was recorded.

For SP2, the ambient air was commonly sampled from the compass deck by a 3-m-long conductive tube through the dryer to dry up the particles, and then introduced to each instrument installed at the environmental research room. WIBS4 and OPC instruments were installed at the compass deck. The ambient air was directory introduced to the instruments.

(4-2) Ambient air sampling

Ambient air samplings were carried out by air samplers installed at compass deck. Ambient particles were collected on the quartz filter (size: 8" × 10"), polycarbonate (ϕ =54mm) filter and nuclepore membrane filter (ϕ =47mm) along cruise track to analyze their composition and ice nuclei ability using a high-volume air sampler (HVS, 120SL, KIMOTO), NANO sampler (model 3182, Kanomax) and a handmade air sampler operated at flow rate of 740L/min, 40 L/min and 10L/min, respectively. To avoid collecting particles emitted from the funnel of the own vessel, the sampling period was controlled automatically by using a "wind-direction selection system". Particles whose size in the 2.5-10, 1.0-2.5, and 0.5-1.0 μm were collected on each polycarbonate filter, while all size particles were collected on nuclepore membrane filter. These sampling logs are listed in Tables 2.8-1, 2.8-2 and 2.8-3. All samples are going to be analyzed in laboratory.

(4-3) Snow and rain

Snow and rain samples were corrected using metal tray and rain sampler, respectively. Sea ices were also sampled. These sampling logs are listed in Table 2.8-4. To investigate the interaction from aerosols to rain/snow, these samples are going to be analyzed in laboratory.

(4-5) CO and O3

Ambient air was continuously sampled on the compass deck and drawn through ~20-m-long Teflon tubes connected to a gas filter correlation CO analyzer (Model 48C, Thermo Fisher Scientific) and a UV photometric ozone analyzer (Model 49C, Thermo Fisher Scientific), located in the Research Information Center. The data will be used for characterizing air mass origins.

(5) Observation log

Table 2.8-1: Logs of ambient particles sampling on the quartz filter

On board ID	Date Collected					Latitude			Longitude		
	YYYY	MM	DD	hh:mm:ss	UTC/JST	Deg.	Min.	N/S	Deg.	Min.	E/W
MR18-05C-HV-001	2018	10	25	7:56	UTC	40	33.94	N	141	37.47	E
MR18-05C-HV-002	2018	10	27	2:08	UTC	41	27.18	N	152	3.17	E
MR18-05C-HV-003	2018	10	29	0:32	UTC	47	12.58	N	161	48.8	E
MR18-05C-HV-004	2018	10	31	0:42	UTC	53	16.85	N	171	23.42	E
MR18-05C-HV-005	2018	11	2	0:56	UTC	60	40.36	N	176	50.39	W
MR18-05C-HV-006	2018	11	4	0:54	UTC	65	54.83	N	168	41.89	W
MR18-05C-HV-007	2018	11	6	0:40	UTC	73	5.23	N	168	44.23	W
MR18-05C-HV-008	2018	11	8	1:40	UTC	72	15.07	N	158	59.82	W
MR18-05C-HV-009	2018	11	9	23:30	UTC	73	18	N	160	54.98	W
MR18-05C-HV-010	2018	11	12	0:40	UTC	72	44.97	N	162	59.87	W
MR18-05C-HV-011	2018	11	14	0:01	UTC	72	53.39	N	162	28.98	W
MR18-05C-HV-012	2018	11	16	0:14	UTC	72	55.06	N	162	19.46	W
MR18-05C-HV-013	2018	11	18	2:01	UTC	72	44.96	N	163	0.25	W
MR18-05C-HV-014	2018	11	20	1:28	UTC	72	45.22	N	162	59.81	W
MR18-05C-HV-015	2018	11	22	0:17	UTC	71	35.87	N	163	50.9	W
MR18-05C-HV-016	2018	11	25	0:26	UTC	65	40.71	N	168	37.02	W
MR18-05C-HV-017	2018	11	27	23:40	UTC	57	53.09	N	178	1.02	E
MR18-05C-HV-018	2018	11	29	23:57	UTC	52	10.57	N	169	37.04	E
MR18-05C-HV-019	2018	12	2	0:06	UTC	47	23.32	N	161	34.62	E
MR18-05C-HV-020	2018	12	4	0:13	UTC	40	42.73	N	150	51.16	E
MR18-05C-HV-021	2018	12	5	0:09	UTC	38	4.84	N	145	56.22	E

Table 2.8-2: Logs of ambient particles sampling on the polycarbonate filter

On board ID	Date Collected					Latitude			Longitude		
	YYYY	MM	DD	hh:mm:ss	UTC/JST	Deg.	Min.	N/S	Deg.	Min.	E/W
MR18-05C-NANO-001	2018	10	25	7:56	UTC	40	33.94	N	141	37.47	E
MR18-05C-NANO-002	2018	10	27	2:08	UTC	41	27.18	N	152	3.17	E
MR18-05C-NANO-003	2018	10	29	0:32	UTC	47	12.58	N	161	48.8	E
MR18-05C-NANO-004	2018	10	31	0:42	UTC	53	16.85	N	171	23.42	E
MR18-05C-NANO-005	2018	11	2	0:56	UTC	60	40.36	N	176	50.39	W
MR18-05C-NANO-006	2018	11	4	0:54	UTC	65	54.83	N	168	41.89	W
MR18-05C-NANO-007	2018	11	8	1:40	UTC	72	15.07	N	158	59.82	W
MR18-05C-NANO-008	2018	11	12	0:40	UTC	72	44.97	N	162	59.87	W
MR18-05C-NANO-009	2018	11	16	0:14	UTC	72	55.06	N	162	19.46	W
MR18-05C-NANO-010	2018	11	20	1:28	UTC	72	45.22	N	162	59.81	W
MR18-05C-NANO-011	2018	11	25	0:26	UTC	65	40.71	N	168	37.02	W
MR18-05C-NANO-012	2018	11	27	23:40	UTC	57	53.09	N	178	1.02	E
MR18-05C-NANO-013	2018	11	29	23:57	UTC	52	10.57	N	169	37.04	E
MR18-05C-NANO-014	2018	12	2	0:06	UTC	47	23.32	N	161	34.62	E
MR18-05C-NANO-015	2018	12	4	0:13	UTC	40	42.73	N	150	51.16	E
MR18-05C-NANO-016	2018	12	5	0:09	UTC	38	4.84	N	145	56.22	E

Table 2.8-3: Logs of ambient particles sampling on the nuclepore filter.

On board ID	Date Collected					Latitude			Longitude		
	YYYY	MM	DD	hh:mm:ss	UTC/JST	Deg.	Min.	N/S	Deg.	Min.	E/W
MR18-05C-IN-001	2018	10	25	7:56	UTC	40	33.94	N	141	37.47	E
MR18-05C-IN-002	2018	10	27	2:08	UTC	41	27.18	N	152	3.17	E
MR18-05C-IN-003	2018	10	29	0:32	UTC	47	12.58	N	161	48.8	E
MR18-05C-IN-004	2018	10	31	0:42	UTC	53	16.85	N	171	23.42	E
MR18-05C-IN-005	2018	11	2	0:56	UTC	60	40.36	N	176	50.39	W
MR18-05C-IN-006	2018	11	4	0:54	UTC	65	54.83	N	168	41.89	W
MR18-05C-IN-007	2018	11	6	0:40	UTC	73	5.23	N	168	44.23	W
MR18-05C-IN-008	2018	11	8	1:40	UTC	72	15.07	N	158	59.82	W
MR18-05C-IN-009	2018	11	9	23:30	UTC	73	18	N	160	54.98	W
MR18-05C-IN-010	2018	11	12	0:40	UTC	72	44.97	N	162	59.87	W
MR18-05C-IN-011	2018	11	14	0:01	UTC	72	53.39	N	162	28.98	W
MR18-05C-IN-012	2018	11	16	0:14	UTC	72	55.06	N	162	19.46	W
MR18-05C-IN-013	2018	11	18	2:01	UTC	72	44.96	N	163	0.25	W
MR18-05C-IN-014	2018	11	20	1:28	UTC	72	45.22	N	162	59.81	W
MR18-05C-IN-015	2018	11	22	0:17	UTC	71	35.87	N	163	50.9	W
MR18-05C-IN-016	2018	11	25	0:26	UTC	65	40.71	N	168	37.02	W
MR18-05C-IN-017	2018	11	27	23:40	UTC	57	53.09	N	178	1.02	E
MR18-05C-IN-018	2018	11	29	23:57	UTC	52	10.57	N	169	37.04	E
MR18-05C-IN-019	2018	12	2	0:06	UTC	47	23.32	N	161	34.62	E
MR18-05C-IN-020	2018	12	4	0:13	UTC	40	42.73	N	150	51.16	E
MR18-05C-IN-021	2018	12	5	0:09	UTC	38	4.84	N	145	56.22	E

Table 2.8-4: List of snow and rain sampling

On board ID	Date Collected					Latitude			Longitude		
	YYYY	MM	DD	hh:mm:ss	UTC/JST	Deg.	Min.	N/S	Deg.	Min.	E/W
MR1805C-RS-001	2018	10	28	5:00	UTC	44	54.07	N	157	40.49	E
MR1805C-RS-002	2018	10	29	0:35	UTC	47	12.58	N	161	48.80	E
MR1805C-RS-003	2018	10	29	23:40	UTC	49	35.68	N	165	37.46	E
MR1805C-RS-004	2018	10	30	23:40	UTC	53	06.34	N	171	08.90	E
MR1805C-RS-005	2018	10	31	7:35	UTC	54	26.76	N	172	53.25	E
MR1805C-RS-006	2018	11	02	0:50	UTC	60	40.66	N	176	50.00	W
MR1805C-RS-007	2018	11	06	7:40	UTC	73	00.04	N	165	15.19	W
MR1805C-RS-008	2018	11	07	4:30	UTC	73	17.32	N	161	08.78	W
MR1805C-RS-009	2018	11	07	6:30	UTC	73	30.20	N	162	00.18	W
MR1805C-RS-010	2018	11	08	4:30	UTC	71	59.95	N	158	16.45	W
MR1805C-RS-011	2018	11	08	23:10	UTC	72	09.48	N	162	37.69	W
MR1805C-RS-012	2018	11	09	3:00	UTC	71	59.81	N	163	23.39	W
MR1805C-RS-013	2018	11	11	0:00	UTC	73	06.13	N	161	35.15	W
MR1805C-RS-014	2018	11	11	5:30	UTC	72	45.40	N	163	00.15	W
MR1805C-RS-015	2018	11	11	7:50	UTC	72	30.10	N	163	59.83	W
MR1805C-RS-016	2018	11	12	0:40	UTC	72	44.97	N	162	59.09	W
MR1805C-RS-017	2018	11	12	7:55	UTC	72	00.04	N	166	00.02	W
MR1805C-RS-018	2018	11	13	8:00	UTC	72	00.09	N	166	00.02	W
MR1805C-RS-019	2018	11	14	0:00	UTC	72	57.92	N	162	07.82	W
MR1805C-RS-020	2018	11	15	0:00	UTC	73	03.17	N	161	29.25	W
MR1805C-RS-021	2018	11	15	8:00	UTC	72	21.41	N	164	34.49	W
MR1805C-RS-022	2018	11	17	4:41	UTC	72	13.23	N	165	07.29	W
MR1805C-RS-023	2018	11	19	23:50	UTC	72	55.40	N	162	12.66	W
MR1805C-RS-024	2018	11	20	8:00	UTC	72	00.03	N	165	59.50	W
MR1805C-RS-025	2018	11	20	23:50	UTC	73	00.57	N	162	09.27	W
MR1805C-RS-026	2018	11	21	2:00	UTC	72	45.16	N	163	01.91	W
MR1805C-RS-027	2018	11	21	4:08	UTC	72	29.83	N	163	59.75	W
MR1805C-RS-028	2018	11	21	6:24	UTC	72	14.78	N	165	59.45	W
MR1805C-RS-029	2018	11	21	8:50	UTC	71	59.36	N	166	01.41	W
MR1805C-RS-030	2018	11	21	11:00	UTC	71	44.96	N	166	59.99	W
MR1805C-RS-031	2018	11	21	23:30	UTC	71	29.07	N	163	37.80	W
MR1805C-RS-032	2018	11	23	0:04	UTC	69	47.73	N	168	44.59	W
MR1805C-RS-033	2018	11	25	0:30	UTC	66	40.07	N	168	36.30	W
MR1805C-RS-034	2018	11	29	7:35	UTC	53	35.59	N	171	33.70	E
MR1805C-RS-035	2018	11	30	0:00	UTC	52	10.14	N	169	36.39	E
MR1805C-RS-036	2018	12	02	0:00	UTC	47	24.45	N	161	36.39	E
MR1805C-RS-037	2018	12	02	8:50	UTC	46	00.88	N	159	15.27	E
MR1805C-RS-038	2018	12	04	23:50	UTC	38	06.66	N	145	59.47	E
MR1805C-RS-039	2018	12	05	8:43	UTC	37	07.74	N	144	06.02	E

(6) Preliminary results

In the cruise, we obtain several events for black carbon mass concentration and O3, corresponding to Figures 2.8-1 and 2.8-2, respectively. We are going to analyze more detail in the future.

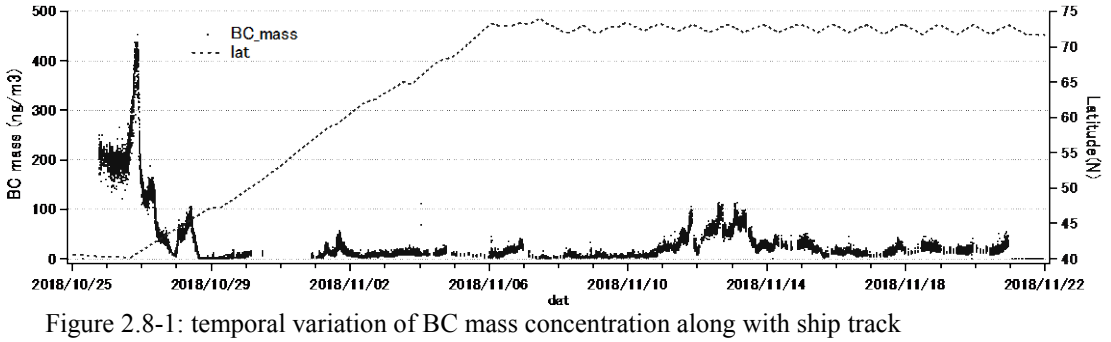

Figure 2.8-1: temporal variation of BC mass concentration along with ship track

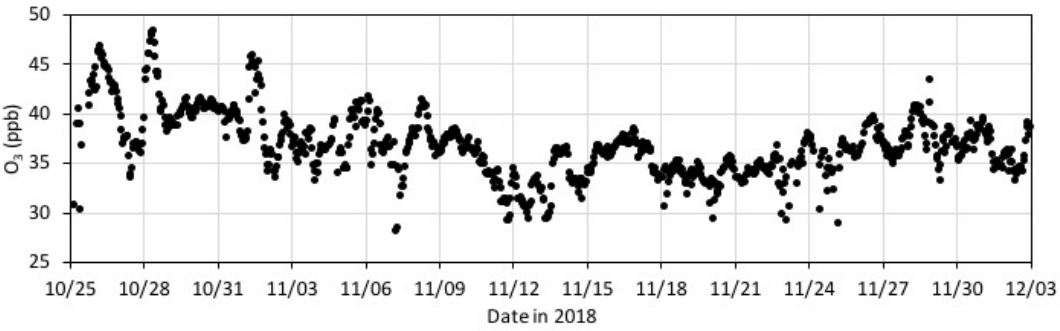

Figure 2.8-2: temporal variation of O3 mass concentration along with ship track

(7) Data archives

These data obtained in this cruise will be submitted to the Data Management Group of JAMSTEC, and will be opened to the public via "Data Research System for Whole Cruise Information in JAMSTEC (DARWIN)" in JAMSTEC web site.

<http://www.godac.jamstec.go.jp/darwin/e>

2.9 Precipitation

2.9.1 Disdrometer

(1) Personnel

Fumikazu Taketani	JAMSTEC	- PI
Masaki Katsumata	JAMSTEC	- not on board
Biao Geng	JAMSTEC	- not on board
Kyoko Taniguchu	JAMSTEC	- not on board

(2) Objectives

The disdrometer can continuously obtain size distribution of raindrops. The objective of this observation is (a) to reveal microphysical characteristics of the rainfall, depends on the type, temporal stage, etc. of the precipitating clouds, (b) to retrieve the coefficient to convert radar reflectivity (especially from C-band radar in Section 2.3) to the rainfall amount, and (c) to validate the algorithms and the products of the satellite-borne precipitation radars; TRMM/PR and GPM/DPR.

(3) Instrumentations and Methods

Two “Laser Precipitation Monitor (LPM)” (Adolf Thies GmbH & Co) are utilized. It is an optical disdrometer. The instrument consists of the transmitter unit which emit the infrared laser, and the receiver unit which detects the intensity of the laser come thru the certain path length in the air. When a precipitating particle fall thru the laser, the received intensity of the laser is reduced. The receiver unit detect the magnitude and the duration of the reduction and then convert them onto particle size and fall speed. The sampling volume, i.e. the size of the laser beam “sheet”, is 20 mm (W) x 228 mm (D) x 0.75 mm (H).

The number of particles are categorized by the detected size and fall speed and counted every minutes. The categories are shown in Table 2.9.1-1.

The LPMs are installed on the top (roof) of the anti-rolling system, as shown in Figure 2.9.1-1. One is installed at the corner at the bow side and the starboard side, while the other at the corner at the bow and the port side. This is to select the data from upwind side.

(4) Preliminary Results

The data have been obtained all through the cruise, except non-permitted territorial waters and EEZs. An example of the obtained data is shown in Figure 2.9.1-2. The further analyses for the rainfall amount, drop-size-distribution parameters, etc., will be carried out after the cruise.

(5) Data Archive

All data obtained during this cruise will be submitted to the JAMSTEC Data Management Group (DMG).

(6) Acknowledgment

The operations are supported by Japan Aerospace Exploration Agency (JAXA) Precipitation Measurement Mission (PMM).

Figure 2.9.1-1: The location of the LPM sensors, on the panorama photo looking down toward the bow (from a tower for the radome of the C-band radar). Red broken circle shows the location of LPM sensors.

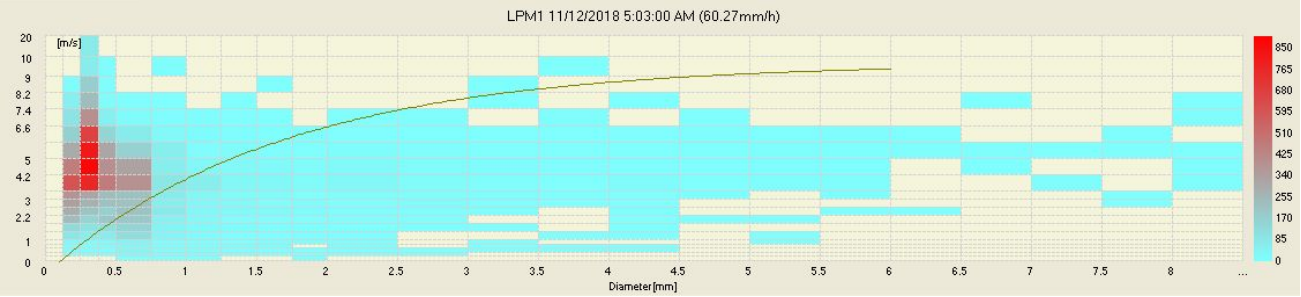

Figure 2.9.1-2: An example of 1-minute raw data, obtained by LPM at 0503UTC on Nov. 12, 2018. Data is shown by two-dimensional histogram to display numbers of observed raindrops categorized by diameter (x-axis) and fall speed (y-axis).

Table 2.9.1-1: Categories of the particle size and the fall speed.

Particle Size			Fall Speed		
Class	Diameter [mm]	Class width [mm]	Class	Speed [m/s]	Class width [m/s]
1	≥ 0.125	0.125	1	≥ 0.000	0.200
2	≥ 0.250	0.125	2	≥ 0.200	0.200
3	≥ 0.375	0.125	3	≥ 0.400	0.200
4	≥ 0.500	0.250	4	≥ 0.600	0.200
5	≥ 0.750	0.250	5	≥ 0.800	0.200
6	≥ 1.000	0.250	6	≥ 1.000	0.400
7	≥ 1.250	0.250	7	≥ 1.400	0.400
8	≥ 1.500	0.250	8	≥ 1.800	0.400
9	≥ 1.750	0.250	9	≥ 2.200	0.400
10	≥ 2.000	0.500	10	≥ 2.600	0.400
11	≥ 2.500	0.500	11	≥ 3.000	0.800
12	≥ 3.000	0.500	12	≥ 3.400	0.800
13	≥ 3.500	0.500	13	≥ 4.200	0.800
14	≥ 4.000	0.500	14	≥ 5.000	0.800
15	≥ 4.500	0.500	15	≥ 5.800	0.800
16	≥ 5.000	0.500	16	≥ 6.600	0.800
17	≥ 5.500	0.500	17	≥ 7.400	0.800
18	≥ 6.000	0.500	18	≥ 8.200	0.800
19	≥ 6.500	0.500	19	≥ 9.000	1.000
20	≥ 7.000	0.500	20	≥ 10.000	10.000
21	≥ 7.500	0.500			
22	≥ 8.000	unlimited			

2.9.2 Micro Rain Radar

(1) Personnel

Fumikazu Taketani	JAMSTEC	- PI
Masaki Katsumata	JAMSTEC	- not on board
Biao Geng	JAMSTEC	- not on board
Kyoko Taniguchi	JAMSTEC	- not on board

(2) Objectives

The micro rain radar (MRR) is a compact vertically-pointing Doppler radar, to detect vertical profiles of rain drop size distribution. The objective of this observation is to understand detailed vertical structure of the precipitating systems.

(3) Instruments and Methods

The MRR-2 (METEK GmbH) was utilized. The specifications are in Table 2.9.2-1. The antenna unit was installed at the starboard side of the anti-rolling systems (see Figure 2.9.2-1), and wired to the junction box and laptop PC inside the vessel.

The data was averaged and stored every one minute. The vertical profile of each parameter was obtained every 100 meters in range distance (i.e. height) up to 3100 meters. The recorded parameters were; Drop size distribution, radar reflectivity, path-integrated attenuation, rain rate, liquid water content and fall velocity.

Figure 2.9.2-1: Photo of the antenna unit of MRR

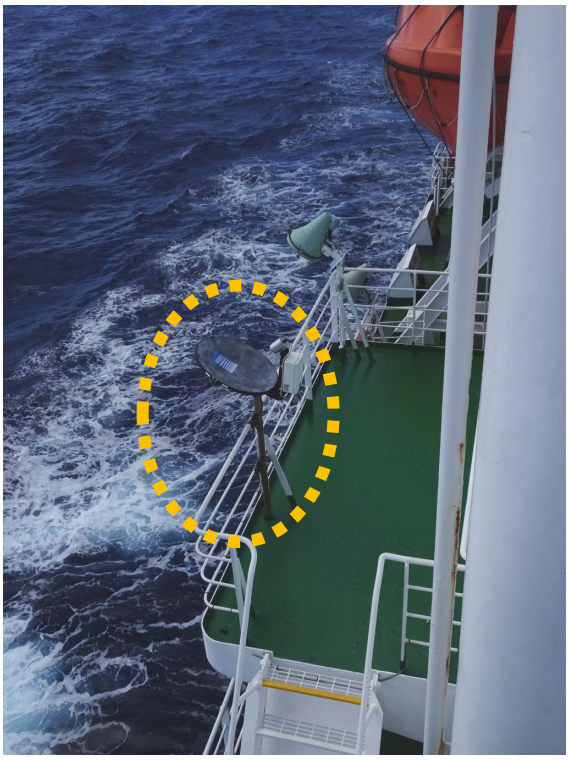

Table 2.9.2-1: Specifications of the MRR-2.

Transmitter power	50 mW
Operating mode	FM-CW
Frequency	24.230 GHz
	(modulation 1.5 to 15 MHz)
3dB beam width	1.5 degrees
Spurious emission	< -80 dBm / MHz
Antenna Diameter	600 mm
Gain	40.1 dBi

(4) Preliminary Results

The data have been obtained all through the cruise, except non-permitted territorial waters and EEZs. Figure 2.9.2-2 displays an example of the time-height cross section for one day. The temporal variation reasonably corresponds to the rainfall measured by the Mirai Surface Met sensors (see Section 2.4), C-band radar (see Section 2.3), etc. The further analyses will be after the cruise.

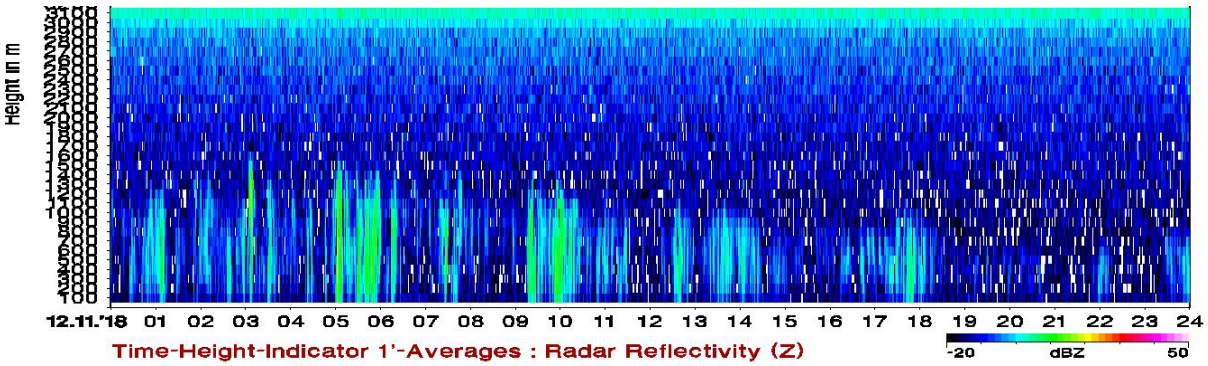

Figure 2.9.2-2: An example of the time-height cross section of the radar reflectivity, for 24 hours from 00UTC on November 12.

(5) Data Archive

All data obtained during this cruise will be submitted to the JAMSTEC Data Management Group (DMG).

(6) Acknowledgment

The operations are supported by Japan Aerospace Exploration Agency (JAXA) Precipitation Measurement Mission (PMM).

2.10 Water vapor

(1) Personnel

Fumikazu Taketani	JAMSTEC	- PI
Masaki Katsumata	JAMSTEC	- not on board
Mikiko Fujita	JAMSTEC	- not on board
Kyoko Taniguchi	JAMSTEC	- not on board

(2) Objective

Recording the GNSS satellite data to estimate the total column integrated water vapor content of the atmosphere.

(3) Instrumentations and Method

The GNSS satellite data was archived to the receiver (Trimble NetR9) with 5 sec interval. The GNSS antenna (Margrin) was set on the roof of radar operation room. The observations were carried out all thru the cruise.

(4) Results

We will calculate the total column integrated water from observed GNSS satellite data after the cruise.

(5) Data archive

Raw data is recorded as T02 format and stream data every 5 seconds. These raw datasets are available from Mikiko Fujita of JAMSTEC. Corrected data will be submitted to JAMSTEC Marine-Earth Data and Information Department and will be archived there.

2.11 Lidar

(1) Personnel

Fumikazu Taketani	JAMSTEC	- PI
Masaki Katsumata	JAMSTEC	- not on board
Kyoko Taniguchi	JAMSTEC	- not on board

(2) Objectives

The objective of this observation is to capture vertical distribution of clouds, aerosols, and water vapor in high temporal and spatial resolutions by measuring backscattering lights from targets.

(3) Instrumentations and Methods

Mirai lidar system transmits 10 Hz pulse laser in three wavelengths: 1064 nm, 532 nm, and 335 nm. For clouds, and aerosol observations, the system detects Mie scattering at these wavelengths The separate detections of parallel and perpendicular components at 532 nm and 355 nm in the system obtain additional characteristics of the targets. The system also detects Raman water vapor signals at 660 nm and 408 nm, and Raman nitrogen signals at 607 nm and 387 nm at nighttime. Based on signal rations of the Raman water vapor and the Raman nitrogen, the system offers water vapor mixing ratio profiles.

(4) Preliminary Results

The lidar system observed lower atmosphere from 24 October, 2018 to 30 November, 2018 UTC in this cruise. All data will be reviewed after the cruise.

Figures 2.11-1 shows preliminary results of 1064 nm and 532 nm obtained on 3 November 2018 UTC. The red colored areas in the top and middle panels of Figures 2.11-1 indicate continuous cloud cover from beginning of the day. The cloud base height is approximately 1 km ASL. Thick aerosol layer (darker blue areas) remains within 1 km even after cloud dissipation at 7:00 UTC. The signal ratios of Raman water vapor and Raman nitrogen illustrate higher water vapor contents within the 1km layer (Figure 2.11-2).

(5) Data Archive

All data obtained during this cruise will be submitted to the JAMSTEC Data Management Group (DMG).

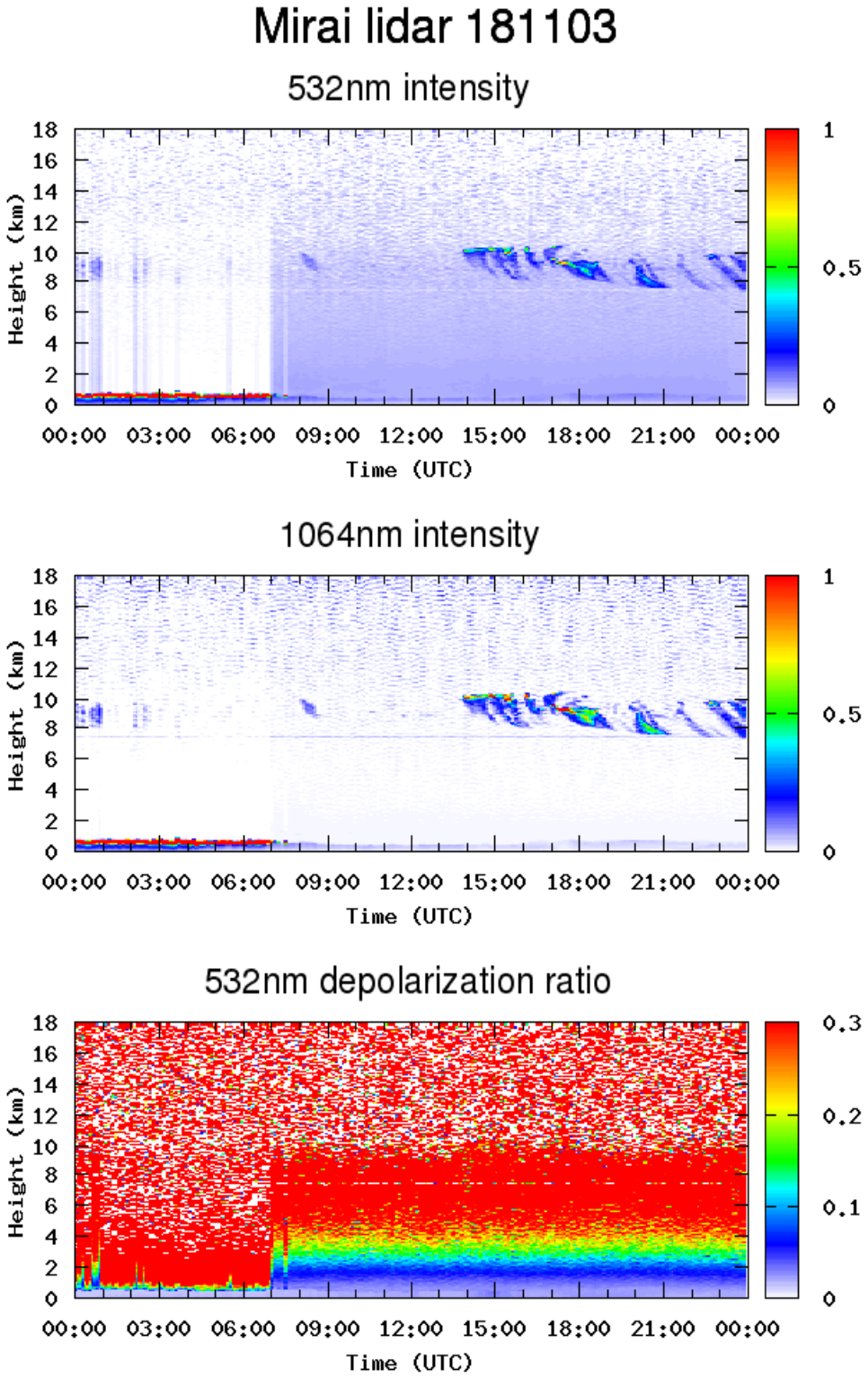

Figure 2.11-1: Preliminary result of 532 nm (top) and 1064 nm (middle) backscattering intensity, and 532 nm depolarization ratio (bottom) obtained on 3 November 2018 UTC.

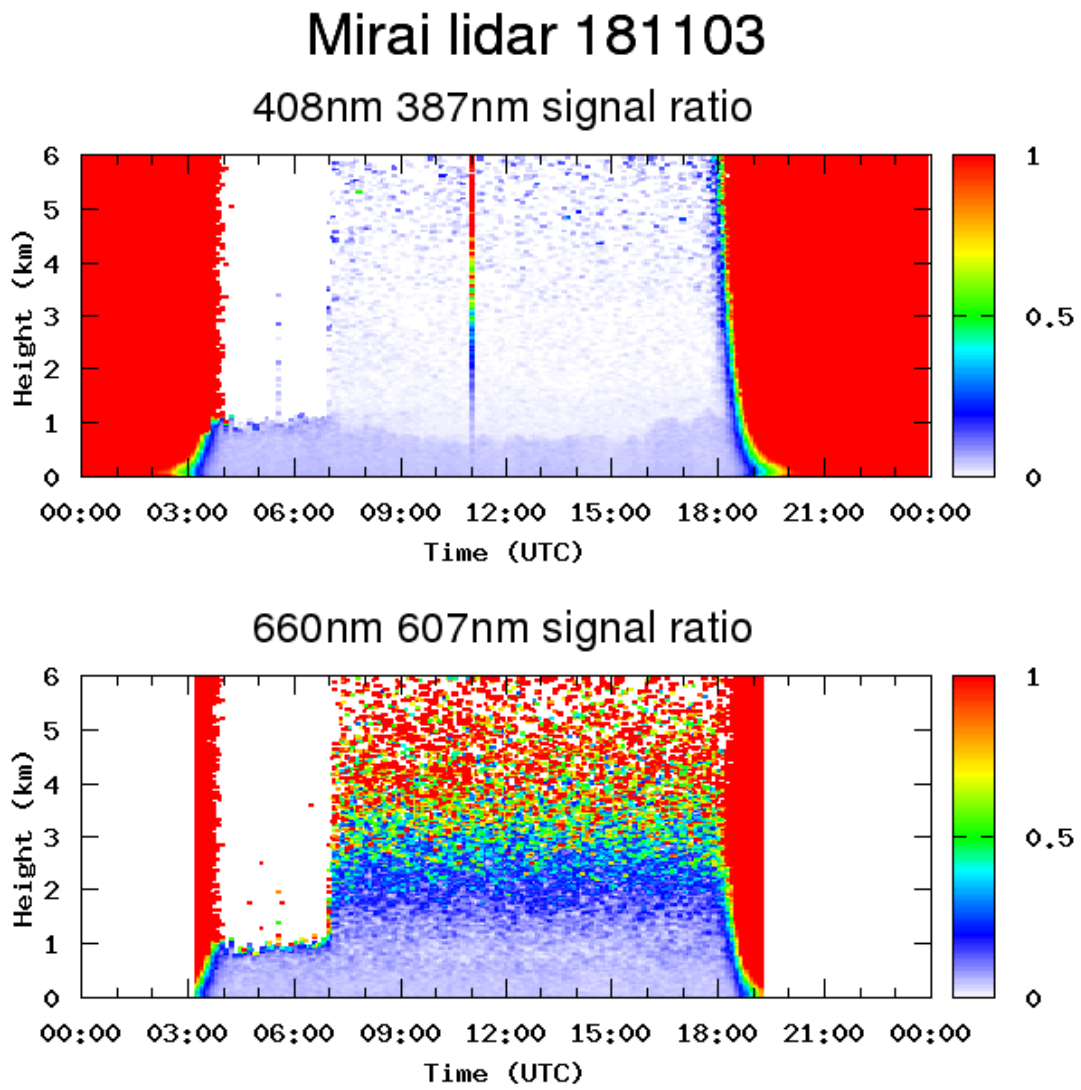

Figure 2.11-2: Preliminary result of Raman water vapor and Raman nitrogen signal ratio obtained on 3 November 2018 UTC. The top panel is the ratio of 408 nm and 387 nm, while the bottom panel is the ratio of 660 nm and 607 nm.

2.12 Greenhouse gasses observation

(1) Personnel

Yasunori Tohjima	NIES	-PI, not on board
Shigeyuki Ishidoya	AIST	- not on board
Fumikazu Taketani	JAMSTEC	
Chunmao Zhu	JAMSTEC	
Shinji Morimoto	Tohoku Univ.	- not on board
Shuji Aoki	Tohoku Univ.	- not on board
Ryo Fujita	Tohoku Univ.	- not on board
Hideki Nara	NIES	- not on board
Daisuke Goto	NIPR	- not on board
Prabir Patra	JAMSTEC	- not on board
Hiroshi Uchida	JAMSTEC	- not on board
Shohei Murayama	AIST	- not on board

(2) Objective

(2-1) Continuous observations of CO_2, CH_4 and CO mixing ratios

The Arctic region is considered to be vulnerable to the global warming, which would potentially enhance emissions of the greenhouse gases including CO_2 and CH_4 from the carbon pools in the Arctic regions into the atmosphere. The objective of this study is to detect the increases in the atmospheric greenhouse gas levels associated with the ongoing global warming in the Arctic region in the early stage. The continuous observations of the atmospheric CO_2 and CH_4 mixing ratios during this MR16-06 cruise would allow us to detect the enhanced mixing ratios associated with the regional emissions and to estimate the distribution of the regional emission sources. The atmospheric CO mixing ratios, which were also observed at the same time, can be used as an indicator of the anthropogenic emissions associated with the combustion processes.

(2-2) Discrete flask sampling

In order to clarify spatial variations and air-sea exchanges of the greenhouse gases at northern high latitude, whole air samples were corrected into 40 stainless-steel flasks on-board R/V MIRAI (MR18-05). The collected air samples will be analyzed for the mixing ratios of CO_2, O_2, Ar, CH_4, CO, N_2O and SF_6 and the stable isotope ratios of CO_2 and CH_4.

(3) Parameters

(3-1) Continuous observations of CO_2, CH_4 and CO mixing ratios

Mixing ratios of atmospheric CO_2, CH_4, and CO.

(3-2) Discrete flask sampling

Mixing ratios of atmospheric CO_2, O_2 (O_2/N_2 ratio), Ar (Ar/N_2 ratio), CH_4, CO, N_2O and SF_6, $d^{13}C$ and $d^{18}O$ of CO_2, $d^{13}C$ and dD of CH_4.

(4) Instruments and Methods

(4-1) Continuous observations of CO_2, CH_4 and CO mixing ratios

Atmospheric CO_2, CH_4, and CO mixing ratios were measured by a wavelength-scanned cavity ring-down spectrometer (WS-CRDS, Picarro, G2401). An air intake, capped with an inverted stainless steel beaker covered with stainless steel mesh, was placed on the right-side of the upper deck. A diaphragm pump (GAST, MOA-P108) was used to draw in the outside air at a flow rate of ~8 L min^{-1}. Water vapor in the sample air was removed to a dew pint of about 2°C and about -35°C by passing it through a thermoelectric dehumidifier (KELK, DH-109) and a Nafion drier (PERMA PURE, PD-50T-24), respectively. Then, the dried sample air was introduced into the WS-CRDS at a flow rate of 100 ml min^{-1}. The WS-CRDS were automatically calibrated every 50 hour by introducing 3 standard airs with known CO_2, CH_4 and CO mixing ratios. The analytical precisions for CO_2, CH_4 and CO mixing ratios are about 0.02 ppm, 0.3 ppb and 3 ppb, respectively.

(4-2) Discrete flask sampling

The air sampling equipment consisted of an air intake, a piston pump (GAST LOA), a water trap, solenoid valves (CKD), an ethanol bath as refrigerant, a flow meter and an immersion cooler (EYELA ECS-80). Ambient air was pumped using a piston pump from an air intake, dried cryogenically and filled into a 1 L stainless-steel flask at a pressure of 0.55 MPa.

(5) Station list or Observation log

The continuous observations of CO_2, CH_4 and CO mixing ratios were conducted during the entire cruise. Sampling logs of the discrete flask sampling are listed in Table 2.12-1.

(6) Data archives

These data obtained in this cruise will be submitted to the Data Management Group (DMG) of JAMSTEC, and will opened to the public via "R/V Mirai Data Web Page" in JAMSTEC home page.

.

Table 2.12-1: List of logs of the discrete flask sampling

On board ID	Date Collected					Latitude			Longitude		
	YYYY	MM	DD	hh:mm:ss	UTC	Deg.	Min.	N/S	Deg.	Min.	E/W
MR1805C-F001	2018	10	26	0:30	UTC	40	17.096	N	145	54.697	E
MR1805C-F002	2018	10	27	0.19653	UTC	41	47.92	N	152	35.55	E
MR1805C-F003	2018	10	28	0.20139	UTC	44	53.106	N	157	38.840	E
MR1805C-F004	2018	10	29	0.19792	UTC	47	12.645	N	161	48.727	E
MR1805C-F005	2018	10	30	0.2	UTC	50	19.0595	N	166	51.2978	E
MR1805C-F006	2018	10	31	0.20556	UTC	53	59.944	N	172	18.56	E
MR1805C-F007	2018	11	01	0.19861	UTC	57	53.634	N	177	55.619	E
MR1805C-F008	2018	11	02	0.20278	UTC	61	19.968	N	175	58.89	W
MR1805C-F009	2018	11	03	0.19931	UTC	64	0.703	N	171	52.295	W
MR1805C-F010	2018	11	04	0.19861	UTC	66	33.076	N	168	44.951	W
MR1805C-F011	2018	11	05	0.18056	UTC	69	30.0381	N	168	44.9561	W
MR1805C-F012	2018	11	06	0.19653	UTC	73	0.395	N	167	5.3245	W
MR1805C-F013	2018	11	07	0.26667	UTC	73	30.148	N	162	0.2526	W
MR1805C-F014	2018	11	08	0.19653	UTC	71	59.9265	N	158	20.6185	W
MR1805C-F015	2018	11	09	0.19722	UTC	72	3.3651	N	164	12.1003	W
MR1805C-F016	2018	11	10	0.19792	UTC	72	44.5353	N	162	59.0955	W
MR1805C-F017	2018	11	11	0.2375	UTC	72	44.0612	N	163	3.2363	W
MR1805C-F018	2018	11	12	0.19097	UTC	72	21.0973	N	164	35.5046	W
MR1805C-F019	2018	11	13	0.19722	UTC	72	18.918	N	164	43.7163	W
MR1805C-F020	2018	11	14	0.16042	UTC	72	28.7377	N	164	5.0433	W
MR1805C-F021	2018	11	15	0.21319	UTC	72	38.13	N	163	25.448	W
MR1805C-F022	2018	11	16	0.18403	UTC	72	27.8445	N	164	8.9236	W
MR1805C-F023	2018	11	17	0.18056	UTC	72	14.992	N	165	0.05	W
MR1805C-F024	2018	11	18	0.18125	UTC	72	29.9711	N	163	59.9276	W
MR1805C-F025	2018	11	19	0.19792	UTC	72	29.8806	N	163	59.942	W
MR1805C-F026	2018	11	20	0.15069	UTC	72	30.092	N	164	0.1396	W
MR1805C-F027	2018	11	21	0.16597	UTC	72	29.7705	N	163	59.4838	W
MR1805C-F028	2018	11	22	0.17361	UTC	71	21.7151	N	163	0.6619	W
MR1805C-F029	2018	11	23	0.33264	UTC	68	20.344	N	168	44.1133	W
MR1805C-F030	2018	11	24	0.00764	UTC	68	2.6742	N	167	46.9818	W
MR1805C-F031	2018	11	25	0.25	UTC	64	40.1687	N	169	6.5	W
MR1805C-F032	2018	11	26	0.19722	UTC	62	47.264	N	173	29.8221	W
MR1805C-F033	2018	11	27	0.21458	UTC	59	52.983	N	176	3.9167	W
MR1805C-F034	2018	11	28	0.16042	UTC	57	15.3766	N	176	58.9801	E
MR1805C-F035	2018	11	29	0.21389	UTC	53	51.2348	N	171	56.1537	E
MR1805C-F036	2018	11	30	0.14931	UTC	51	48.4757	N	169	7.6067	E
MR1805C-F037	2018	12	01	0.21389	UTC	49	34.8277	N	165	26.0274	E
MR1805C-F038	2018	12	02	0.02639	UTC	47	18.3638	N	161	26.3817	E
MR1805C-F039	2018	12	03	0.19444	UTC	43	43.1	N	155	30.56	E
MR1805C-F040	2018	12	04	0.14514	UTC	40	11.4559	N	150	03.5101	E

2 .13 Sea ice radar

(1) Personnel

Jun Inoue	NIPR	-PI
Kazuho Yoshida	NME	
Souichiro Sueyoshi	NME	
Shinya Okumura	NME	
Takehito Hattori	MIRAI Crew	

(2) Objectives

In the sea ice areas, a marine radar is an important tool for the detection of sea ice and icebergs. In order to decide the route optimally in the ice-covered area, radar images can be applied to the route search algorithm. Those images would be useful to develop the system.

(3) Parameters

Capture format: JPEG

Capture interval: 30 seconds

Resolution: 1,280×1,024 pixel

Color tone: 256 gradation

(4) Instruments and methods

R/V MIRAI is equipped with an Ice Navigation Radar, “sigma S6 Ice Navigator (Rutter Inc.)”. The ice navigation radar, the analog signal from the x-band radar is converted by a modular radar interface and displayed as a digital video image (Figure 2.12-1). The sea ice radar is equipped with a screen capture function and saves at arbitrary time intervals.

(5) Observation Period

04 Nov. 2018 - 25 Nov. 2017

(6) Data archives

These data obtained in this cruise will be submitted to the Data Management Group of JAMSTEC, and will be opened to the public via “Data Research System for Whole Cruise Information in JAMSTEC (DARWIN)” in JAMSTEC web site.

<http://www.godac.jamstec.go.jp/darwin/e>

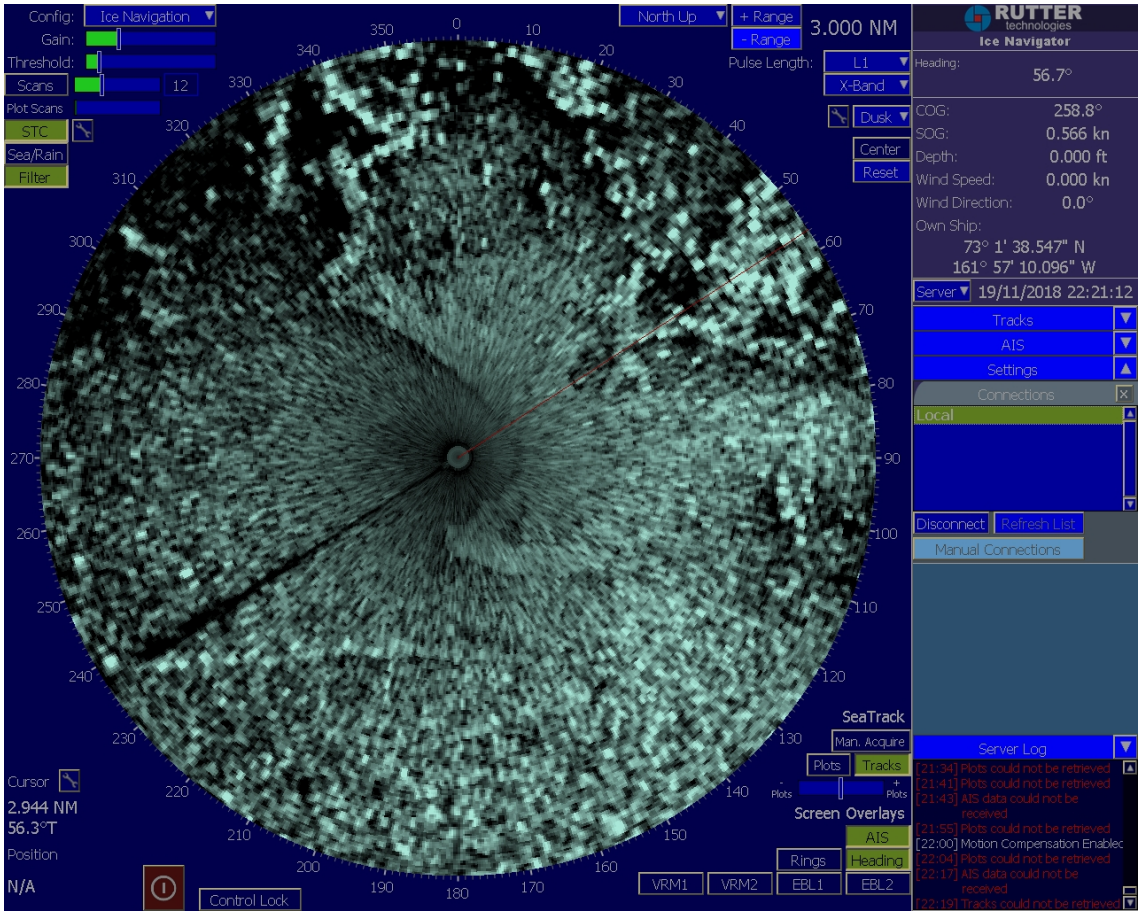

Figure 2.12-1: An example of a sea-ice image by the sea ice radar

3. Physical Oceanography

3.1. CTD cast and water sampling

(1) Personnel

Jun Inoue	NIPR	- PI
Rio Kobayashi	MWJ	
Kenich Katayama	MWJ	
Shungo Oshitani	MWJ	
Keisuke Takeda	MWJ	

(2) Objective

Investigation of oceanic structure and water sampling.

(3) Parameters

Temperature (Primary and Secondary)
Conductivity (Primary and Secondary)
Pressure
Dissolved Oxygen (Primary “RINKOIII” and Secondary “SBE43”)
Fluorescence (Primary and Secondary)
Beam Transmission
Turbidity
Altimeter

(4) Instruments and Methods

CTD/Carousel Water Sampling System, which is a 36-position Carousel Water Sampler (CWS) with Sea-Bird Electronics, Inc. CTD (SBE9plus), was used during Sta1. 12-liter sample Bottles were used for sampling seawater. The sensors attached on the CTD were temperature (primary and secondary), conductivity (primary and secondary), pressure, dissolved oxygen (primary:RINKOIII, secondary:SBE43), fluorescence (primary and secondary), beam transmission, turbidity and altimeter. Salinity was calculated by measured values of pressure, conductivity and temperature. The CTD/CWS was deployed from starboard on working deck.

Specifications of the sensors are listed below.

Two sets of temperature, conductivity and dissolved oxygen (SBE43) were prepared for backup. “SET_A” used for CTD cast 001M001, “SET_B” used for CTD cast 001M002 – 002M002.

CTD: SBE911plus CTD system

Under water unit: SBE9plus (S/N: 09P54451-1027, Sea-Bird Electronics, Inc.)

Pressure sensor: Digiquartz pressure sensor (S/N: 117457)

Calibrated Date: 26 Feb. 2018

Carousel water sampler: SBE32 (S/N: 3227443-0391, Sea-Bird Electronics, Inc.)

Temperature sensors:

SET_A

Primary: SBE03-04/F (S/N: 031464, Sea-Bird Electronics, Inc.)

Calibrated Date: 23 Feb. 2018

Secondary: SBE03-04/F (S/N: 031524, Sea-Bird Electronics, Inc.)

Calibrated Date: 27 Feb. 2018

SET_B

Primary: SBE03-04/F (S/N: 031525, Sea-Bird Electronics, Inc.)

Calibrated Date: 22 Feb. 2018

Secondary: SBE03-04/F (S/N: 031359, Sea-Bird Electronics, Inc.)

Calibrated Date: 03 May. 2018

Conductivity sensors:

SET_A

Primary: SBE04C (S/N: 043036, Sea-Bird Electronics, Inc.)

Calibrated Date: 16 Feb. 2018

Secondary: SBE04-02/0 (S/N: 041206, Sea-Bird Electronics, Inc.)

Calibrated Date: 15 Feb. 2018

SET_B

Primary: SBE04C (S/N: 042435, Sea-Bird Electronics, Inc.)

Calibrated Date: 15 Feb. 2018

Secondary: SBE04C (S/N: 042854, Sea-Bird Electronics, Inc.)

Calibrated Date: 16 Feb. 2018

Dissolved Oxygen sensor:

Primary: RINKOIII (S/N: 0287_163011BA, JFE Advantech Co., Ltd.)

Calibrated Date: 05 Oct. 2018

SET_A

Secondary: SBE43 (S/N: 430330, Sea-Bird Electronics, Inc.)

Calibrated Date: 06 Feb. 2018

SET_B

Secondary: SBE43 (S/N: 432211, Sea-Bird Electronics, Inc.)

Calibrated Date: 03 Feb. 2018

Fluorescence:

Primary: Chlorophyll Fluorometer (S/N: 3618, Seapoint Sensors, Inc.)

Gain setting: 30X, 0-5 ug/l

Calibrated Date: None

Offset: 0.000

Secondary: Chlorophyll Fluorometer (S/N: 3700, Seapoint Sensors, Inc.)

Gain setting: 3X, 0-50 ug/l

Calibrated Date: None

Offset: 0.000

Transmission meter: C-Star (S/N CST-1726DR, WET Labs, Inc.)

Calibrated Date: 27 Aug. 2018

Turbidity: Turbidity Meter (S/N: 14953)

Gain setting: 100X

Scale factor: 1.000

Calibrated Date: None

Altimeter: Benthos PSA-916T (S/N: 1157, Teledyne Benthos, Inc.)

Submersible Pump:

Primary: SBE5T (S/N: 055816, Sea-Bird Electronics, Inc.)

Secondary: SBE5T (S/N: 054595, Sea-Bird Electronics, Inc.)

Bottom contact switch: (Sea-Bird Electronics, Inc.)

Deck unit: SBE11plus (S/N 11P54451-0872, Sea-Bird Electronics, Inc.)

Configuration file: MR1805C_A.xmlcon (SET_A)
001M001
MR1805C_B.xmlcon (SET_B)
001M002 – 002M002

The CTD raw data were acquired on real time using the Seasave-Win32 (ver.7.23.2) provided by Sea-Bird Electronics, Inc. and stored on the hard disk of the personal computer. Seawater was sampled during the up cast by sending fire commands from the personal computer.

For depths where vertical gradient of water properties were exchanged to be large, the bottle was exceptionally fired after waiting from the stop for 60 seconds to enhance exchanging the water between inside and outside of the bottle. 30 seconds below thermocline to stabilize then fire. 164 casts of CTD measurements were conducted (Table 3.1-1).

Data processing procedures and used utilities of SBE Data Processing-Win32 (ver.7.26.7.114) and SEASOFT were as follows:

(The process in order)

DATCNV: Convert the binary raw data to engineering unit data. DATCNV also extracts bottle information where scans were marked with the bottle confirm bit during acquisition. The duration was set to 3.0 seconds, and the offset was set to 0.0 seconds.

TCORP (original module): Corrected the pressure sensitivity of the temperature (SBE3) sensor.
S/N 031464: -7.75293156e-09 (degC/dbar)
S/N 031524: -2.5868e-07 (degC/dbar)
S/N 031525: 1.714e-08 (degC/dbar)
S/N 031359: -2.29885054e-007 (degC/dbar)

RINKOCOR (original module): Corrected the time dependent, pressure induced effect (hysteresis) of the RINKOIII profile data.

RINKOCORROS (original module): Corrected the time dependent, pressure induced effect (hysteresis) of the RINKOIII bottle information data by using the hysteresis

corrected profile data.

BOTTLESUM: Create a summary of the bottle data. The data were averaged over 3.0 seconds.

ALIGNCTD: Convert the time-sequence of sensor outputs into the pressure sequence to ensure that all calculations were made using measurements from the same parcel of water. Dissolved oxygen data are systematically delayed with respect to depth mainly because of the long time constant of the dissolved oxygen sensor and of an additional delay from the transit time of water in the pumped pluming line. This delay was compensated by 2 seconds advancing dissolved oxygen sensor (SBE43) output (dissolved oxygen voltage) relative to the temperature data. RINKOIII voltage (User polynomial 0) was advanced 1 second, transmission data, beam attenuation and transmission voltage were advanced 2 seconds.

WILDEDIT: Mark extreme outliers in the data files. The first pass of WILDEDIT obtained the accurate estimate of the true standard deviation of the data. The data were read in blocks of 1000 scans. Data greater than 10 standard deviations were flagged. The second pass computed a standard deviation over the same 1000 scans excluding the flagged values. Values greater than 20 standard deviations were marked bad. This process was applied to pressure, depth, temperature, conductivity, dissolved oxygen voltage (RINKO III and SBE43).

CELLTM: Remove conductivity cell thermal mass effects from the measured conductivity. Typical values used were thermal anomaly amplitude alpha = 0.03 and the time constant 1/beta = 7.0.

FILTER: Perform a low pass filter on pressure and depth data with a time constant of 0.15 second. In order to produce zero phase lag (no time shift) the filter runs forward first then backward

WFILTER: Perform a median filter to remove spikes in the fluorescence data (primary and secondary), transmission data, transmission beam attenuation, transmission voltage, turbidity. A median value was determined by 49 scans of the window.

SECTIONU (original module of SECTION): Select a time span of data based on scan number in order to reduce a file size. The minimum number was set to be the starting time when the CTD package was beneath the sea-surface after activation of the pump. The maximum number of was set to be the end time when the package came up from the surface.

LOOPEDIT: Mark scans where the CTD was moving less than the minimum velocity of 0.0 m/s (traveling backwards due to ship roll).

DESPIKE (original module): Remove spikes of the data. A median and mean absolute deviation was calculated in 1-dbar pressure bins for both down and up cast, excluding the flagged values. Values greater than 4 mean absolute deviations from the median were marked bad for each bin. This process was performed twice for temperature, conductivity and dissolved oxygen (RINKOIII and SBE43) voltage.

DERIVE: Compute dissolved oxygen (SBE43).

BINAVG: Average the data into 1-dbar pressure bins.

BOTTOMCUT (original module): Deletes discontinuous scan bottom data, when it's created by BINAVG.

DERIVE: Compute salinity, potential temperature, and sigma-theta.

SPLIT: Separate the data from the input .cnv file into down cast and up cast files.

(5) Station list

During this cruise, 164 casts of CTD observation were carried out. Date, time and locations of the CTD casts are listed in Table 3.1-1. In bottom attack of shallow casts, bottom contact switch was also used.

(6) Preliminary Results

During this cruise, we judged noise, spike or shift in the data of some casts. These were as follows.

001M001: Dissolved Oxygen (SBE43) voltage

Down 51 db – 57 db: spike

001M002: Turbidity

Up 1970 db – 1 db: noise

005M001: Primary Salinity

Down 59 db – 66 db: shift

006M001: Beam Transmission voltage

Down 20 db – 23 db: spike

Down 59 db – 62 db: spike

030M001: Beam Transmission voltage

Down 4 db - 7 db: spike

Turbidity

Down 4 db – 7 db: spike

042M001: Secondary Fluorescence

Down 197 db – Down 205 db: spike

044M001: Beam Transmission voltage

Down 36 db – 39 db: spike

050M001: Beam Transmission voltage

Down 4 db – 6 db: spike

Primary Fluorescence

Down 27 db – 35 db: spike

051M001: Primary Fluorescence

Down 21 db – 24 db: spike

042M002: Beam Transmission voltage

Down 57 db – 62 db: spike

064M001: Primary Temperature

Down 67 db – 104 db: shift

Primary Salinity

Down 67 db – 104 db: shift

Dissolved Oxygen (SBE43)

Down 67 db – 104 db: shift

048M003: Primary Salinity

Down 91 db – 93 db: spike

Secondary Temperature

Down 38 db – 41 db: spike

Secondary Salinity

Down 38 db – 41 db: spike

066M001: Turbidity

Down 36 db – 54 db: spike

056M005: Secondary Salinity

Down 47 db – 50 db: spike

056M007: Primary Fluorescence

Down 42 db – 44 db: spike

058M007: Beam Transmission voltage

Down 2 db - 4 db: spike

Turbidity

Down 2 db – 5 db: spike

065M006: Beam Transmission voltage

Down 3 db – 5 db: spike

Turbidity

Down 2 db – 5 db: spike

058M007: Beam Transmission voltage

Down 3 db – 5 db: spike

Turbidity

Down 3 db – 9 db: spike

058M010: Beam Transmission voltage

Down 3 db – 5 db: bad data

Turbidity

Down 3 db – 6 db: bad data

062M010: Beam Transmission voltage

Down 35 db – 40 db: spike

065M007: Beam Transmission voltage

Down 2 db – 4 db: spike

068M011: Beam Transmission voltage

Down 25 db – 34 db: spike

067M003: Beam Transmission voltage

Down 2 db – 5 db: spike

Turbidity

Down 1 db – 8 db: bad data

048M012: Primary Temperature

Down 10 db – Up 19 db: shift

Primary Salinity

Down 10 db – Up 11 db: shift

Dissolved Oxygen (SBE43)

Down 10 db – 12 db: shift

067M004: Primary Temperature

Primary Salinity

Secondary Temperature

Secondary Salinity

Dissolved Oxygen (SBE43 and RINKOIII)

Down and Up : bad data

Beam Transmission voltage

Down 1 db – 3 db: spike

Turbidity

Down 1 db – 3 db: spike

069M001: Primary Temperature

Down 28 db: spike

Down 30 db – 33 db: spike

Primary Salinity

Down 28 db: spike

Down 31 db – 32 db: spike

073M001: Beam Transmission voltage

Down 2 db – 5 db: spike

Turbidity

Down 2 db – 5 db: spike

019M002: Turbidity

Down 35 db – 39 db: Range out

007M002: Beam Transmission voltage

Down 2 db – 4 db: spike

004M002: Beam Transmission voltage

Down 2 db – 5 db: spike

002M002: Beam Transmission voltage

Down 53 db – 61 db: spike

(7) Data archive

These data obtained in this cruise will be submitted to the Data Management Group of JAMSTEC, and will be opened to the public via "Data Research System for Whole Cruise Information in JAMSTEC (DARWIN)" in JAMSTEC web site.

<http://www.godac.jamstec.go.jp/darwin/e>

(8) Others

067M004: Temperature (primary and secondary), Salinity (primary and secondary) and Dissolved Oxygen (SBE43 and RINKOIII) were bad data in this cast because primary and secondary pump was not working during observation.

Table 3.1-1: MR18-05C CTD cast table

Stnnbr	Castno	Date(UTC)	Time(UTC)		BottomPosition		Depth (m)	Wire Out (m)	HT Above Bottom (m)	Max Depth (m)	Max Pressure (dbar)	CTD Filename	Remark
		(mmddyy)	Start	End	Latitude	Longitude							
001	1	102918	00:18	02:20	47-12.63N	161-48.73E	5612.0	1981.8	-	1975.9	2002.0	001M001	SET_A calibration cast
001	2	102918	04:06	06:04	47-12.63N	161-48.73E	5612.0	1978.1	-	1974.9	2001.0	001M002	SET_B calibration cast
002	1	110218	09:24	09:30	62-00.85N	175-04.04W	79.6	69.1	5.7	73.3	74.0	002M001	DBO1.1
003	1	110218	10:17	10:23	62-03.16N	175-13.06W	81.0	73.7	5.0	75.3	76.0	003M001	DBO1.2
004	1	110218	12:14	12:22	62-13.40N	174-52.73W	76.0	64.7	4.4	70.3	71.0	004M001	DBO1.3
005	1	110218	13:50	13:55	62-23.50N	174-34.20W	70.8	60.8	5.1	65.4	66.0	005M001	DBO1.4
006	1	110218	15:30	15:36	62-28.15N	174-05.27W	68.2	59.7	4.6	62.4	63.0	006M001	DBO1.5
007	1	110218	17:23	17:28	62-33.67N	173-33.24W	66.6	55.3	5.2	59.4	60.0	007M001	DBO1.6
008	1	110218	18:59	19:05	62-47.18N	173-30.34W	67.9	58.4	4.5	63.4	64.0	008M001	DBO1.7
009	1	110218	20:41	20:48	63-01.80N	173-27.84W	71.8	63.9	4.1	66.3	67.0	009M001	DBO1.8
010	1	110218	22:42	22:48	63-16.93N	173-05.38W	69.2	60.6	4.2	64.4	65.0	010M001	DBO1.9
011	1	110318	01:34	01:37	63-36.25N	172-35.54W	53.6	42.1	5.3	48.5	49.0	011M001	DBO1.10
012	1	110318	10:28	10:34	64-40.35N	169-55.08W	47.5	39.7	4.9	41.6	42.0	012M001	DBO2.1
013	1	110318	12:36	12:41	64-57.69N	169-53.42W	47.9	39.0	5.0	42.6	43.0	013M001	DBO2.4
014	1	110318	14:32	14:37	64-59.48N	169-08.40W	48.8	39.7	5.3	42.6	43.0	014M001	DBO2.5
015	1	110318	16:29	16:33	64-40.87N	169-05.73W	46.0	37.3	5.2	39.6	40.0	015M001	DBO2.2
016	1	110318	18:36	18:39	64-40.28N	168-13.87W	38.6	31.6	5.1	32.7	33.0	016M001	DBO2.3
017	1	110418	01:35	01:39	65-59.75N	168-45.12W	53.4	44.8	4.6	48.5	49.0	017M001	
018	1	110418	04:20	04:25	66-30.00N	168-45.05W	54.1	47.6	4.1	49.5	50.0	018M001	
019	1	110418	07:15	07:20	67-00.10N	168-44.90W	45.6	36.8	4.4	40.6	41.0	019M001	

020	1	110418	09:56	10:00	67-30.12N	168-44.98W	49.5	41.7	5.6	43.6	44.0	020M001	
021	1	110418	11:11	11:15	67-40.99N	168-55.09W	50.2	41.3	4.4	45.5	46.0	021M001	DBO3.8
022	1	110418	12:23	12:28	67-47.00N	168-35.93W	50.7	41.5	6.1	43.6	44.0	022M001	DBO3.7
023	1	110418	13:34	13:40	67-53.86N	168-14.44W	57.7	49.1	4.7	52.5	53.0	023M001	DBO3.6
024	1	110418	14:49	14:54	68-00.86N	167-52.19W	53.4	45.2	4.6	47.5	48.0	024M001	DBO3.5
025	1	110418	16:06	16:11	68-07.82N	167-29.83W	50.3	40.4	5.3	43.6	44.0	025M001	DBO3.4
026	1	110418	16:55	17:00	68-11.27N	167-18.74W	48.3	39.9	4.0	43.6	44.0	026M001	DBO3.3
027	1	110418	17:53	17:58	68-14.66N	167-07.83W	43.5	34.7	4.4	38.6	39.0	027M001	DBO3.2
028	1	110418	18:43	18:47	68-18.07N	166-56.34W	34.7	25.7	4.7	29.7	30.0	028M001	DBO3.1
029	1	110418	22:24	22:28	68-29.92N	168-44.72W	54.1	45.4	5.6	47.5	48.0	029M001	
030	1	110518	01:39	01:44	69-00.13N	168-44.60W	52.1	43.7	4.5	47.5	48.0	030M001	
031	1	110518	04:28	04:33	69-30.15N	168-44.85W	52.1	41.5	4.3	46.5	47.0	031M001	
032	1	110518	07:21	07:24	69-59.91N	168-45.11W	40.4	33.3	4.7	35.6	36.0	032M001	
033	1	110518	10:06	10:09	70-29.99N	168-44.75W	38.9	30.0	5.6	32.7	33.0	033M001	
034	1	110518	12:52	12:57	71-00.08N	168-44.95W	44.3	36.0	5.2	38.6	39.0	034M001	
035	1	110518	15:35	15:40	71-30.03N	168-44.86W	48.6	39.7	4.9	42.6	43.0	035M001	
036	1	110518	18:21	18:27	72-00.03N	168-44.97W	50.5	40.2	4.4	45.5	46.0	036M001	
037	1	110518	21:09	21:12	72-30.04N	168-44.94W	57.7	50.0	5.3	52.4	53.0	037M001	
038	1	110618	00:01	00:06	72-59.88N	168-45.14W	62.4	52.6	4.3	56.4	57.0	038M001	
039	1	110618	01:41	01:47	73-15.08N	168-45.07W	78.1	69.6	5.5	72.2	73.0	039M001	
040	1	110618	16:05	16:15	73-00.17N	159-59.98W	198.0	184.7	10.2	188.9	191.0	040M001	wave buoy deploy
041	1	110618	20:57	21:20	73-16.88N	158-59.12W	1698.0	531.8	-	500.2	506.0	041M001	wave buoy deploy
042	1	110718	03:51	04:08	73-15.33N	161-00.12W	367.0	353.7	8.1	355.0	359.0	042M001	
043	1	110718	06:24	06:33	73-30.19N	162-00.21W	196.0	182.3	10.4	185.0	187.0	043M001	

044	1	110718	08:42	08:51	73-45.02N	163-00.54W	198.0	181.0	10.7	183.0	185.0	044M001	
045	1	110718	10:57	11:08	73-59.89N	163-59.94W	253.0	241.1	9.9	243.3	246.0	045M001	
046	1	110718	14:05	14:12	73-30.07N	164-00.07W	111.0	95.7	10.9	98.0	99.0	046M001	
047	1	110718	16:23	16:29	73-15.09N	163-00.17W	98.3	85.3	10.5	87.1	88.0	047M001	
048	1	110718	18:53	18:59	73-00.02N	162-00.04W	111.2	95.4	9.2	98.0	99.0	048M001	
049	1	110718	21:09	21:13	72-45.02N	160-59.80W	52.3	45.2	4.1	47.5	48.0	049M001	
050	1	110718	23:22	23:26	72-30.09N	160-00.01W	47.6	39.1	4.5	42.6	43.0	050M001	
051	1	110818	01:40	01:44	72-15.07N	158-59.84W	51.3	42.1	5.4	45.5	46.0	051M001	
052	1	110818	03:58	04:03	71-59.99N	158-00.19W	64.9	55.3	4.7	59.4	60.0	052M001	
053	1	110818	07:40	07:44	71-59.93N	159-59.67W	29.9	21.7	5.2	23.8	24.0	053M001	
054	1	110818	10:04	10:07	72-14.93N	160-59.89W	35.1	26.8	4.8	29.7	30.0	054M001	
055	1	110818	12:32	12:36	72-29.88N	161-59.81W	41.2	32.9	5.4	35.6	36.0	055M001	
056	1	110818	14:49	14:54	72-44.97N	162-59.68W	57.4	48.0	5.6	51.5	52.0	056M001	
057	1	110818	17:10	17:15	73-00.03N	164-00.22W	82.4	75.0	5.6	77.2	78.0	057M001	
058	1	110818	20:05	20:08	72-30.13N	163-59.88W	49.4	41.3	4.2	44.5	45.0	058M001	
059	1	110818	22:18	22:21	72-14.94N	163-00.34W	39.9	32.9	4.7	34.6	35.0	059M001	
060	1	110918	00:52	00:55	72-00.11N	162-00.34W	31.2	23.7	5.1	25.7	26.0	060M001	
061	1	110918	04:10	04:14	72-00.10N	163-59.92W	39.9	32.7	4.8	34.6	35.0	061M001	
062	1	110918	06:39	06:45	72-15.02N	164-59.88W	45.8	38.0	4.5	40.6	41.0	062M001	
063	1	110918	22:47	23:00	73-17.79N	160-55.00W	367.0	360.5	5.4	358.9	363.0	063M001	MIZ
042	2	111018	00:10	00:25	73-15.14N	161-00.71W	374.0	371.4	4.6	370.8	375.0	042M002	
048	2	111018	02:32	02:39	73-00.15N	161-59.37W	114.0	100.5	9.7	101.9	103.0	048M002	
056	2	111018	05:38	05:42	72-45.26N	162-58.06W	57.8	49.8	4.9	52.4	53.0	056M002	
058	2	111018	07:58	08:02	72-30.03N	163-59.75W	49.4	40.8	5.2	43.5	44.0	058M002	

062	2	111018	10:43	10:47	72-15.01N	164-59.89W	46.0	36.9	4.8	40.6	41.0	062M002	
064	1	111018	22:01	22:15	73-08.12N	161-23.26W	250.0	238.5	9.4	238.4	241.0	064M001	MIZ
048	3	111118	01:03	01:11	72-59.95N	161-59.21W	112.0	99.8	8.5	100.9	102.0	048M003	
056	3	111118	03:29	03:34	72-45.04N	162-59.69W	57.9	49.4	5.4	51.5	52.0	056M003	
058	3	111118	07:42	07:47	72-30.05N	163-59.89W	49.6	42.1	5.2	43.5	44.0	058M003	
062	3	111118	10:44	10:48	72-14.99N	164-59.85W	46.4	38.4	4.9	40.6	41.0	062M003	
064	2	111118	20:46	20:56	73-06.60N	161-35.18W	198.0	189.6	10.3	188.9	191.0	064M002	MIZ
048	4	111118	22:25	22:31	73-00.04N	162-00.01W	108.0	100.0	9.9	100.9	102.0	048M004	
056	4	111218	00:58	01:03	72-45.03N	162-59.76W	57.9	50.7	4.8	52.4	53.0	056M004	
058	4	111218	03:17	03:22	72-30.04N	163-59.92W	49.7	41.7	5.2	43.5	44.0	058M004	
062	4	111218	05:40	05:45	72-15.13N	164-59.47W	45.7	38.6	5.6	39.6	40.0	062M004	
065	1	111218	07:58	08:02	72-00.06N	166-00.01W	45.9	39.1	4.7	40.6	41.0	065M001	
066	1	111218	20:50	20:58	73-04.59N	161-45.95W	158.0	153.1	9.8	153.3	155.0	066M001	MIZ
048	5	111218	22:21	22:28	72-59.96N	161-59.70W	108.0	97.2	9.4	98.9	100.0	048M005	
056	5	111318	00:50	00:55	72-45.18N	162-59.76W	57.5	50.7	5.6	51.5	52.0	056M005	
058	5	111318	03:10	03:15	72-29.98N	164-00.20W	49.0	38.8	4.8	43.5	44.0	058M005	
062	5	111318	05:38	05:42	72-15.05N	165-00.29W	44.5	34.9	5.4	39.6	40.0	062M005	
065	2	111318	07:58	08:02	72-00.10N	166-00.49W	46.0	37.3	4.7	40.6	41.0	065M002	
066	2	111318	21:12	21:20	73-04.53N	161-47.37W	159.0	148.5	9.8	149.4	151.0	066M002	MIZ
048	6	111318	22:47	22:54	73-00.01N	161-59.73W	113.0	100.0	9.3	100.9	102.0	048M006	
056	6	111418	01:16	01:21	72-44.86N	162-59.73W	57.5	50.9	4.7	52.4	53.0	056M006	
058	6	111418	03:33	03:37	72-29.94N	164-00.32W	48.9	41.7	4.8	43.5	44.0	058M006	
062	6	111418	05:48	05:52	72-14.96N	165-00.05W	45.7	35.3	5.3	39.6	40.0	062M006	
065	3	111418	08:10	08:14	71-59.92N	165-59.96W	45.6	36.4	5.4	39.6	40.0	065M003	

064	3	111418	21:46	21:58	73-07.91N	161-33.69W	261.0	253.6	9.4	255.2	258.0	064M003	MIZ
056	7	111518	03:55	04:00	72-44.98N	162-59.46W	57.8	48.5	6.2	51.5	52.0	056M007	
058	7	111518	06:43	06:47	72-30.03N	163-59.58W	49.0	38.4	5.1	43.5	44.0	058M007	
062	7	111518	09:03	09:07	72-15.03N	165-00.01W	46.0	35.6	5.6	39.6	40.0	062M007	
065	4	111518	11:20	11:24	72-00.04N	166-00.22W	45.6	36.9	4.5	40.6	41.0	065M004	
066	3	111518	21:13	21:22	73-06.26N	161-52.57W	199.0	186.7	9.7	187.0	189.0	066M003	MIZ
048	8	111518	23:16	23:22	73-00.02N	162-00.28W	109.0	97.2	9.9	98.0	99.0	048M008	
056	8	111618	01:44	01:49	72-44.94N	163-00.14W	57.2	51.1	4.8	52.4	53.0	056M008	
058	8	111618	04:00	04:04	72-30.00N	164-00.19W	48.9	39.9	4.8	43.5	44.0	058M008	
062	8	111618	06:17	06:20	72-14.98N	165-00.23W	45.1	36.8	4.4	40.6	41.0	062M008	
065	5	111618	08:27	08:32	71-59.99N	166-00.42W	45.8	37.7	5.7	39.6	40.0	065M005	
048	9	111618	20:45	20:51	73-00.90N	162-02.03W	116.0	100.7	10.1	101.9	103.0	048M009	MIZ
056	9	111618	23:41	23:45	72-45.13N	162-59.34W	57.3	52.6	4.5	53.4	54.0	056M009	
058	9	111718	02:03	02:07	72-30.13N	164-00.04W	49.0	41.7	5.2	43.5	44.0	058M009	
062	9	111718	04:18	04:21	72-14.99N	165-00.04W	45.5	38.0	4.6	40.6	41.0	062M009	
065	6	111718	06:31	06:35	72-00.00N	166-00.12W	45.7	36.0	4.7	40.6	41.0	065M006	
067	1	111718	08:49	08:53	71-45.08N	167-00.03W	46.0	37.3	4.2	42.6	43.0	067M001	
064	4	111718	21:53	22:05	73-07.94N	161-31.91W	269.0	255.6	9.2	257.2	260.0	064M004	MIZ
048	10	111718	23:42	23:48	73-00.04N	161-59.64W	114.0	99.0	10.2	100.9	102.0	048M010	
056	10	111818	02:08	02:12	72-45.08N	163-00.07W	58.6	48.9	5.1	52.4	53.0	056M010	
058	10	111818	04:23	04:26	72-29.97N	163-59.93W	49.5	38.8	5.0	43.5	44.0	058M010	
062	10	111818	06:36	06:41	72-15.01N	164-59.96W	46.0	35.5	4.6	40.6	41.0	062M010	
065	7	111818	08:48	08:52	71-59.97N	165-59.86W	46.5	37.1	4.8	40.6	41.0	065M007	
067	2	111818	11:04	11:08	71-45.08N	167-00.13W	47.0	37.7	4.3	42.6	43.0	067M002	

064	5	111818	22:45	22:53	73-05.85N	161-38.05W	186.0	175.9	10.0	175.1	177.0	064M005	MIZ
048	11	111918	00:10	00:16	73-00.09N	162-00.46W	111.0	97.4	10.0	99.9	101.0	048M011	
056	11	111918	02:29	02:33	72-45.18N	162-59.78W	56.9	51.3	5.1	52.4	53.0	056M011	
058	11	111918	04:43	04:47	72-29.88N	163-59.94W	49.0	40.8	5.0	43.5	44.0	058M011	
062	11	111918	06:56	07:00	72-15.02N	165-00.32W	45.2	38.4	5.0	41.6	42.0	062M011	
065	8	111918	09:06	09:10	72-00.12N	166-00.43W	46.3	36.9	4.8	40.6	41.0	065M008	
067	3	111918	11:16	11:20	71-45.06N	167-00.41W	48.3	37.9	5.0	41.6	42.0	067M003	
048	12	111918	22:37	22:44	73-01.63N	161-57.86W	119.3	107.3	9.8	107.9	109.0	048M012	MIZ
056	12	112018	01:26	01:30	72-45.23N	162-59.81W	58.4	50.5	5.4	52.4	53.0	056M012	
058	12	112018	03:44	03:48	72-30.03N	164-00.13W	48.9	41.3	4.8	43.5	44.0	058M012	
062	12	112018	05:56	06:00	72-15.09N	165-00.36W	44.9	35.5	5.2	40.6	41.0	062M012	
065	9	112018	08:08	08:12	72-00.06N	166-00.55W	46.0	34.5	4.7	40.6	41.0	065M009	
067	4	112018	10:19	10:23	71-45.11N	167-00.09W	46.8	37.1	4.8	41.6	42.0	067M004	
056	13	112118	01:54	01:59	72-45.28N	163-01.29W	59.1	49.2	4.5	53.4	54.0	056M013	
058	13	112118	04:09	04:13	72-29.86N	163-59.89W	47.8	39.1	4.6	43.5	44.0	058M013	
062	13	112118	06:26	06:30	72-14.81N	164-59.53W	44.5	37.5	5.0	39.6	40.0	062M013	
065	10	112118	08:44	08:48	71-59.86N	166-00.19W	45.1	37.5	5.5	39.6	40.0	065M010	
067	5	112118	11:04	11:07	71-44.97N	166-59.98W	47.6	36.0	6.6	39.6	40.0	067M005	
068	1	112218	00:51	00:55	71-37.03N	163-46.38W	41.0	32.2	4.9	35.6	36.0	068M001	DBO4.6
069	1	112218	01:43	01:47	71-33.28N	163-34.64W	42.9	31.6	5.6	35.6	36.0	069M001	DBO4.5a
070	1	112218	02:34	02:37	71-29.45N	163-23.27W	42.1	32.3	4.6	36.6	37.0	070M001	DBO4.5
071	1	112218	03:23	03:27	71-25.83N	163-12.10W	42.5	34.5	4.3	37.6	38.0	071M001	DBO4.4a
072	1	112218	04:14	04:17	71-21.75N	163-00.64W	45.5	35.8	5.9	38.6	39.0	072M001	DBO4.4
073	1	112218	05:49	05:53	71-17.84N	162-49.49W	45.1	36.9	5.1	39.6	40.0	073M001	DBO4.3a

034	2	112218	16:41	16:44	71-00.17N	168-45.00W	43.7	34.4	5.7	37.6	38.0	034M002	
033	2	112218	19:46	19:50	70-30.05N	168-44.97W	38.1	29.6	4.7	32.7	33.0	033M002	
032	2	112218	22:49	22:53	69-59.93N	168-44.51W	38.6	30.5	5.8	33.7	34.0	032M002	
020	2	112318	12:34	12:37	67-30.04N	168-44.76W	46.8	35.0	13.0	35.6	36.0	020M002	
026	2	112418	02:33	02:37	68-11.26N	167-19.09W	47.3	34.2	9.5	37.6	38.0	026M002	DBO3.3
027	2	112418	03:34	03:37	68-14.35N	167-07.72W	43.3	32.7	7.0	35.6	36.0	027M002	DBO3.2
028	2	112418	04:37	04:40	68-18.05N	166-56.60W	34.4	27.0	5.2	28.7	29.0	028M002	DBO3.1
019	2	112418	12:37	12:41	67-00.33N	168-44.53W	45.2	33.3	6.7	37.6	38.0	019M002	
018	2	112418	19:35	19:38	66-29.96N	168-44.95W	54.0	45.0	4.9	47.5	48.0	018M002	
017	2	112418	22:31	22:34	66-00.00N	168-44.99W	52.9	45.0	5.1	47.5	48.0	017M002	
016	2	112518	06:14	06:17	64-40.22N	168-15.20W	37.5	23.0	10.6	26.7	27.0	016M002	DBO2.3
014	2	112518	10:42	10:45	64-59.37N	169-08.90W	47.3	34.7	8.7	38.6	39.0	014M002	DBO2.5
013	2	112518	12:41	12:45	64-57.52N	169-53.37W	47.1	33.8	10.2	37.6	38.0	013M002	DBO2.4
012	2	112518	14:24	14:28	64-40.16N	169-55.15W	46.5	37.9	6.7	39.6	40.0	012M002	DBO2.1
011	2	112518	22:35	22:39	63-35.96N	172-36.32W	52.0	44.5	5.3	47.5	48.0	011M002	DBO1.10
010	2	112618	00:49	00:54	63-16.82N	173-04.37W	67.9	58.6	5.4	62.4	63.0	010M002	DBO1.9
009	2	112618	02:04	02:09	63-16.75N	173-27.56W	71.8	61.0	4.6	66.3	67.0	009M002	DBO1.8
008	2	112618	04:50	04:55	62-47.28N	173-30.12W	68.5	61.6	4.7	63.4	64.0	008M002	DBO1.7
007	2	112618	06:29	06:35	62-33.68N	173-33.02W	65.0	57.5	5.5	59.4	60.0	007M002	DBO1.6
006	2	112618	08:13	08:17	62-28.15N	174-05.15W	67.5	56.8	4.6	62.4	63.0	006M002	DBO1.5
005	2	112618	09:43	09:48	62-23.49N	174-34.38W	71.2	59.7	6.5	63.4	64.0	005M002	DBO1.4
004	2	112618	11:08	11:13	62-13.10N	174-52.74W	75.6	59.7	9.7	64.4	65.0	004M002	DBO1.3
003	2	112618	12:37	12:42	62-02.92N	175-12.85W	80.2	71.8	4.9	74.3	75.0	003M002	DBO1.2
002	2	112618	13:24	13:30	62-00.53N	175-03.76W	79.7	65.0	9.6	68.3	69.0	002M002	DBO1.1

3.2. Salinity measurements

(1) Personnel

Jun INOUE	NIPR	- PI
Masahiko MURATA	JAMSTEC	
Shungo OSHITANI	MWJ	

(2) Objective

To provide calibrations for the measurements of salinity collected from CTD casts, bucket and the continuous sea surface water monitoring system (TSG).

(3) Method

a. Salinity Sample Collection

Seawater samples were collected with 12 liter water sampling bottles and TSG. The salinity sample bottle of the 250ml brown glass bottle with screw cap was used for collecting the sample water. Each bottle was rinsed 3 times with the sample water, and was filled with sample water to the bottle shoulder. All of sample bottle were sealed with a plastic cone and a screw cap because we took into consideration the possibility of storage for about a month. The cone was rinsed 3 times with the sample seawater before its use. Each bottle was stored for more than 12 hours in the laboratory before the salinity measurement.

The kind and number of samples taken are shown as follows ;

Table 3.2-1: Kind and number of samples

Kind of Samples	Number of Samples
Samples for CTD	68
Samples for Bucket	79
Samples for TSG	34
Total	181

b. Instruments and Method

The salinity analysis was carried out on R/V MIRAI during the cruise of MR18-05C using the salinometer

(Model 8400B “AUTOSAL” ; Guildline Instruments Ltd.: S/N 62556) with an additional peristaltic-type intake pump (Ocean Scientific International, Ltd.). A pair of precision digital thermometers (1502A; FLUKE: S/N B78466 and B81550) were used for monitoring the ambient temperature and the bath temperature of the salinometer.

The specifications of the AUTOSAL salinometer and thermometer are shown as follows ;

Salinometer (Model 8400B “AUTOSAL” ; Guildline Instruments Ltd.)

Measurement Range	:	0.005 to 42 (PSU)
Accuracy	:	Better than ±0.002 (PSU) over 24 hours without re-standardization
Maximum Resolution	:	Better than ±0.0002 (PSU) at 35 (PSU)

Thermometer (1502A: FLUKE)

Measurement Range	:	16 to 30 deg C (Full accuracy)
Resolution	:	0.001 deg C
Accuracy	:	0.006 deg C (@ 0 deg C)

The measurement system was almost the same as Aoyama *et al.* (2002). The salinometer was operated in the air-conditioned ship's laboratory at a bath temperature of 24 deg C. The ambient temperature varied from approximately 21 deg C to 23 deg C, while the bath temperature was very stable and varied within +/- 0.002 deg C on rare occasion. The measurement for each sample was done with a double conductivity ratio and defined as the median of 31 readings of the salinometer. Data collection was started 5 seconds after filling the cell with the sample and it took about 10 seconds to collect 31 readings by a personal computer. Data were taken for the sixth and seventh filling of the cell. In the case of the difference between the double conductivity ratio of these two fillings being smaller than 0.00002, the average value of the double conductivity ratio was used to calculate the bottle salinity with the algorithm for the practical salinity scale, 1978 (UNESCO, 1981).

If the difference was greater than or equal to 0.00003, an eighth filling of the cell was done. In the case of the difference between the double conductivity ratio of these two fillings being smaller than 0.00002, the average value of the double conductivity ratio was used to calculate the bottle salinity. The measurement was conducted in about 4 hours per day and the cell was cleaned with soap after the measurement of the day.

(4) Results

a. Standard Seawater

Standardization control of the salinometer was set to 613 and all measurements were done at this setting. The value of STANDBY was 24+5135-5140 and that of ZERO was 0.0±0000-0001. The conductivity ratio of IAPSO Standard Seawater batch P161 was 0.99987 (double conductivity ratio was 1.99974) and was used as the standard for salinity. 16 bottles of P161 were measured.

Figure 3.2-1 shows the time series of the double conductivity ratio of the Standard Seawater batch P161. The average of the double conductivity ratio was 1.99970 and the standard deviation was 0.00004 which is equivalent to 0.0008 in salinity.

Figure 3.2-2 shows the time series of the double conductivity ratio of the Standard Seawater batch P161 after correction. The average of the double conductivity ratio after correction was 1.99974 and the standard deviation was 0.00001, which is equivalent to 0.0003 in salinity.

The specifications of SSW used in this cruise are shown as follows ;

Batch	:	P161
Conductivity ratio	:	0.99987
Salinity	:	34.995
Use by	:	3rd Mar. 2020

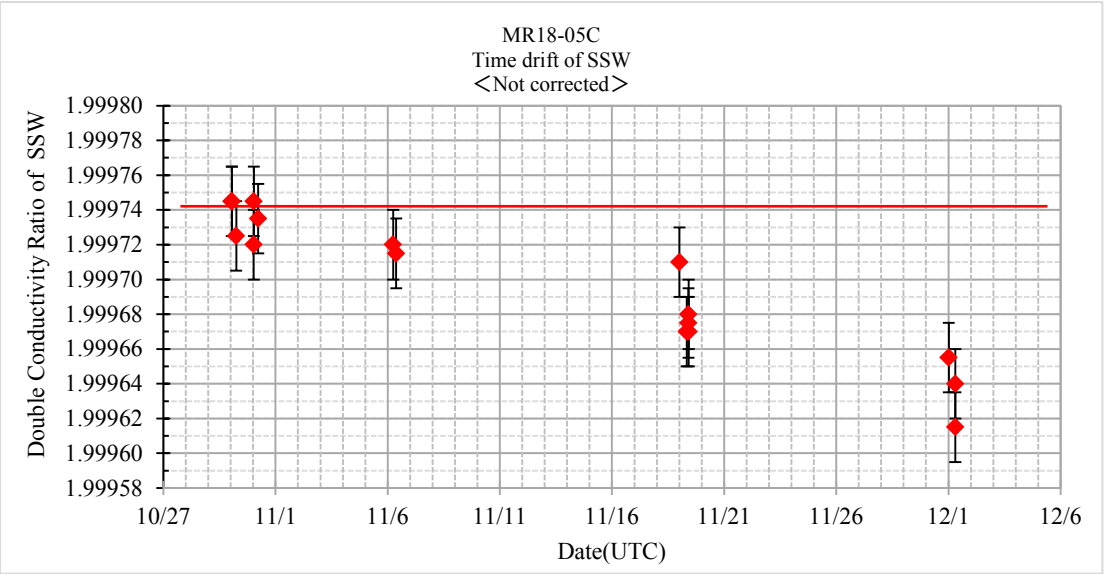

Figure 3.2-1: Time series of double conductivity ratio for the Standard Seawater batch P161 (before correction)

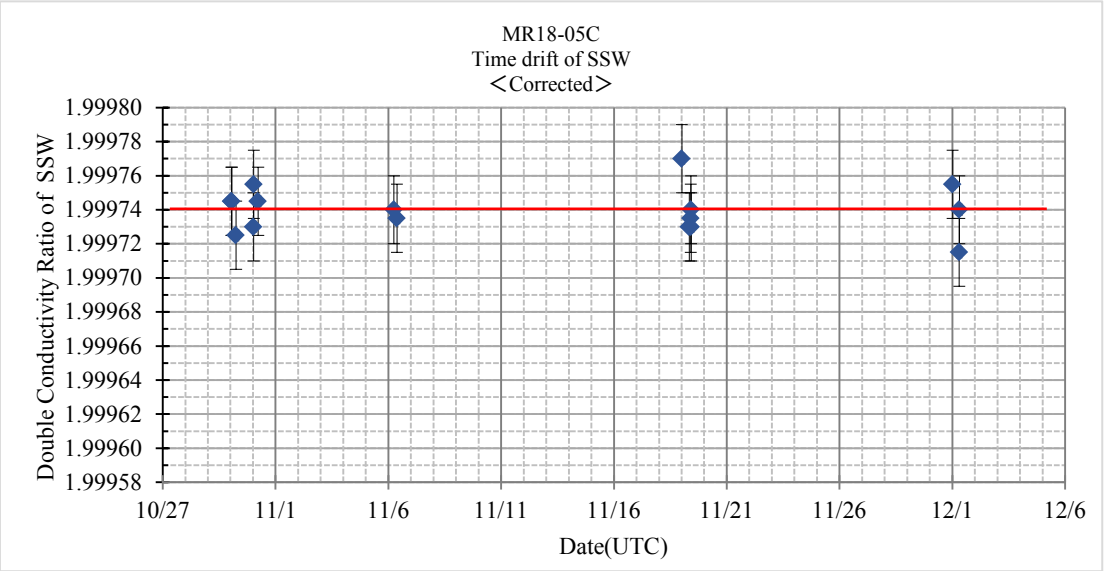

Figure 3.2-2: Time series of double conductivity ratio for the Standard Seawater batch P161 (after correction)

b. Sub-Standard Seawater

Sub-standard seawater was made from surface sea water filtered by a pore size of 0.2 micrometer and stored in a 20 liter container made of polyethylene and stirred for at least 24 hours before measuring. It was measured about every 6 samples in order to check for the possible sudden drifts of the salinometer.

c. Replicate Samples

We estimated the precision of this method using 12 pairs of replicate samples taken from the same water sampling bottle. The average and the standard deviation of absolute difference among 12 pairs of replicate samples were 0.0003 and 0.0003 in salinity, respectively.

(5) Data archive

These raw datasets will be submitted to JAMSTEC Data Management Group (DMG).

(6) Reference

Aoyama, M., T. Joyce, T. Kawano and Y. Takatsuki : Standard seawater comparison up to P129. Deep-Sea Research, I, Vol. 49, 1103～1114, 2002

UNESCO : Tenth report of the Joint Panel on Oceanographic Tables and Standards. UNESCO Tech. Papers in Mar. Sci., 36, 25 pp., 1981

3.3. XCTD

(1) Personnel

Jun Inoue	NIPR	-PI
Kazuho Yoshida	NME	
Sueyoshi Souichirou	NME	
Shinya Okumura	NME	
Takehito Hattori	MIRAI Crew	

(2) Objective

To obtain vertical profiles of sea water temperature and salinity (calculated by the function of temperature, pressure (depth), and conductivity).

(3) Parameters

The range and accuracy of parameters measured by the XCTD (eXpendable Conductivity, Temperature & Depth profiler) are as follows;

Parameter	Range	Accuracy
Conductivity	0 ~ 60 [mS/cm]	+/- 0.03 [mS/cm]
Temperature	-2 ~ 35 [deg-C]	+/- 0.02 [deg-C]
Depth	0 ~ 1000 [m]	5 [m] or 2 [%] (either of them is major)

(4) Instruments and Methods

We observed the vertical profiles of the sea water temperature and conductivity measured by XCTD-1 manufactured by Tsurumi-Seiki Co. (TSK). The signal was converted by MK-150N(TSK) and was recorded by AL-12B software (Ver.1.1.4, TSK). We launched 17 probes by using the automatic launcher. The summary of XCTD observation log is shown in Table 3.3.-1.

Table 3.3-1: XCTD observation log

SST: Sea Surface Temperature [deg-C] measured by TSG (Thermo Salino Graph).

SSS: Sea Surface Salinity [PSU] measured by TSG.

No.	Station No.	Date [YYYY/MM/DD]	Time [hh:mm]	Latitude [degN]	Longitude [deg]	Depth [m]	SST [deg-C]	SSS [PSU]	Probe S/N
1	XCTD.01	2018/11/06	04:52	73-00.0128N	167-00.0765W	57	1.995	31.990	17121099
2	XCTD.02	2018/11/06	06:37	72-59.9960N	166-00.0234W	58	1.381	31.912	17121104
3	XCTD.03	2018/11/06	08:08	73-00.0008N	164-59.3369W	64	1.653	31.908	18086029
4	XCTD.04	2018/11/06	09:39	73-00.0138N	164-00.0774W	82	-0.009	31.006	17121105
5	XCTD.05	2018/11/06	11:11	73-00.0226N	163-00.0619W	91	-0.235	30.946	17121102
6	XCTD.06	2018/11/06	12:44	73-00.0336N	162-00.0220W	109	0.650	31.560	17121103
7	XCTD.07	2018/11/06	14:14	72-59.9769N	161-00.0262W	104	0.676	31.477	17121101
8	St.48-7	2018/11/15	01:02	72-59.8699N	161-59.9746W	113	-0.787	31.190	17121100
9	St.67-4	2018/11/20	10:35	71-45.3145N	167-00.5475W	45	1.240	31.200	17121098
10	St.48-13	2018/11/20	23:02	73-00.2512N	161-59.1306W	114	0.384	31.974	17121090
11	St.29-2	2018/11/23	07:01	68-30.0800N	168-44.8545W	54	1.448	31.523	17121093
12	St.21-2	2018/11/23	18:40	67-40.9587N	168-55.3432W	50	1.948	31.479	17121095
13	St.22-2	2018/11/23	20:07	67-46.9916N	168-36.0374W	50	1.953	31.551	17121087
14	St.23-2	2018/11/23	21:46	67-53.9061N	168-14.2120W	57	1.714	31.531	17121086
15	St.24-2	2018/11/23	23:47	68-00.8357N	167-51.9582W	52	1.824	31.534	17121089
16	St.25-2	2018/11/24	01:24	68-07.6491N	167-07.6491W	49	2.254	31.715	17121092
17	St.15-2	2018/11/25	08:16	64-40.6872N	169-05.3858W	45	1.572	32.156	18086017

(5) Data archives

These data obtained in this cruise will be submitted to the Data Management Group of JAMSTEC and will be opened to the public via “Data Research System for Whole Cruise Information in JAMSTEC (DARWIN)” in JAMSTEC web site. <http://www.godac.jamstec.go.jp/darwin/e>

3.4. Shipboard ADCP

(1) Personnel

Jun Inoue	NIPR	- PI
Kazuho Yoshida	NME	
Sueyoshi Souichirou	NME	
Shinya Okumura	NME	
Takehito Hattori	MIRAI Crew	

(2) Objectives

To obtain continuous measurement data of the current profile along the ship's track.

(3) Parameters

Major parameters for the measurement, Direct Command, are shown in Table 3.4.-1.

Table 3.4-1: Major parameters

Bottom-Track Commands	
BP = 001	Pings per Ensemble (almost less than 1,200m depth)
Environmental Sensor Commands	
EA = 04500	Heading Alignment (1/100 deg)
ED = 00065	Transducer Depth (0 - 65535 dm)
EF = +001	Pitch/Roll Divisor/Multiplier (pos/neg) [1/99 - 99]
EH = 00000	Heading (1/100 deg)
ES = 35	Salinity (0-40 pp thousand)
EX = 00000	Coordinate Transform (Xform:Type; Tilts; 3Bm; Map)
EZ = 10200010	Sensor Source (C; D; H; P; R; S; T; U)
	C (1): Sound velocity calculates using ED, ES, ET (temp.)
	D (0): Manual ED
	H (2): External synchro
	P (0), R (0): Manual EP, ER (0 degree)
	S (0): Manual ES
	T (1): Internal transducer sensor
	U (0): Manual EU
EV = 0	Heading Bias (1/100 deg)
Timing Commands	
TE = 00:00:02.00	Time per Ensemble (hrs:min:sec.sec/100)
TP = 00:02.00	Time per Ping (min:sec.sec/100)
Water-Track Commands	
WA = 255	False Target Threshold (Max) (0-255 count)
WC = 120	Low Correlation Threshold (0-255)
WD = 111 100 000	Data Out (V; C; A; PG; St; Vsum; Vsum^2; #G; P0)
WE = 1000	Error Velocity Threshold (0-5000 mm/s)
WF = 0400	Blank After Transmit (cm)
WN = 100	Number of depth cells (1-128)
WP = 00001	Pings per Ensemble (0-16384)
WS = 800	Depth Cell Size (cm)
WV = 0390	Radial Ambiguity Velocity (cm/s)

(4) Instruments and methods

Upper ocean current measurements were made in this cruise, using the hull-mounted Acoustic Doppler

Current Profiler (ADCP) system. For most of its operation, the instrument was configured for water-tracking mode. Bottom-tracking mode, interleaved bottom-ping with water-ping, was made to get the calibration data for evaluating transducer misalignment angle in the shallow water. The system consists of following components;

1. R/V MIRAI has installed the Ocean Surveyor for vessel-mount ADCP (frequency 76.8 kHz; Teledyne RD Instruments, USA). It has a phased-array transducer with single ceramic assembly and creates 4 acoustic beams electronically. We mounted the transducer head rotated to a ship-relative angle of 45 degrees azimuth from the keel.
2. For heading source, we use ship's gyro compass (Tokyo Keiki, Japan), continuously providing heading to the ADCP system directory. Additionally, we have Inertial Navigation Unit (Phins, Ixblue, France) which provide high-precision heading, attitude information, pitch and roll. They are stored in ".N2R" data files with a time stamp.
3. Differential GNSS system (Star Pack-D, Fugro, Netherlands) providing precise ship's position.
4. We used VmDas software version 1.49 (TRDI) for data acquisition.
5. To synchronize time stamp of ping with Computer time, the clock of the logging computer is adjusted to GPS time server every 10 minutes.
6. Fresh water is charged in the sea chest to prevent bio fouling at transducer face.
7. The sound speed at the transducer does affect the vertical bin mapping and vertical velocity measurement, and that is calculated from temperature, salinity (constant value; 35.0 PSU) and depth (6.5 m; transducer depth) by equation in Medwin (1975).

Data were configured for "8 m" layer intervals starting about 19m below sea surface. In the shallow water (Depth < 100m), layer interval was changed to "6m", so that starting about 17m below sea surface. Data were recorded every ping as raw ensemble data (.ENR). Additionally, 10 seconds averaged data were recorded as short-term average (.STA). 300 seconds averaged data were long-term average (.LTA), respectively.

(5) Preliminary results

Figure 3.4-1 shows the time series plot of the current velocity during the fixed observation line (round-trip from FP3 to marginal ice zone).

(6) Observation Log

24 Oct. 2018 to 06 Dec 2018

(7) Data archives

These data obtained in this cruise will be submitted to the Data Management Group of JAMSTEC and will be opened to the public via "Data Research System for Whole Cruise Information in JAMSTEC (DARWIN)" in JAMSTEC web site.

<http://www.godac.jamstec.go.jp/darwin/e>

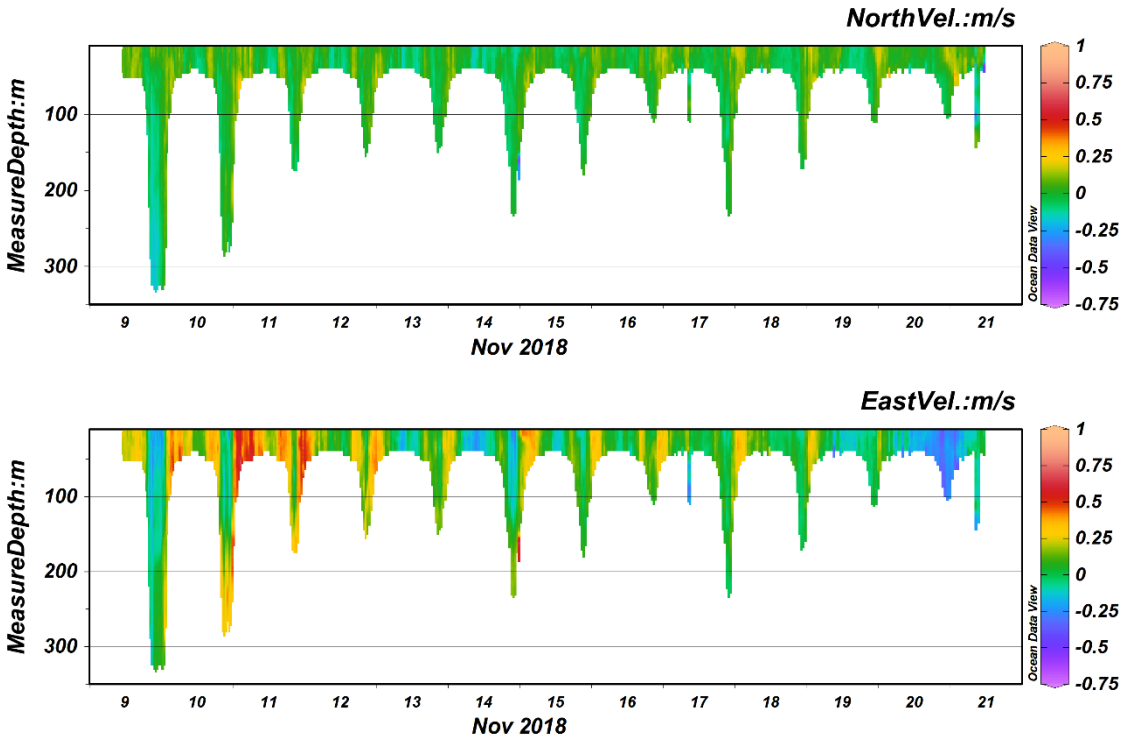

Figure 3.4-1: The time series plot of the current velocity

3.5. Surface wave measurement by drifting wave buoys

(1) Personnel

Jun Inoue	NIPR	- PI
Takuji Waseda	The University of Tokyo	- not on board
Tsubasa Kodaira	The University of Tokyo	- not on board
Takehiko Nose	The University of Tokyo	

(2) Objectives

Recent research has recognized surface ocean waves as one of the key physical processes in sea ice freeze up in autumn in the western Arctic Ocean. By deploying two drifting wave buoys in partially ice-covered water and adjacent open water, we aimed to study wave characteristics during the back and forth sea ice advance and retreat primarily driven by surface winds. On-ice winds bring relatively warm air over open water as well as surface waves; waves are decayed through damping and scattering as they enter ice-covered waters, and wave attenuation and sea ice break up observation are the key processes we aimed to capture. Furthermore, wave growth over ice-covered water during off-ice winds are also of interest.

(3) Parameters

Wave heights (Hm0, Hmax), periods (Tp, Tz and moment periods) and Power Spectral Density (PSD). Air temperature, sea surface temperature, atmospheric air pressure (only Piper-A #14), and GPS coordinates.

(4) Instruments and methods

Two drifting type surface wave buoys were manufactured, Piper-A #13 and #14. They are a variant version of the Waves in Ice buoy (WII buoy) deployed during the 2016 R/V Mirai cruise when two months of wave data were collected in the ice-free Beaufort Sea. The system was developed in cooperation with P.A.S. Consultants, Australia (hardware) and A. Kohout of NIWA (post-processing software). Since daylight hours are limited in November, a double battery pack system was designed with the auxiliary pack placed in the keel.

The buoy initially draws power from the auxiliary battery, and when the voltage drops below 9 V, the system switches to the main battery source. The motion of floating buoys is measured by 9-axis inertial moment unit, and an onboard processing unit analyzes data on board the buoy. Data acquisition duration is ~11 minutes (640 s). Default sampling intervals are 15 minutes but can be changed to longer intervals to prolong battery life, e.g., half an hour and two hours. Processed data (statistical quantities and power spectral density) and metadata are transferred by the Iridium satellite link to a server maintained by P.A.S. Consultants. These are also available on the Web based Dashboard page. Raw data are stored in the SD card.

(5) Preliminary Results

Piper-A #14 was deployed in open water at 16:28 UTC on the 6th November at 73-00.32 N, 159-59.60 W. The instrument transmitted data until 21:45 UTC on the same day and ceased transmission thereafter. The penultimate reading showed the auxiliary battery voltage dropped abruptly. According to P.A.S.'s log, the switch to the main battery source was confirmed; however, no further data were transmitted. Given the nature of the failure, a catastrophic cause is speculated such as being crashed by an object or water leakage.

Piper-A #13 was deployed in partially ice-covered water at 22:18 UTC on the 6th of November at 73-18.91 N, 158-54.34 W. The first sighting of sea ice was remnants of old ice at around 19:40 UTC followed by a combination of old and new ice patches and strips. The #13 buoy was deployed in waters when several bands of brash ice were observed. Somewhat similar to #14, #13's auxiliary battery pack failed at around 06:00 UTC on the 8th of November. The cause remains unknown, however, based on two failures, it is speculated the design to house a secondary battery pack in the keel was not suited in the harsh environments of the Arctic Ocean. Note that a 3-week field test was conducted in the Sagami Bay, Kanagawa using the #13 buoy using only the keel battery pack prior to the Arctic deployment; therefore, the keel system passed a field test at least under typical oceanic conditions.

Figure 3.5-1 shows the wave statistics recorded by #13. During the first two days, wave heights between 1—2.5 m with 6—8 seconds peak periods were measured. Sea state at the buoy site gradually decreased as winds became calm and the buoy drifted farther into the ice field. Indeed, the buoy drifted westward faster

than the members expected and not consistent with the local winds. The buoy and R/V Mirai tracks are provided in Figure 3.5-2 Following the 12th of November, no discernible waves were recorded. Although an on-ice wave event occurred on the 15th of November, which was observed by R/V Mirai, the buoy wave heights remained small despite a detection of a small peak in the processed PSD. This will be further analyzed to maximize the collected data in combination with the shipboard wave observation.

It is reasonable to conjecture that had a significant on-ice wind event occurred several days after the deployment, more apparent wave decay signal may have been observed, i.e., the buoy was deployed in a favorable location. A wave observational experiment in ice-covered water is a challenging task; in addition to precise planning considering ship time, it also requires an element of luck such as the timing of wave event occurrences.

Piper-A #13 sampling intervals have been reduced to save battery life. Furthermore, as the Arctic enters winter, the buoy will be put to a sleep mode where only GPS coordinates are transmitted to the server.

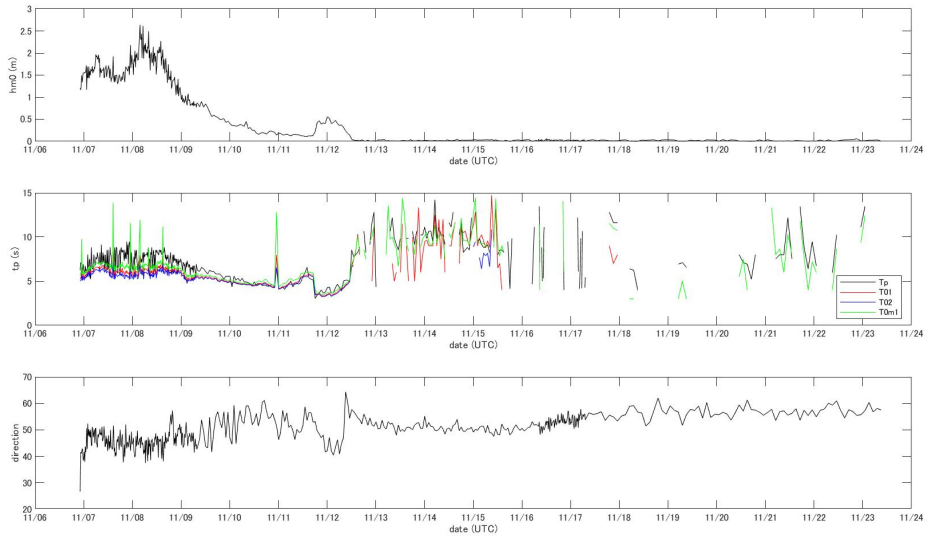

Figure 3.5-1: Significant wave height (top), periods (middle), and direction (bottom) measured by Piper-A #13 between the 6th and the 23rd of November 2018.

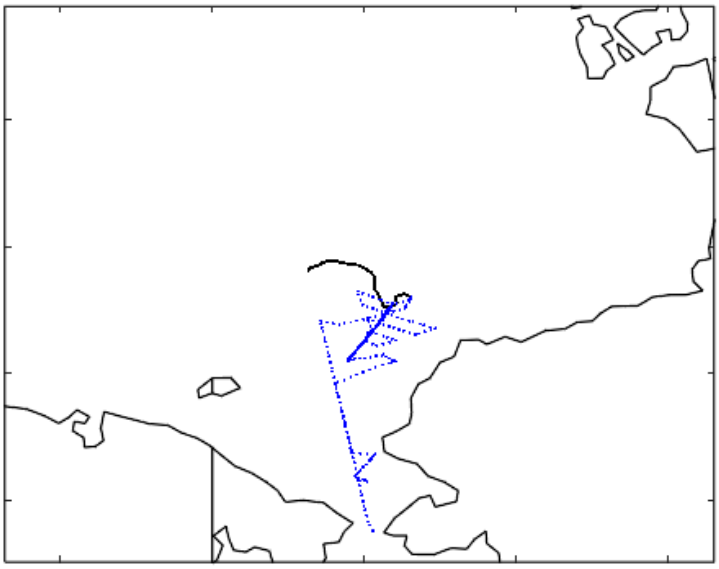

Figure 3.5-2: Piper-A #13 (black) and R/V Mirai (dotted blue) tracks.

(6) Data archive

Data obtained during this cruise will be submitted to the Data Management Group of JAMSTEC and open to public via “Data Research System for Whole Cruise Information in JAMSTEC (DARWIN)” on the JAMSTEC Web site. <http://www.godac.jamstec.go.jp/darwin/e>

3.6 Shipboard inertial moment unit

(1) Personnel

Jun Inoue	NIPR	- PI
Takuji Waseda	The University of Tokyo	- not on board
Tsubasa Kodaira	The University of Tokyo	- not on board
Takehiko Nose	The University of Tokyo	

(2) Objectives

Accurate shipboard wave observation can potentially be a valuable source of wave data. This is especially true for a vessel like R/V Mirai as it sails all over the World Oceans. Shipboard measurements require sufficient knowledge about the vessel response to waves of various frequencies, which is known as Response Amplitude Operator (RAO) in the study of floating bodies. Combining shipboard inertial moment unit (IMU) data, R/V Mirai's microwave Doppler radar wave sensors at the bow and stern of the ship, and numerical models, we aim to estimate the ship's response function and, therefore, usable wave data during the cruise.

(3) Parameters

Wave heights (Hm0, Hmax), periods (Tp, Tz and moment periods) and Power Spectral Density (PSD), pitch and roll, and GPS coordinates.

(4) Instruments and methods

Piper-C #15 was also developed by the same companies mentioned in Section 3.5 (4). This model was designed to be deployed on consolidated sea ice floes, and NIWA have had successes in the Antarctica. It uses the same methods as the Piper-A for processing measured data.

(5) Observation period and the use of data

The Piper-C #15 buoy logged wave data from the 23rd of October when R/V Mirai sailed from the Sekinehama port and continued logging until the 6th of December. It was turned off during the periods of calm sea states or choppy wind seas with short wavelengths. The instrument suffered from intermittent failures between the 8th—27th of November when air temperatures were low. After extensive correspondence with the manufacturer, three possible causes have been identified: reduced battery capacity due to elevated internal resistance in low temperatures, diode complication under low temperatures, and the condensation on the circuit board. Recommendations will be provided to P.A.S. Consultants to mitigate recurring issues including placing the circuit board in an air-tight enclosure, the addition of desiccant moisture absorber, and the use of lithium batteries.

(6) Data archive

Data obtained during this cruise will be submitted to the Data Management Group of JAMSTEC and open to public via "Data Research System for Whole Cruise Information in JAMSTEC (DARWIN)" on the JAMSTEC Web site. <http://www.godac.jamstec.go.jp/darwin/e>

4. Chemical and Biological Oceanography

4.1. Dissolved oxygen

(1) Personnel

Akihiko Murata	JAMSTEC	- PI
Erii Irie	MWJ	
Keitaro Matsumoto	MWJ	
Elena Hayashi	MWJ	

(2) Objective

Determination of dissolved oxygen in seawater by Winkler titration.

(3) Parameters

Dissolved oxygen

(4) Instruments and Methods

Following procedure is based on winkler method (Dickson, 1996; Culberson, 1991).

a. Instruments

Burette for sodium thiosulfate and potassium iodate:

Automatic piston burette (APB-510 / APB-610 / APB-620) manufactured by Kyoto Electronic Manufacturing Co. Ltd. / 10 cm3 of titration vessel

Detector:

Automatic photometric titrator (DOT-15X) manufactured by Kimoto Electronic Co. Ltd.

Software:

DOT_Terminal Ver. 1.3.1

b. Reagents

Pickling Reagent I:

Manganese chloride solution (3 mol dm-3)

Pickling Reagent II:

Sodium hydroxide (8 mol dm-3) / sodium iodide solution (4 mol dm-3)

Sulfuric acid solution (5 mol dm-3)

Sodium thiosulfate (0.025 mol dm-3)

Potassium iodate (0.001667 mol dm-3)

c. Sampling

Seawater samples were collected with Niskin bottle attached to the CTD-system and surface bucket sampler. Seawater for oxygen measurement was transferred from sampler to a volume calibrated flask (ca. 100 cm3). Three times volume of the flask of seawater was overflowed. Temperature was measured by digital thermometer during the overflowing. Then two reagent solutions (Reagent I and II) of 1 cm3 each were added immediately into the sample flask and the stopper was inserted carefully into the flask. The sample flask was then shaken vigorously to mix the contents and to disperse the precipitate finely throughout. After the precipitate has settled at least halfway down the flask, the flask was shaken again vigorously to disperse the precipitate. The sample flasks containing pickled samples were stored in a laboratory until they were titrated.

d. Sample measurement

At least two hours after the re-shaking, the pickled samples were measured on board. 1 cm3 sulfuric acid solution and a magnetic stirrer bar were added into the sample flask and stirring began. Samples were titrated by sodium thiosulfate solution whose morality was determined by potassium iodate solution. Temperature of sodium thiosulfate during titration was recorded by a digital thermometer. During this cruise, we measured dissolved oxygen concentration using 2 sets of the titration apparatus. Dissolved oxygen concentration (μmol kg-1) was calculated by sample temperature during seawater sampling,salinity of the bottle sampling, flask

volume, and titrated volume of sodium thiosulfate solution without the blank.

e. Standardization and determination of the blank

Concentration of sodium thiosulfate titrant was determined by potassium iodate solution. Pure potassium iodate was dried in an oven at 130ºC. 1.7835g potassium iodate weighed out accurately was dissolved in deionized water and diluted to final weight of 5 kg in a flask. 10 cm3 of the standard potassium iodate solution was added to a flask using a volume-calibrated dispenser. Then 90 cm3 of deionized water, 1 cm3 of sulfuric acid solution, and 1 cm3 of pickling reagent solution II and I were added into the flask in order. Amount of titrated volume of sodium thiosulfate (usually 5 times measurements average) gave the morality of sodium thiosulfate titrant.

The oxygen in the pickling reagents I (1 cm3) and II (1 cm3) was assumed to be 7.6×10^{-8} mol (Murray et al., 1968).The blank due to other than oxygen was determined as follows.1 and 2 cm3 of the standard potassium iodate solution were added to two flasks respectively using a calibrated dispenser. Then 100 cm3 of deionized water, 1 cm3 of sulfuric acid solution, and 1 cm3 of pickling reagent solution II and I each were added into the flask in order. The blank was determined by difference between the first (1 cm3 of KIO_3) titrated volume of the sodium thiosulfate and the second (2 cm3 of KIO_3) one. The results of 3 times blank determinations were averaged.

(5) Observation log

a. Standardization and determination of the blank

Results of the standardization and the blank determination during this cruise are illustrated in Table 4.5-1.

Table 4.5-1: Results of the standardization and the blank determinations during cruise.

Date (yyyy/mm/dd)	Potassium iodate ID	Sodium thiosulfate ID	DOT-01X (No.9)		DOT-01X (No.10)		Stations
			E.P. (cm^3)	Blank (cm^3)	E.P. (cm^3)	Blank (cm^3)	
2018/10/28	K1805D01	T1806C	3.968	0.003	3.969	0.000	001M001, 001M002
2018/11/02	K1805D02	T1806C	3.967	0.003	3.968	0.004	002M001, 003M001, 004M001, 007M001, 011M001, 012M001, 015M001, 017M001, 019M001, 021M001, 026M001, 030M001, 032M001, 034M001, 036M001, 039M001, 040M001
2018/11/06	K1805D03	T1806C	3.967	0.006			041M001, 042M001, 044M001, 047M001, 050M001, 052M001, 054M001, 057M001, 060M001, 062M001, 063M001, 056M002, 062M002, 064M001, 056M003, 062M003, 064M002, 040M001, 056M004
2018/11/12	K1805D04	T1806C	3.967	0.005			062M004, 066M001, 056M005, 062M005, 066M002, 056M006, 062M006, 064M003, 056M007, 062M007, 066M003, 056M008, 062M008, 048M009, 056M009
2018/11/17	K1805D05	T1806C	3.968	0.007			062M009, 067M001, 064M004, 056M010, 062M010, 067M002, 064M005, 056M011, 062M011, 067M003, 048M012, 062M012, 067M004, 056M013, 062M013, 067M005, 068M001
2018/11/21	K1805D06	T1806C	3.968	0.005			072M001, 034M002, 032M002, 020M002, 026M002, 019M002, 017M002, 012M002, 011M002, 007M002, 004M002, 002M002,

(6) Results

We collected sea water samples for DO by two CTD casts at a station. The purpose of it was to calibrate the DO sensor attached to the CTD system. Results of the calibration are shown in Figure 4.5-1.

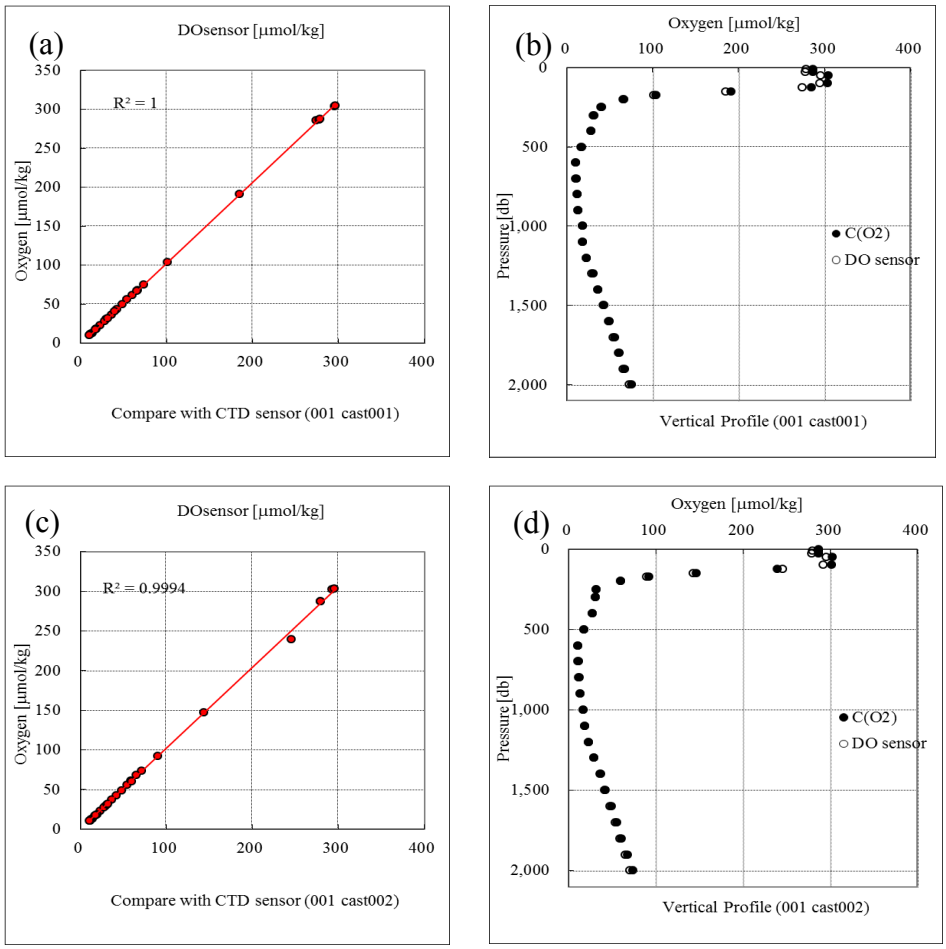

Figure 4.5-1: Results of calibration for DO sensor. (a) and (c): comparison of oxygen measured by the Winkler titration with that by the sensor. (b) and (d): vertical distributions of DO by the Winkler titration and those of the sensor.

(7) Data archives

These data obtained in this cruise will be submitted to the Data Management Group of JAMSTEC, and will be opened to the public via “Data Research System for Whole Cruise Information in JAMSTEC (DARWIN)” in JAMSTEC web site. <http://www.godac.jamstec.go.jp/darwin/e>

(8) Reference

Culberson, C. H. (1991). Dissolved Oxygen. WHPO Publication 91-1.

Dickson, A.G., Determination of dissolved oxygen in sea water by Winkler titration (1996).

In Dickson, A.G., Sabine, C.L. and Christian, J.R. (Eds.), Guide to best practices for ocean CO_2 measurements.

Murray, C. N., Riley, J. P., & Wilson, T. R. S. (1968). The solubility of oxygen in Winklerreagents used for the determination of dissolved oxygen. Deep Sea Res., 15, 237-238.

4.2. Underway DIC

(1) Personnel

Akihiko Murata JAMSTEC - PI

Yasuhiro Arii MWJ

Mikio Kitada MWJ

(2) Objective

Our purpose is to measure total dissolved inorganic carbon (DIC) concentration in surface seawater

(3) Parameter

DIC

(4) Instruments and Methods

Continuous underway measurements of surface seawater C_T were made with the C_T measuring system (Nihon ANS, Inc.) installed in the R/V *Mirai* of JAMSTEC.

The underway water sampling device collects surface seawater in a ~300 ml borosilicate glass bottle automatically after overflow of the 3 times volume. Before measurement, water samples are kept at 20°C. The seawater is then transferred into a pipette (~15 ml), which is kept at 20°C by a water jacket, in which water from a water bath set at 20°C is circulated. CO_2 dissolved in a seawater sample is extracted in a stripping chamber of the CO_2 extraction system by adding phosphoric acid (~10 % v/v) of about 2 ml. The stripping chamber is approx. 25 cm long and has a fine frit at the bottom. The acid is added to the stripping chamber from the bottom of the chamber by pressurizing an acid bottle for a given time to push out the right amount of acid. The pressurizing is made with nitrogen gas (99.9999 %). After the acid is transferred to the stripping chamber, a seawater sample kept in a pipette is introduced to the stripping chamber by the same method as in adding an acid. The seawater reacted with phosphoric acid is stripped of CO_2 by bubbling the nitrogen gas through a fine frit at the bottom of the stripping chamber. The CO_2 stripped in the chamber is carried by the

nitrogen gas (flow rates is 140 ml min^{-1}) to the coulometer through a dehydrating module. The module consists of two electric dehumidifiers (kept at ~2°C) and a chemical desiccant ($Mg(ClO_4)_2$).

(5) Observation log

Cruise track during underway DIC observation is shown in Figure 4.1-1.

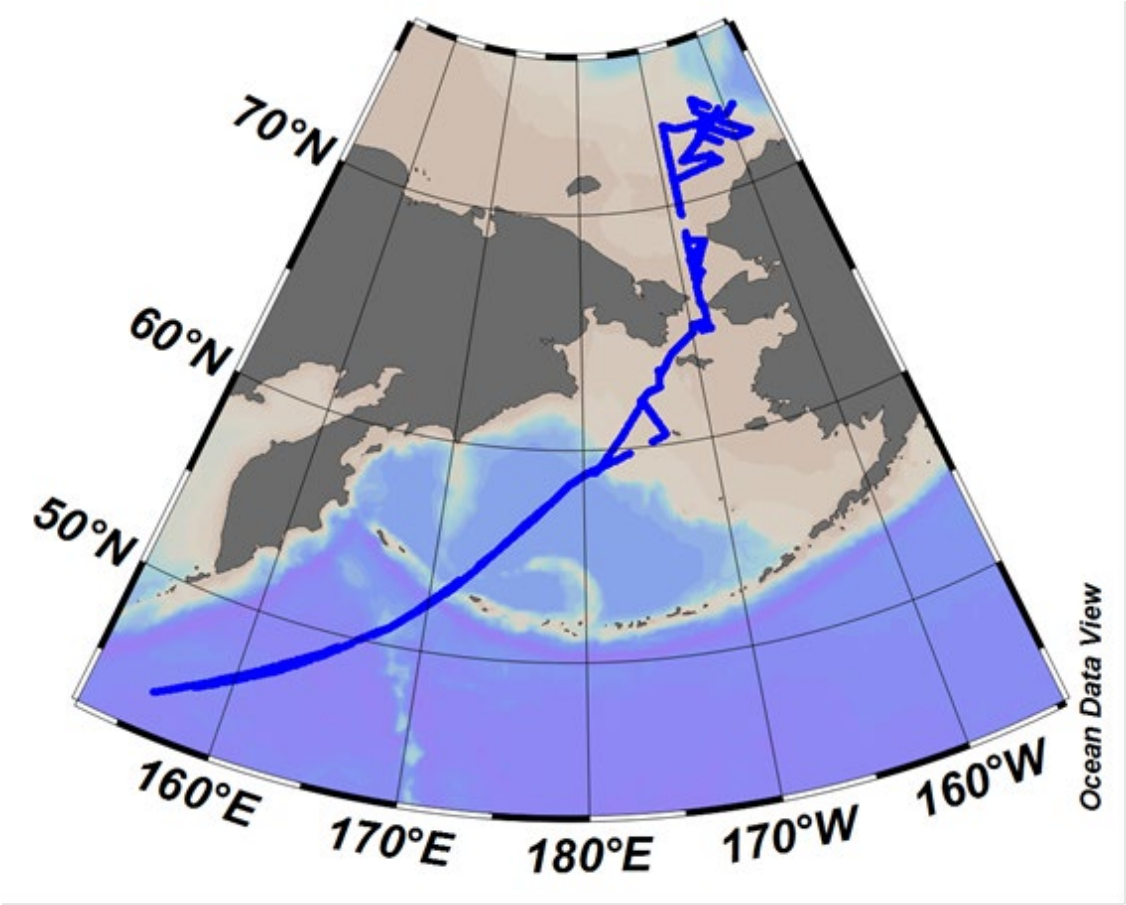

Figure 4.1-1: Cruise track for underway DIC

(6) Results

Temporal variations of surface seawater DIC are shown in Figure 4.1-2, together with SST.

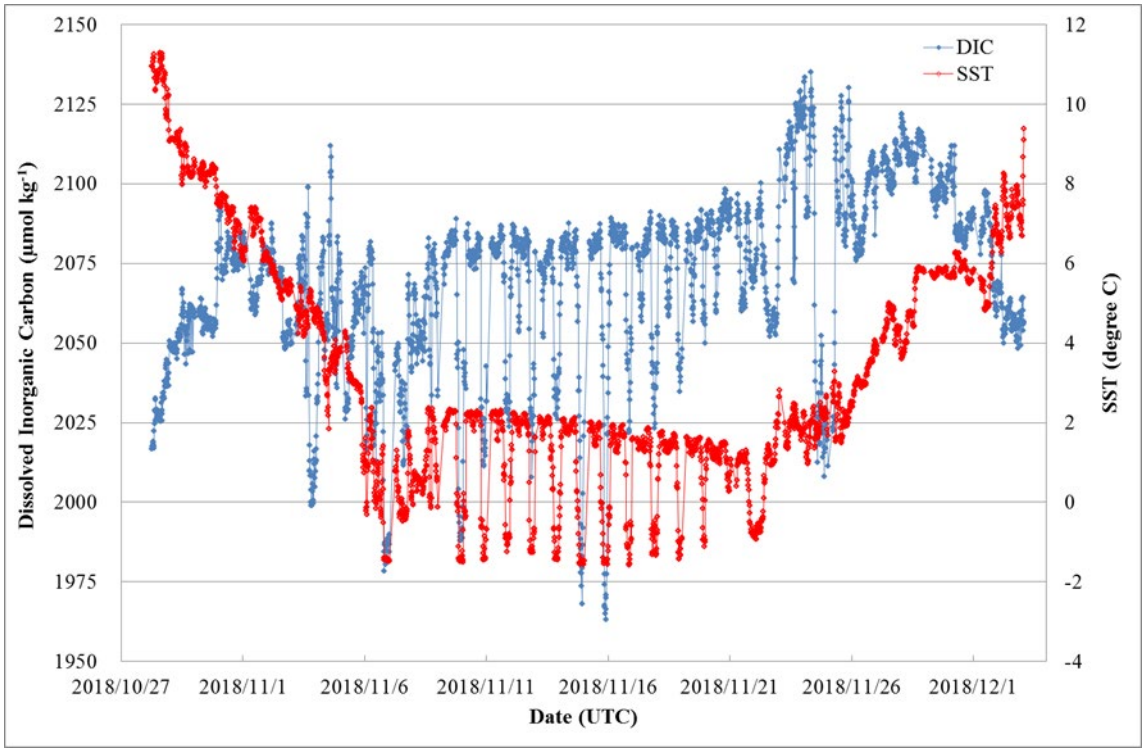

Figure 4.1-2: Temporal variations of surface seawater DIC. Blue and red dots represent surface seawater DIC and SST, respectively.

(7) Date archives

These data obtained in this cruise will be submitted to the Data Management Group (DMG) of JAMSTEC, and will open to the public via "Data Research System for Whole Cruise Information in JAMSTEC (DARWIN)" in JAMSTEC web site.

<http://www.godac.jamstec.go.jp/darwin/e>

4.3. Underway surface water monitoring

(1) Personnel

Akihiko Murata	JAMSTEC	- PI
Erii Irie	MWJ	
Keitaro Matsumoto	MWJ)	
Elena Hayashi	MWJ)	

(2) Objective

Our purpose is to obtain temperature, salinity, dissolved oxygen, fluorescence and total dissolved gas pressure data continuously in near-sea surface water.

(3) Parameters

Temperature

Salinity

Dissolved oxygen

Fluorescence

Turbidity

Total dissolved gas pressure

(4) Instruments and Methods

The Continuous Sea Surface Water Monitoring System (Marine Works Japan Co. Ltd.) has four sensors and automatically measures temperature, salinity, dissolved oxygen, fluorescence, turbidity, and total dissolved gas pressure in near-sea surface water every one minute. This system is located in the sea surface monitoring laboratory and connected to shipboard LAN-system. Measured data, time, and location of the ship were stored in a data management PC. Sea water was continuously pumped up to the laboratory from an

intake placed at the approximately 4.5 m below the sea surface and flowed into the system through a vinyl-chloride pipe. The flow rate of the surface seawater was adjusted to 10 dm^3 min^{-1}.

a. Instruments

Software

Seamoni Ver.1.0.0.0

Sensors

Specifications of the each sensor in this system are listed below.

Temperature and Conductivity sensor

Model:	SBE-45, SEA-BIRD ELECTRONICS, INC.
Serial number:	4563325-0362
Measurement range:	Temperature -5 °C - +35 °C
	Conductivity 0 S m-1 - 7 S m-1
Initial accuracy:	Temperature 0.002 °C
	Conductivity 0.0003 S m-1
Typical stability (per month):	Temperature 0.0002 °C
	Conductivity 0.0003 S m-1
Resolution:	Temperature 0.0001 °C
	Conductivity 0.00001 S m-1

Bottom of ship thermometer

Model:	SBE 38, SEA-BIRD ELECTRONICS, INC.
Serial number:	3852788-0457
Measurement range:	-5 °C - +35 °C

Initial accuracy:	±0.001 °C
Typical stability (per 6 month):	0.001 °C
Resolution:	0.00025 °C

Dissolved oxygen sensor

Model:	RINKO II, JFE ADVANTECH CO. LTD.
Serial number:	13
Measuring range:	0 mg L-1 - 20 mg L-1
Resolution:	0.001 mg L-1 - 0.004 mg L-1 (25 °C)
Accuracy:	Saturation±2%F.S. (non-linear) (1atm, 25°C)

Fluorescence & Turbidity sensor

Model:	C3, TURNER DESIGNS
Serial number:	2300384
Measuring range:	Chlorophyll -1 Chlorophyll in vivo 0 μg L^{-1} – 500 μg L^{-1}
Minimum Detection Limit:	Chlorophyll in vivo 0.03 μg L^{-1}
Measuring range:	Turbidity 0 NTU - 1500 NTU
Minimum Detection Limit:	Turbidity 0.05 NTU

Total dissolved gas pressure sensor

Model:	HGTD-Pro, PRO OCEANUS
Serial number:	37-394-10
Temperature range:	-2 °C - 50 °C
Resolution:	0.0001 %
Accuracy:	0.01 % (Temperature Compensated)
Sensor Drift:	0.02 % per year max (0.001 % typical)

(5) Observation log

Spatial distributions of each property are shown in Figure 4.3-1. We took the surface water samples from this system once a day to compare sensor data with bottle data of salinity, dissolved oxygen, and chlorophyll−a The results are shown in Figure 4.3-2. All the salinity samples were analyzed by the Model 8400B "AUTOSAL" manufactured by Guildline Instruments Ltd. (see 3.2), and dissolve oxygen samples were analyzed by Winkler method (see 4.1), chlorophyll *a* were analyzed by 10-AU manufactured by Turner Designs. (see 4.5).

(a)

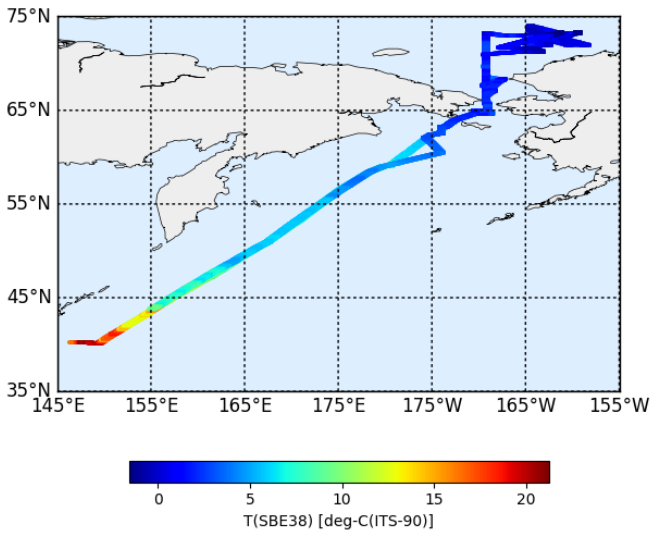

(b)

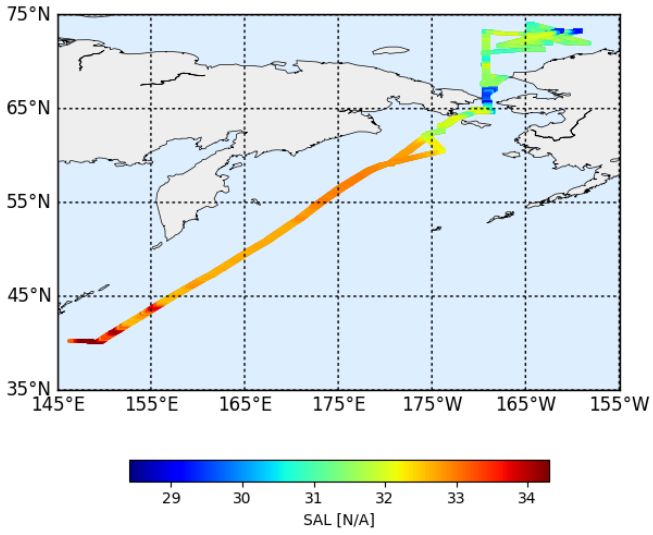

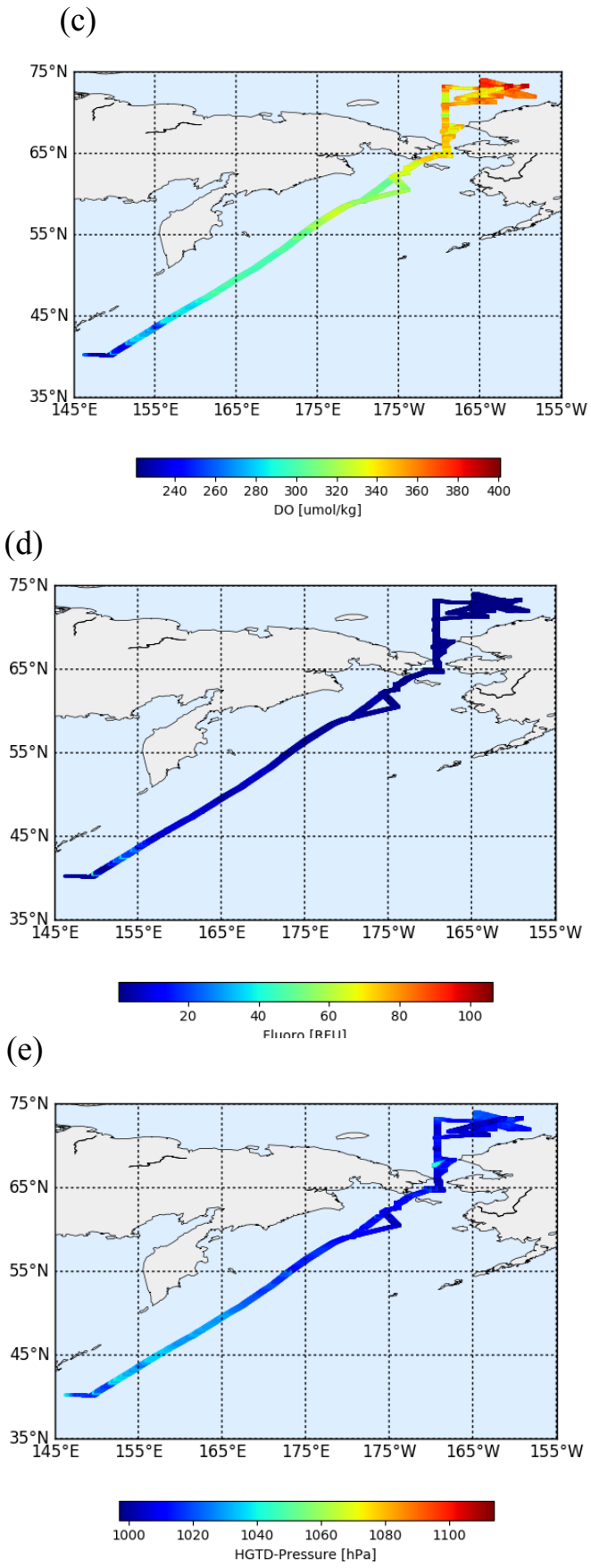

Figure 4.3-1: Spatial and temporal distribution of (a) temperature, (b) salinity, (c) dissolved oxygen, (d) fluorescence, and (e) gas tension in MR18-05C cruise.

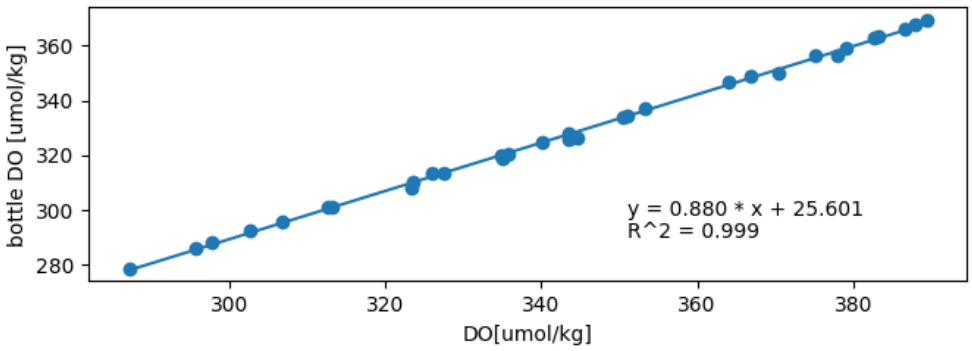

Figure 4.3-2: Correlation of salinity between sensor data and bottle data.

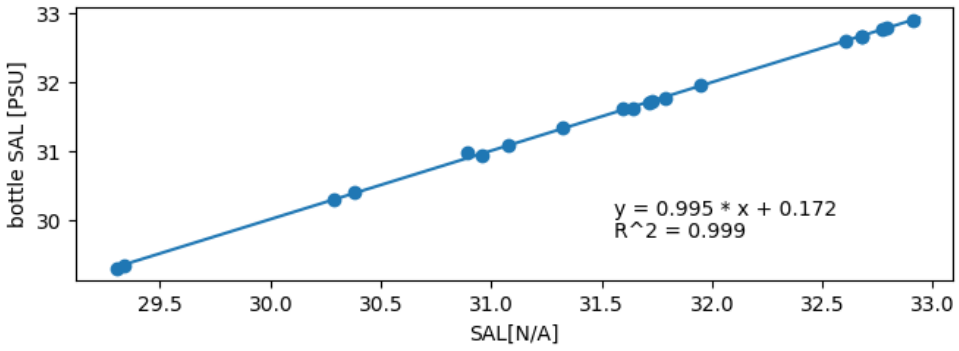

Figure 4.3-3: Correlation of dissolved oxygen between sensor data and bottle data.

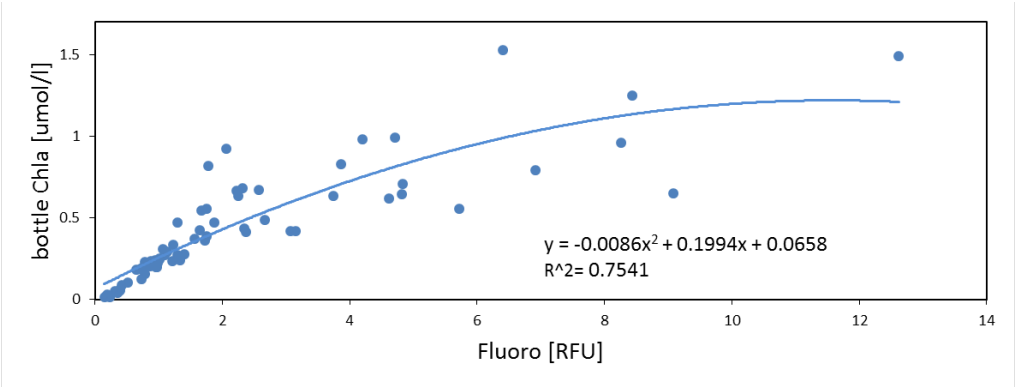

Figure 4.3-4: Correlation of fluorescence between sensor data and bottle data.

(6) Data archives

These data obtained in this cruise will be submitted to the Data Management Group (DMG) of JAMSTEC, and will opened to the public via “Data Research System for Whole Cruise Information in JAMSTEC (DARWIN)” in JAMSTEC web site.

<http://www.godac.jamstec.go.jp/darwin/e>

4.4. Continuous measurement of pCO_2 and pCH_4

(1) Personnel

Akihiko Murata	JAMSTEC	- PI
Yasuhito Arii	MWJ	
Mikio Kitada	MWJ	
Sohiko Kameyama	Hokkaido University	

(2) Objective

Our purpose is in-situ measurement of partial pressure of both carbon dioxide (pCO_2) and methane (pCH_4) in near-sea surface water.

(3) Methods, Apparatus and Performance

CO_2 and CH_4 standard gases (Table 4.3-1), atmospheric air, the both CO_2 and CH_4 equilibrated air with sea surface water were analyzed using an automated system equipped with both a non-dispersive infrared gas analyzer (NDIR; LI-7000, Li-Cor) and Off-Axis Integrated-Cavity output Spectroscopy gas analyzer (Off-Axis ICOS; 911-0011, Los Gatos Research) developed on the basis of Cavity Ring-Down.Spectroscopy. Standard gases and atmospheric air taken from the bow of the ship (approx.13 m above the sea level) were measured every about two hours. Seawater was taken from an intake placed at the approximately 4.5 m below the sea surface and introduced into the equilibrator at the flow rate of (4 - 5) L min-1 by a pump. The equilibrated air was circulated in a closed loop by a pump at flow rate of (0.6 - 0.7) L min-1 through two electric cooling units, a starling cooler, the NDIR and the Off-Axis ICOS.

We also conducted discrete water sampling for surface seawater CH_4 in order to check underway pCH_4 measurements (Table 4.3-2)

(4) Preliminary result

Cruise track during pCO_2 and CH_4 observation is shown in Figure 4.3-1. Temporal variations of CO_2 and CH_4 concentrations were shown in Figures 4.3-2 and 4.3-3, respectively.

(5) Data archive

Data obtained in this cruise will be submitted to the Data Management Group (DMG) of JAMSTEC, and will opened to the public via "Data Research System for Whole Cruise Information in JAMSTEC (DARWIN)" in JAMSTEC web site. <http://www.godac.jamstec.go.jp/darwin/e>

Table 4.3-1: Concentrations of CO_2 and CH_4 standard gases

	CO_2 (ppm)	CH_4 (ppm)
STD 1	219	-
STD 2	328	-
STD 3	389	-
STD 4	418	-
STD 5	240	1.63
STD 6	380	1.92
STD 7	472	2.12

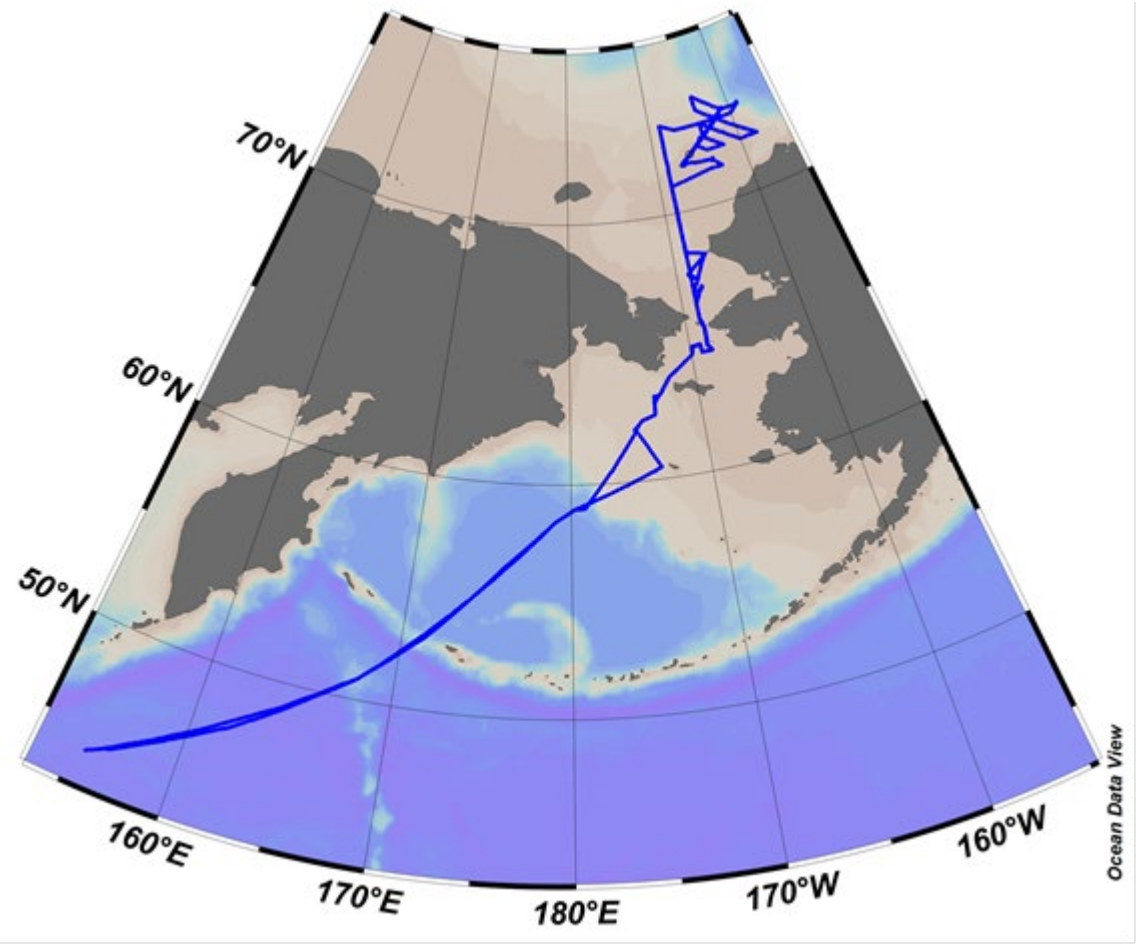

Figure 4.3-1: Observation map

Table 4.3-2: Sampling points for surface seawater CH_4

SystemDate	SystemTime	Latitude	Longitude
yyyy/mm/dd	hh:mm:ss	N/A	N/A
2018/10/31	0:09:52	53-11.94309N	171-15.91828E
2018/11/1	0:22:53	57-12.96491N	176-47.67698E
2018/11/2	0:23:38	60-34.69683N	176-57.36693W
2018/11/3	0:09:24	63-24.53214N	172-49.91367W
2018/11/4	0:07:31	65-44.97368N	168-34.42156W
2018/11/5	0:07:37	68-43.47234N	168-44.13280W
2018/11/6	0:06:54	72-59.87922N	168-45.14976W
2018/11/7	0:15:58	73-14.61569N	159-01.53040W
2018/11/8	0:09:32	72-25.93702N	159-42.00337W
2018/11/9	0:06:07	72-04.33699N	162-16.78914W
2018/11/10	0:07:50	73-15.11135N	161-00.44754W
2018/11/11	0:05:18	73-05.07654N	161-39.18337W
2018/11/12	0:05:36	72-49.19759N	162-36.23286W
2018/11/13	0:05:14	72-49.08525N	162-43.99335W
2018/11/14	0:08:09	72-52.45722N	162-32.24765W
2018/11/15	0:12:58	73-02.45713N	161-36.08413W
2018/11/16	0:06:24	72-56.07307N	162-15.14993W
2018/11/17	0:10:45	72-42.82956N	163-08.22409W
2018/11/18	0:07:22	72-58.95134N	162-05.48354W
2018/11/19	0:06:37	72-59.98725N	162-00.47141W
2018/11/20	0:10:33	72-52.43297N	162-25.64483W
2018/11/21	0:09:05	72-56.80744N	162-15.89955W
2018/11/22	1:15:17	71-35.45614N	163-41.15099W
2018/11/23	0:13:07	69-45.91149N	168-44.82383W
2018/11/24	0:10:07	68-02.57239N	167-47.44667W
2018/11/25	0:14:48	65-42.68384N	168-39.35171W
2018/11/26	0:12:01	63-20.80881N	172-55.65195W
2018/11/27	0:10:29	60-18.72132N	174-14.44304W
2018/11/28	0:09:22	57-51.00585N	177-55.64754E
2018/11/29	0:12:13	54-27.87418N	172-50.14097E
2018/11/30	0:11:31	52-09.21878N	169-35.16701E
2018/12/1	0:07:45	50-00.04681N	166-13.29923E
2018/12/2	0:19:35	47-21.40924N	161-31.47765E
2018/12/3	0:38:50	44-09.82491N	156-18.12004E

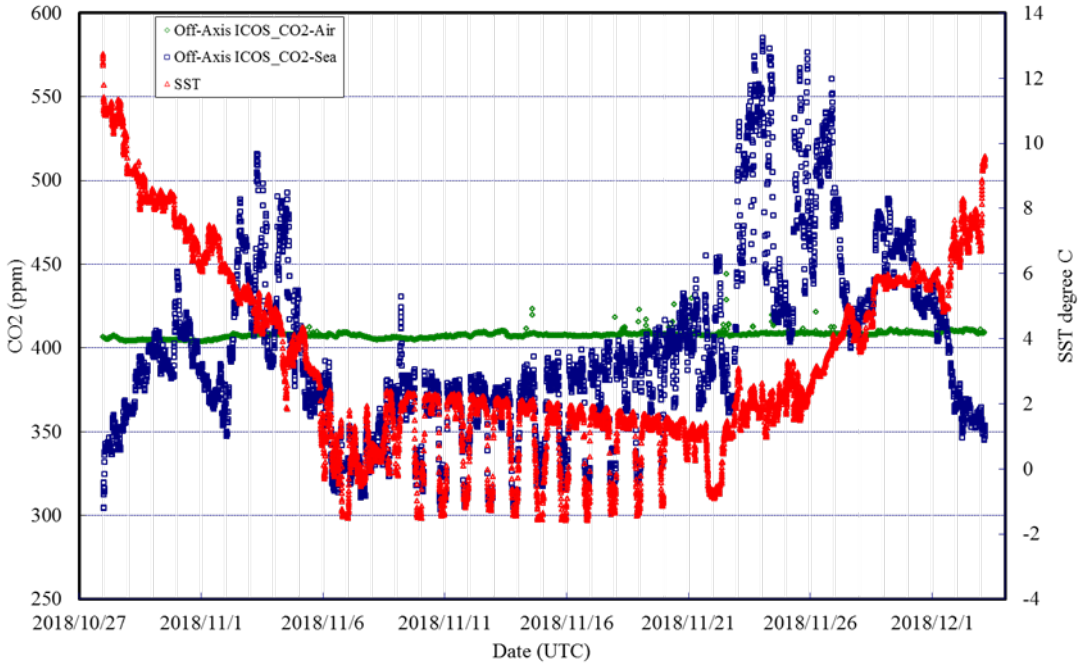

Figure 4.3-2: Temporal variations of atmospheric and surface seawater CO_2

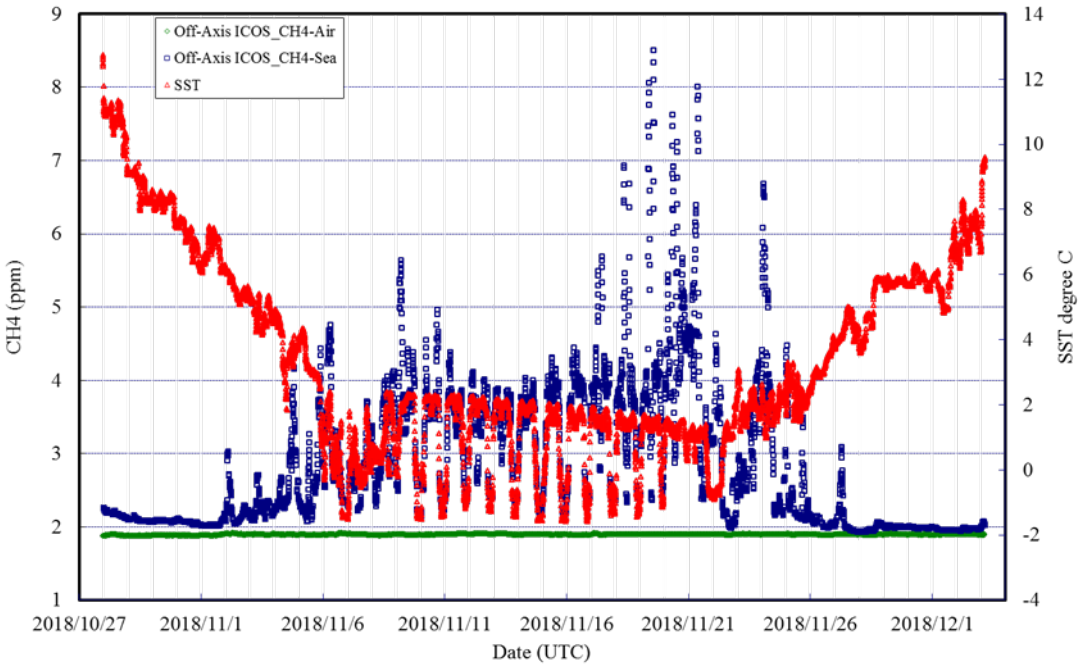

Figure 4.3-3: Temporal variations of atmospheric and surface seawater CH_4

4.5. Chlorophyll *a*

(1) Personnel

Akihiko Murata	JAMSTEC	PI
Keitaro Matsumoto	MWJ	

(2) Objective

Phytoplankton distributes in various species and sizes in the ocean were examined. Phytoplankton species are roughly characterized by the cell size. The objective of this study is to investigate the horizontal distributions of phytoplankton biomass in the Bering Sea and Arctic Ocean, in terms of phytoplankton pigment, chlorophyll *a*.

(3) Parameters

Total chlorophyll *a*

(4) Instruments and methods

We collected samples for total chlorophyll *a* from the surface sea water by bucket sampling. Seawater samples for total chlorophyll *a* were vacuum-filtrated (< 0.02 MPa) through Whatman GF/F filter (25mm-in diameter). Phytoplankton pigments retained on the filters were immediately extracted in a polypropylene tube with 7 ml of *N,N*-dimethylformamide (Wako Pure Chemical Industries Ltd.) (Suzuki and Ishimaru, 1990). The tubes were stored at -20 °C under the dark condition to extract chlorophyll *a* at least for 24 hours.

Chlorophyll *a* concentrations were measured by the fluorometer (10-AU, TURNER DESIGNS), which was previously calibrated against a pure chlorophyll *a* (Sigma-Aldrich Co., LLC). Calibration curves to get chlorophyll *a* concentration were assumed second order equations.To estimate the chlorophyll *a* concentrations, we applied to the fluorometric “Non-acidification method” (Welschmeyer, 1994).

(5) Station list

The number of samples, stations and the sampling positions were shown in Table 4.5-1 and Figure. 4.5-1.

(6) Preliminary results

Spatial distributions of total chlorophyll a are indicated in Figure 4.5-2. From this figure, it is found that biological activity is relatively strong south of 68°N.

(7) Data archives

These data obtained in this cruise will be submitted to the Data Management Group of JAMSTEC, and will be opened to the public via "Data Research System for Whole Cruise Information in JAMSTEC (DARWIN)" in JAMSTEC web site.

<http://www.godac.jamstec.go.jp/darwin/e>

(8) Reference

Suzuki, R., & Ishimaru T. (1990). An improved method for the determination of phytoplankton chlorophyll using N, N-dimethylformamide. *J. Oceanogr. Soc. Japan*, 46, 190-194.

Welschmeyer, N. A. (1994). Fluorometric analysis of chlorophyll *a* in the presence of chlorophyll *b* and pheopigments. *Limnol. Oceanogr.* 39(8), 1985-1992.

Table 4.5-1. Number of samples and casts.

	Number of samples	Number of casts
Total chlorophyll *a*	97	81

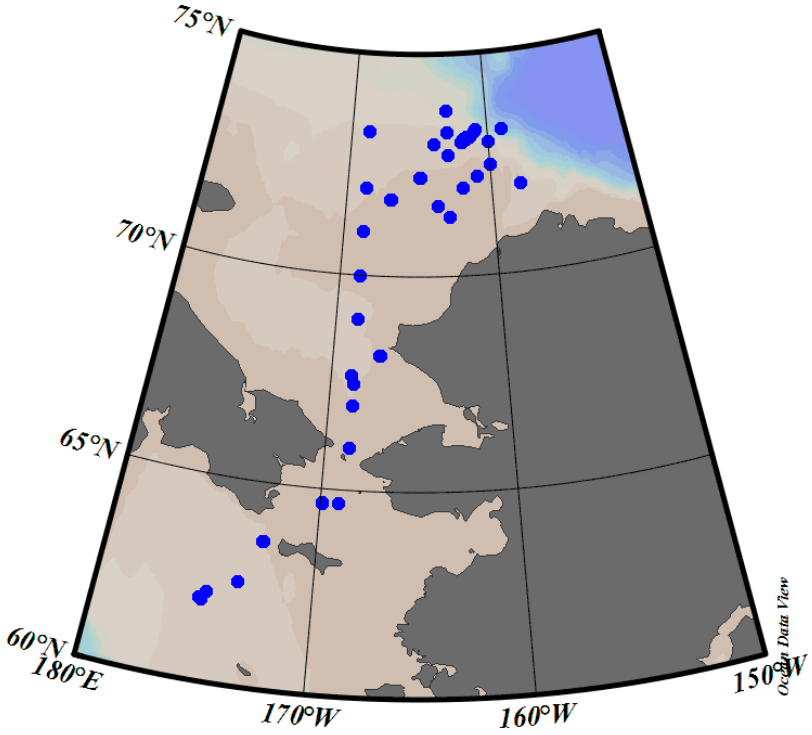

Figure 4.5-1: Sampling positions of total chlorophyll *a*.

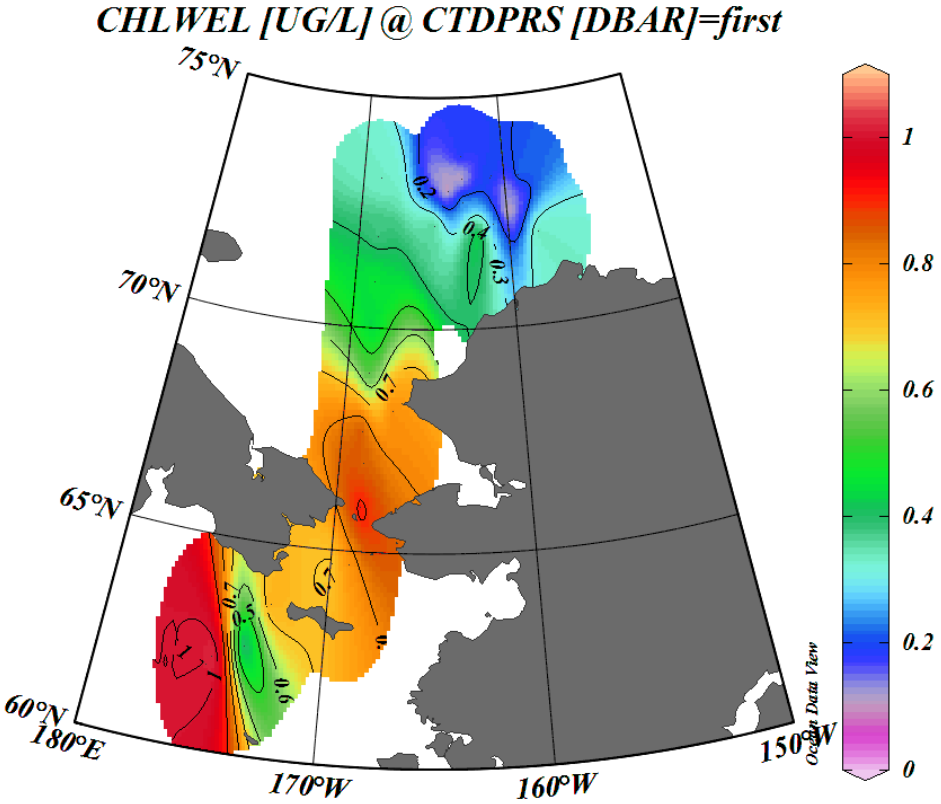

Figure 4.5-2: Spatial distributions of total chlorophyll a.

5. Geology

5.1. Sea Bottom Topography Measurement

(1) Personnel

Jun Inoue	NIPR	-PI
Kazuho Yoshida	NME	
Souichiro Sueyoshi	NME	
Shinya Okumuta	NME	
Takehito Hattori	MIRAI Crew	

(2) Objective

R/V MIRAI is equipped with the Multi Beam Echo Sounding system (MBES; SEABEAM 3012 (L3 Communications ELAC Nautik)). The objective of MBES is collecting continuous bathymetric data along ship's track except shallow depth, to make a contribution to geological and geophysical studies.

Also, R/V MIRAI is equipped with a Sub-Bottom Profiler (SBP), Bathy2010 (SyQwest). The objective of SBP is collecting sub-bottom data along ship's track.

(3) Instruments and Methods

The "SEABEAM 3012" on R/V MIRAI was used for bathymetry mapping during this cruise.

To get accurate sound velocity of water column for ray-path correction of acoustic beams, we determined sound velocities at the depth of 6.62m, the bottom of the ship, by a surface sound velocimeter. We made sound velocity profiles based on the observations of CTD, XCTD and Argo float conducted in this cruise by the equation in Del Grosso (1974).

The system configuration and performance are shown in Table 5.1-1.

Table 5.1-1: SEABEAM 3012 System configuration and performance

Frequency:	12 kHz
Transmit beam width:	2.0 degree
Transmit power:	4 kW
Transmit pulse length:	2 to 20 msec.
Receive beam width:	1.6 degree
Depth range:	50 to 11,000 m
Number of beams:	301 beams (Spacing mode: Equi-angle)
Beam spacing:	1.5 % of water depth (Spacing mode: Equi-distance)
Swath width:	60 to 150 degrees
Depth accuracy:	< 1 % of water depth (average across the swath)

Bathy2010 on R/V MIRAI was used for sub-bottom mapping from 30 Oct. to 01 Nov. and from 26 Nov. to 27 Nov., during the line surveys in Bering Sea. Table 5.1-2 shows system configuration and performance of Bathy2010 system.

Table 5.1-2: Bathy2010 System configuration and performance

Frequency:	3.5 KHz (FM sweep)
Transmit beam width:	23 degree
Transmit pulse length:	0.5 to 50 msec
Strata resolution:	Up to 8 cm with 300 m of bottom penetration according to bottom type
Depth resolution:	0.1 feet, 0.1 m
Depth accuracy:	±10 cm to 100 m, ± 0.3% to 6,000 m
Sound velocity:	1,500 m/s (fix)

(4) Preliminary Results

The results will be published after the primary processing.

(5) Observation Log

MBES: 25 Oct. 2018 to 05 Dec 2018

SBP: 30 Oct. 2018 to 01 Nov. 2018, 26 Nov. 2018 to 27 Nov. 2018

(6) Data archives

These data obtained in this cruise will be submitted to the Data Management Group of JAMSTEC, and will be opened to the public via "Data Research System for Whole Cruise Information in JAMSTEC (DARWIN)" in JAMSTEC web site.

http://www.godac.jamstec.go.jp/darwin/e

(7) Remarks

i) The following periods, MBES data acquisition was suspended due to the work station trouble.
17:19UTC 29 Oct. 2018 - 19:43UTC 29 Oct. 2018
15:19UTC 06 Nov. 2018 - 15:34UTC 06 Nov. 2018

ii) The following periods, Navigation data of MBES was not updated due to the server error.
04:36:56UTC 03 Dec. 2018 - 04:37:14UTC 03 Dec. 2018

iii) The following periods, MBES data acquisition was suspended due to the shallow sea area.
22:22UTC 30 Oct. 2018 - 23:43UTC 31 Oct. 2018
05:24UTC 02 Nov. 2018 - 15:16UTC 06 Nov. 2018
14:26UTC 07 Nov. 2018 - 20:16UTC 09 Nov. 2018
03:00UTC 10 Nov. 2018 - 19:13UTC 13 Nov. 2018
22:55UTC 13 Nov. 2018 - 19:34UTC 14 Nov. 2018
21:18UTC 14 Nov. 2018 - 01:25UTC 15 Nov. 2018
23:36UTC 15 Nov. 2018 - 20:11UTC 16 Nov. 2018
21:41UTC 16 Nov. 2018 - 20:20UTC 17 Nov. 2018
00:12UTC 17 Nov. 2018 - 21:20UTC 18 Nov. 2018
00:39UTC 19 Nov. 2018 - 00:13UTC 27 Nov. 2018

5.2. Sea Surface Gravity Measurement

(1) Personnel

Jun Inoue	NIPR(National Institute of Polar Research) -PI
Kazuho Yoshida	NME (Nippon Marine Enterprises, Ltd.)
Souichiro Sueyoshi	NME
Shinya Okumura	NME
Takehito Hattori	MIRAI Crew

(2) Objective

The local gravity is an important parameter in geophysics and geodesy. We collected gravity data during this cruise.

(3) Parameters

Relative Gravity [CU: Counter Unit]

[mGal] = (coefl: 0.9946) * [CU]

(4) Instruments and Methods

We measured relative gravity using LaCoste and Romberg air-sea gravity meter S-116 (Micro-g LaCoste, LLC) during the cruise. To convert the relative gravity to absolute one, we measured gravity, using portable gravity meter (Scintrex gravity meter CG-5), at Sekinehama and Shimizu port as the reference points.

(5) Preliminary Results

Absolute gravity table is shown in Table 5.2-1

Table 5.2-1: Absolute gravity table of the MR18-05C cruise

No.	Date	UTC	Port	Absolute Gravity [mGal]	Sea Level [cm]	Ship Draft [cm]	Gravity at Sensor * [mGal]	S-116 Gravity [mGal]
#1	24-Oct-18	05:46	Sekinehama	980371.87	218	625	980372.75	12657.21
#2	8-Dec-18	00:05	Shimizu	979729.06	169	663	979729.88	12010.77

*: Gravity at Sensor

= Absolute Gravity + Sea Level*0.3086/100 + (Draft-530)/100*0.2222

(6) Observation Log

24 Oct. 2018 to 08 Dec 2018

(7) Data archives

These data obtained in this cruise will be submitted to the Data Management Group of JAMSTEC, and will be opened to the public via “Data Research System for Whole Cruise Information in JAMSTEC (DARWIN)” in JAMSTEC web site.

<http://www.godac.jamstec.go.jp/darwin/e>

(8) Remarks

i) The following period, Depth and Gyro in GRV data were invalid due to the server error.

04:36:57UTC - 04:37:18UTC 03 Dec. 2018

5.3. Surface Magnetic Field Measurement : Three-components magnetometer

(1) Personnel

Jun Inoue	NIPR	-PI
Kazuho Yoshida	NME	
Souichiro Sueyoshi	NME	
Shinya Okumura	NME	
Takehito Hattori	MIRAI Crew	

(2) Objective

Measurement of magnetic force on the sea is required for the geophysical investigations of marine magnetic anomaly caused by magnetization in upper crustal structure. We measured geomagnetic field using a three-component magnetometer during this cruise.

(3) Instruments and Methods

A shipboard three-component magnetometer system (SFG2018, Tierra Tecnica) is equipped on-board R/V MIRAI. Three-axes flux-gate sensors with ring-cored coils are fixed on the fore mast. Outputs from the sensors are digitized by a 20-bit A/D converter (1 nT/LSB), and sampled at 8 times per second. Yaw (heading), Pitch and Roll are measured by the Inertial Navigation System (INS) for controlling attitude of a Doppler radar. Ship's position (Differential GNSS), speed over ground and gyro data are taken from LAN every second.

The relation between a magnetic-field vector observed on-board, Hob, (in the ship's fixed coordinate system) and the geomagnetic field vector, F, (in the Earth's fixed coordinate system) is expressed as:

$$\mathbf{H}_{ob} = \tilde{\mathbf{A}}\ \tilde{\mathbf{R}}\ \tilde{\mathbf{P}}\ \tilde{\mathbf{Y}}\ \mathbf{F} + \mathbf{H}_p \qquad \text{(a)}$$

where $\tilde{\mathbf{R}}$, $\tilde{\mathbf{P}}$ and $\tilde{\mathbf{Y}}$ are the matrices of rotation due to roll, pitch and heading of a ship, respectively. $\tilde{\mathbf{A}}$ is a 3 x 3 matrix which represents magnetic susceptibility of the ship, and $\mathbf{H}_p$ is a magnetic field vector produced by a permanent magnetic moment of the ship's body. Rearrangement of Eq. (a) makes

$$\tilde{\mathbf{B}}\,\mathbf{H}_{\mathrm{ob}} + \mathbf{H}_{bp} = \tilde{\mathbf{R}}\,\tilde{\mathbf{P}}\,\tilde{\mathbf{Y}}\,\mathbf{F} \qquad \text{(b)}$$

where $\tilde{\mathbf{B}} = \tilde{\mathbf{A}}^{-1}$, and $\mathbf{H}_{bp} = -\tilde{\mathbf{B}}\,\mathbf{H}_{\mathrm{p}}$. The magnetic field, $\mathbf{F}$, can be obtained by measuring , $\tilde{\mathbf{R}}$, $\tilde{\mathbf{P}}$, $\tilde{\mathbf{Y}}$ and $\mathbf{H}_{\mathbf{ob}}$, if $\tilde{\mathbf{B}}$ and $\mathbf{H}_{bp}$ are known. Twelve constants in $\tilde{\mathbf{B}}$ and $\mathbf{H}_{\mathbf{bp}}$ can be determined by measuring variation of $\mathbf{H}_{\mathbf{ob}}$ with $\tilde{\mathbf{R}}$, $\tilde{\mathbf{P}}$, and, $\tilde{\mathbf{Y}}$ at a place where the geomagnetic field, $\mathbf{F}$, is known.

(4) Preliminary Results

The results will be published after the primary processing.

(5) Observation Log

24 Oct. 2018 to 06 Dec 2018

(6) Data archives

These data obtained in this cruise will be submitted to the Data Management Group of JAMSTEC, and will be opened to the public via “Data Research System for Whole Cruise Information in JAMSTEC (DARWIN)” in JAMSTEC web site.

<http://www.godac.jamstec.go.jp/darwin/e>

(7) Remarks

i) For calibration of the ship’s magnetic effect, we made “figure-eight” turns (a pair of clockwise and anti-clockwise rotation) at the following periods and positions.

04:30UTC - 04:55UTC 11 Nov. 2018 around 72-46N, 162-57W

09:01UTC - 09:26UTC 04 Dec. 2018 around 39-31N, 148-41E

ii). The following period, Navigation data (Position, COG, SOG LOG, Heading, Depth) were not updated due to the server error.

04:36:57UTC - 04:37:15UTC 03 Dec. 2018

6. Notice on using

This cruise report is a preliminary but final documentation as of the end of the cruise. This report may not be corrected even if changes on contents (e.g. taxonomic classifications) are found after its publication. This report may also be changed without notice. Data on this cruise report may be raw or unprocessed. If you are going to use or refer to the data written on this report, please ask the Chief Scientist for the latest information. Users of data or results on this cruise report are requested to submit their results to Planning Group, Research Fleet Department, Marine Technology and Engineering Center of JAMSTEC.

E-mail：submit-rv-cruise@jamstec.go.jp